

ATLAS Status Report



113th LHCC Open Session
March 13, 2013

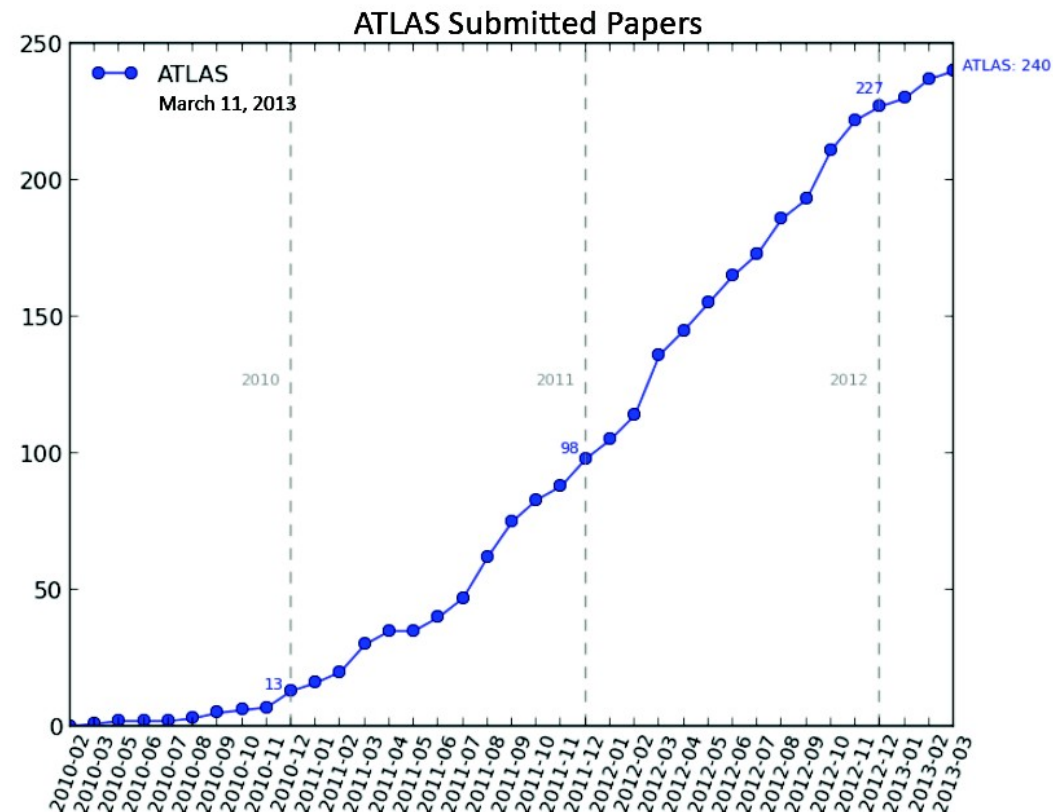
Brian Petersen
CERN

Outline

- 2012 pp data taking
- 2013 p+Pb data taking and first results
- Standard Model measurements
- The new boson
- BSM searches
- Shutdown activities

18 new papers and
36 preliminary results
since the last LHCC

Can only cover a
fraction of these



pp Data Taking and Performance

Integrated Luminosity in 2012

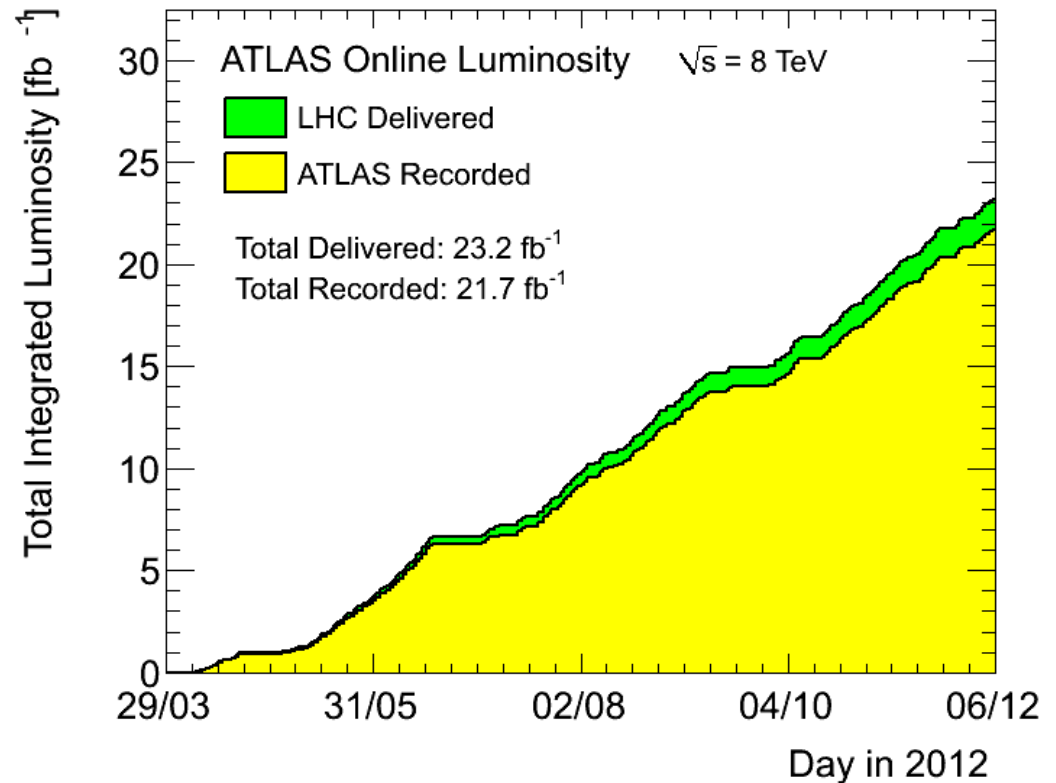
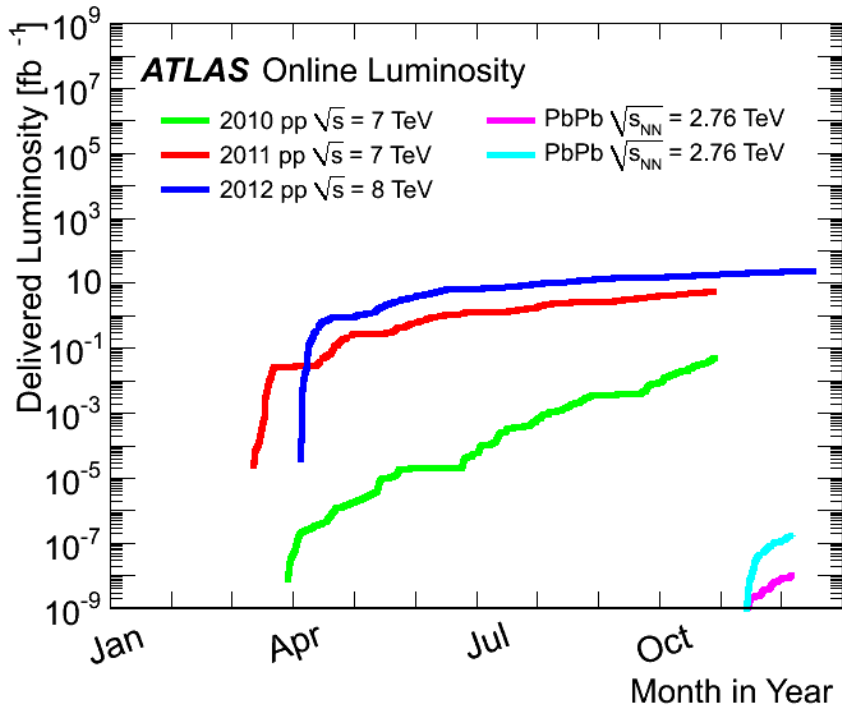
Luminosity is measured with forward detectors and calibrated with beam separation scans (Van der Meer)

ATLAS luminosity in 2012

- Peak Stable Luminosity Delivered:
- Max average interactions per bunch crossing:
- Max Luminosity in fill:
- 2011 Luminosity uncertainty:
- 2012 Luminosity uncertainty:

$7.73 \times 10^{33} \text{ cm}^{-2}\text{s}^{-1}$
 37
 237 pb^{-1}
 1.8%
 2.8% (prelim.)

arXiv:1302.4393
submitted to EPJC



Integrated Luminosity in 2012

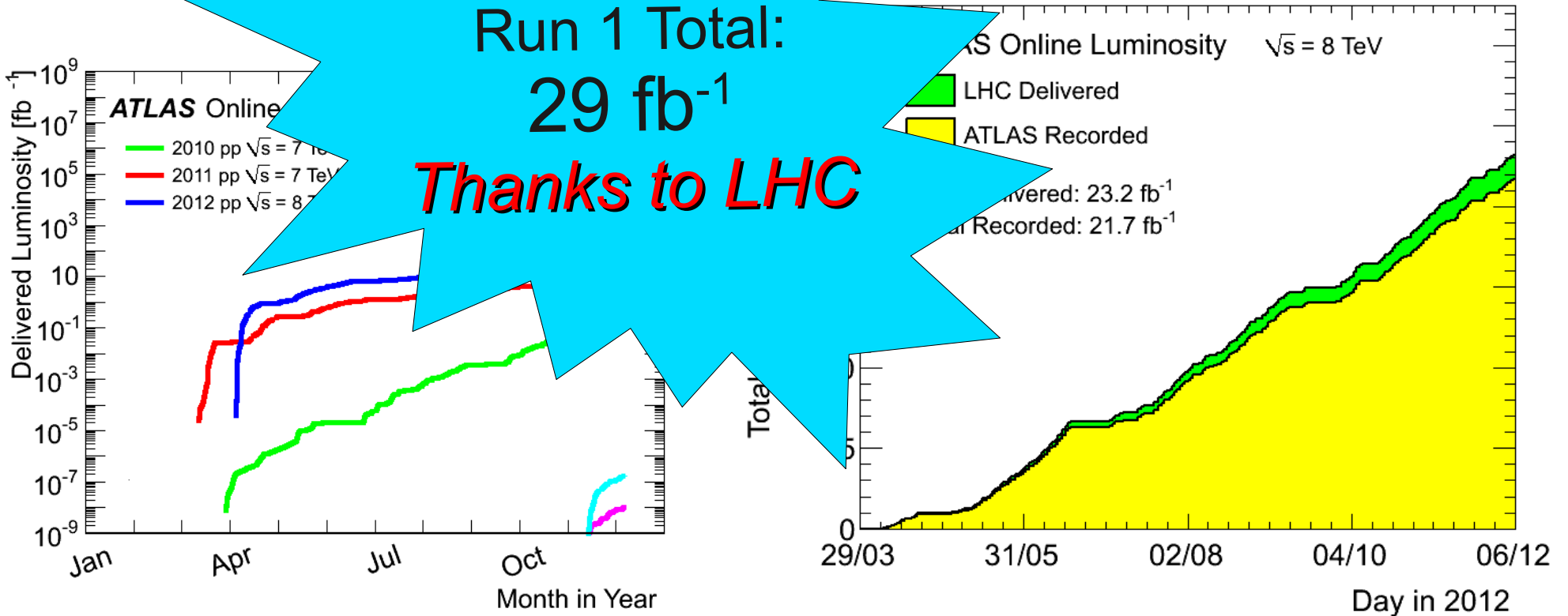
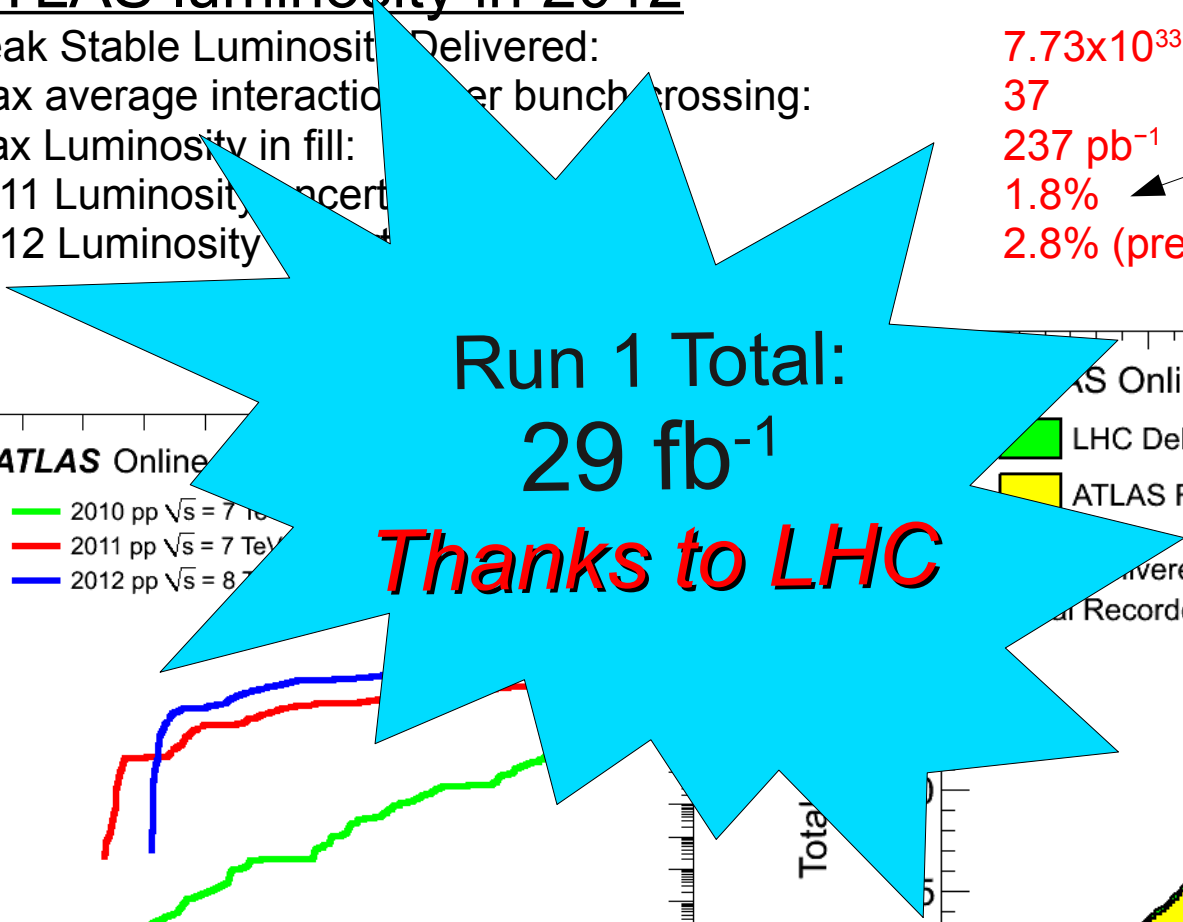
Luminosity is measured with forward detectors and calibrated with beam separation scans (Van der Meer)

ATLAS luminosity in 2012

Peak Stable Luminosity Delivered:
 Max average interaction per bunch crossing:
 Max Luminosity in fill:
 2011 Luminosity Uncertainty:
 2012 Luminosity Uncertainty:

$7.73 \times 10^{33} \text{ cm}^{-2}\text{s}^{-1}$
 37
 237 pb^{-1}
 1.8%
 2.8% (prelim.)

arXiv:1302.4393
 submitted to EPJC



Data Taking and Quality Efficiency

ATLAS p-p run: April-December 2012										
Inner Tracker			Calorimeters		Muon Spectrometer				Magnets	
Pixel	SCT	TRT	LAr	Tile	MDT	RPC	CSC	TGC	Solenoid	Toroid
99.9	99.4	99.8	99.1	99.6	99.6	99.8	100.	99.6	99.8	99.5
All good for physics: 95.8%										
Luminosity weighted relative detector uptime and good quality data delivery during 2012 stable beams in pp collisions at $\sqrt{s}=8$ TeV between April 4 th and December 6 th (in %) – corresponding to 21.6 fb ⁻¹ of recorded data.										

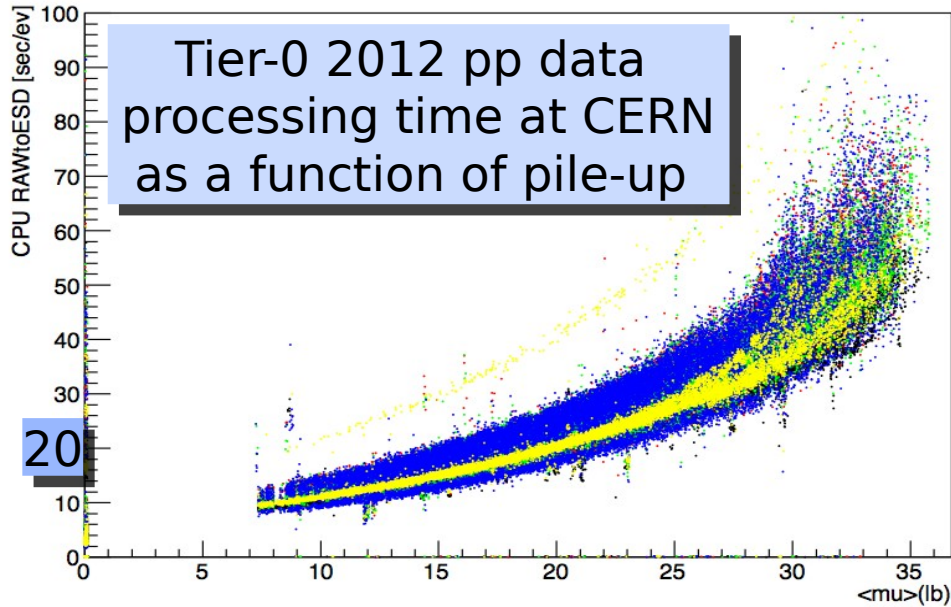
The data-taking efficiency for 2012 was **93.1%**

The good quality data was **95.8%** of the 2012 recorded data

- High DQ partly due recovery from large data reprocessing
- DQ losses at the level of 1% or less for each individual system
- Given the high DQ efficiency, we use a common set of “good quality data” across all analyses

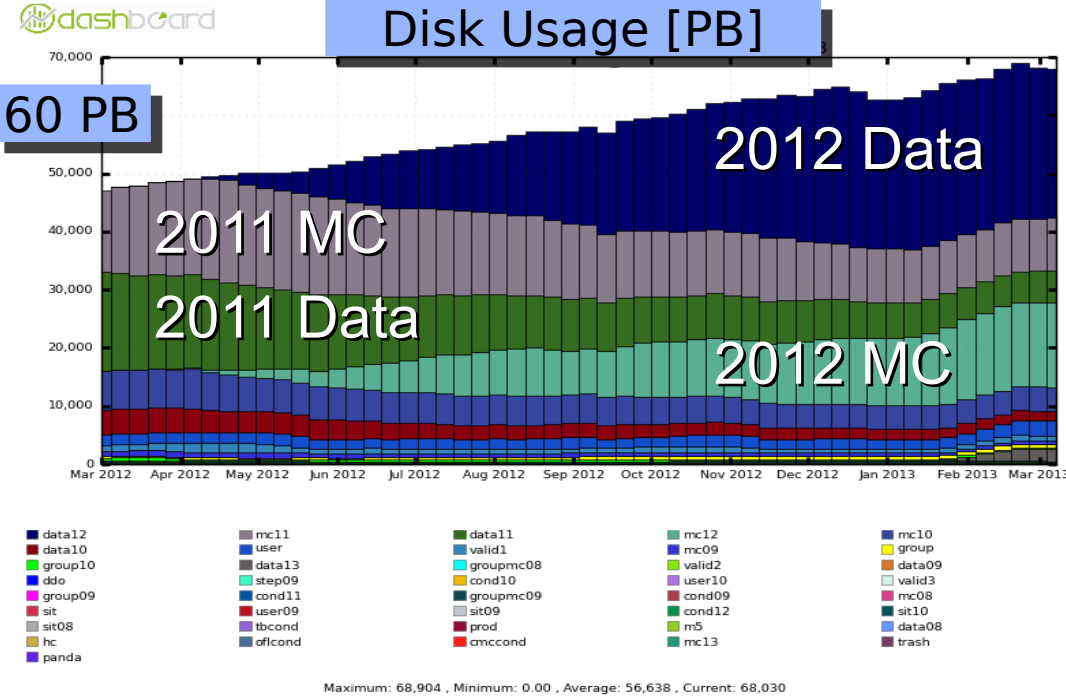
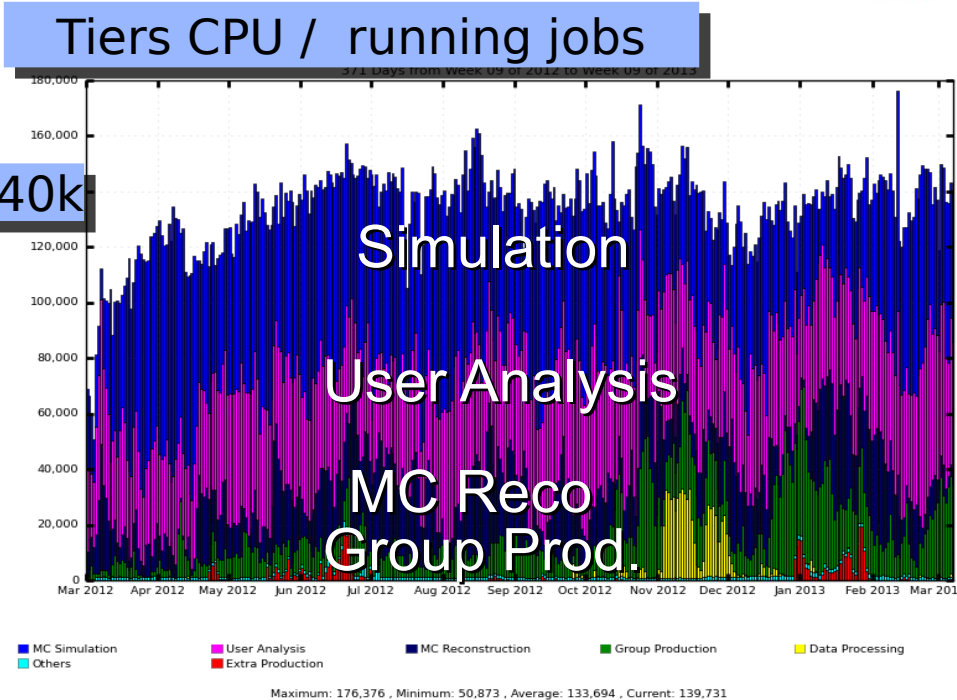
89% of delivered luminosity is used for physics analysis

Computing Resources



ATLAS has utilized the computing resources in its Tiers well:
Many thanks to sites for resources and their excellent operating!

Very challenging conditions, but managed to have a timely throughput for analyses to meet the physics needs



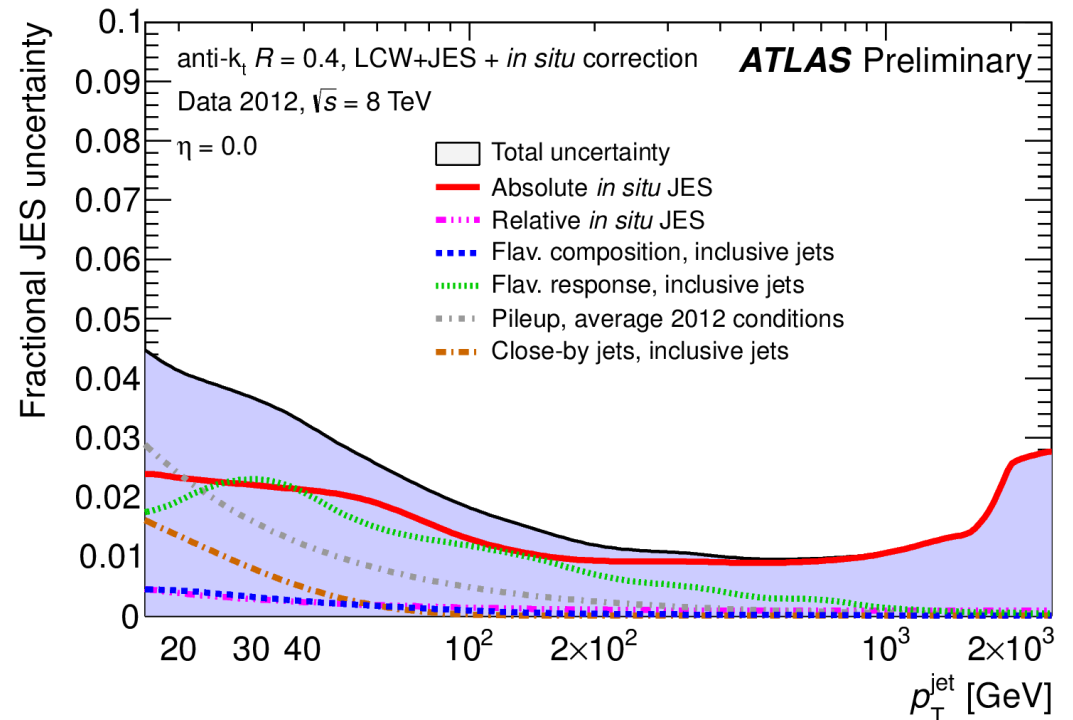
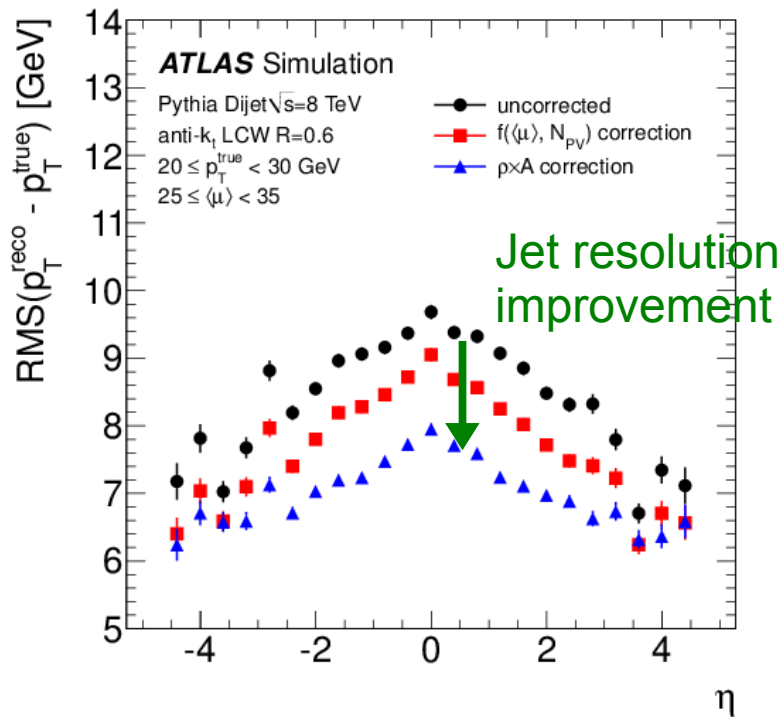
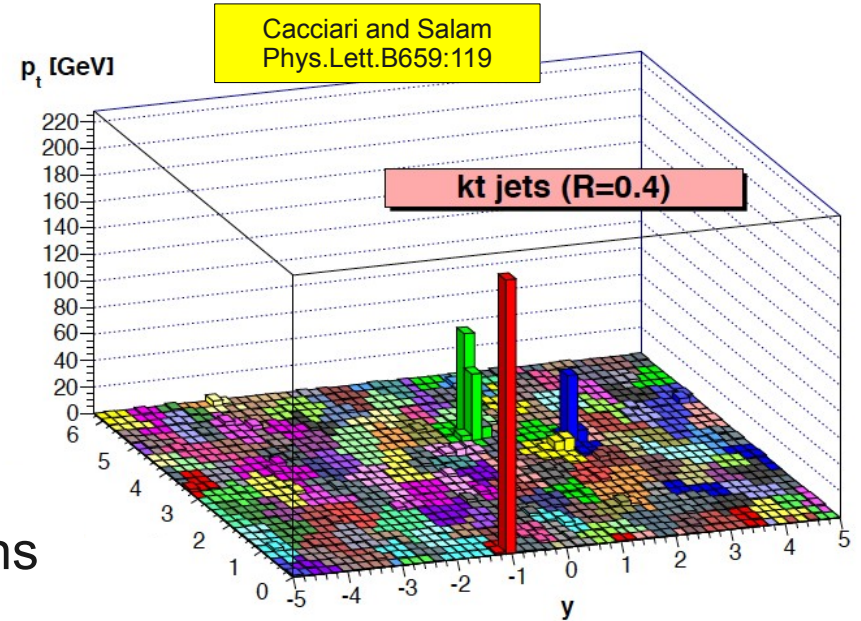
Pileup Subtraction in Jets

Subtract pileup contribution based on jet area, event-by-event:

$$p_T^{\text{jet,corr}} = p_T^{\text{jet}} - \rho \times A_T^{\text{jet}}$$

Residual correction to compensate for noise suppression, occupancy and out-of-time pileup

- Reduces event-by-event pileup fluctuations
Improved jet energy resolution
- Reduced reliance on MC for pileup corrections
Smaller systematic uncertainty



p+Pb

Recorded p+Pb Data

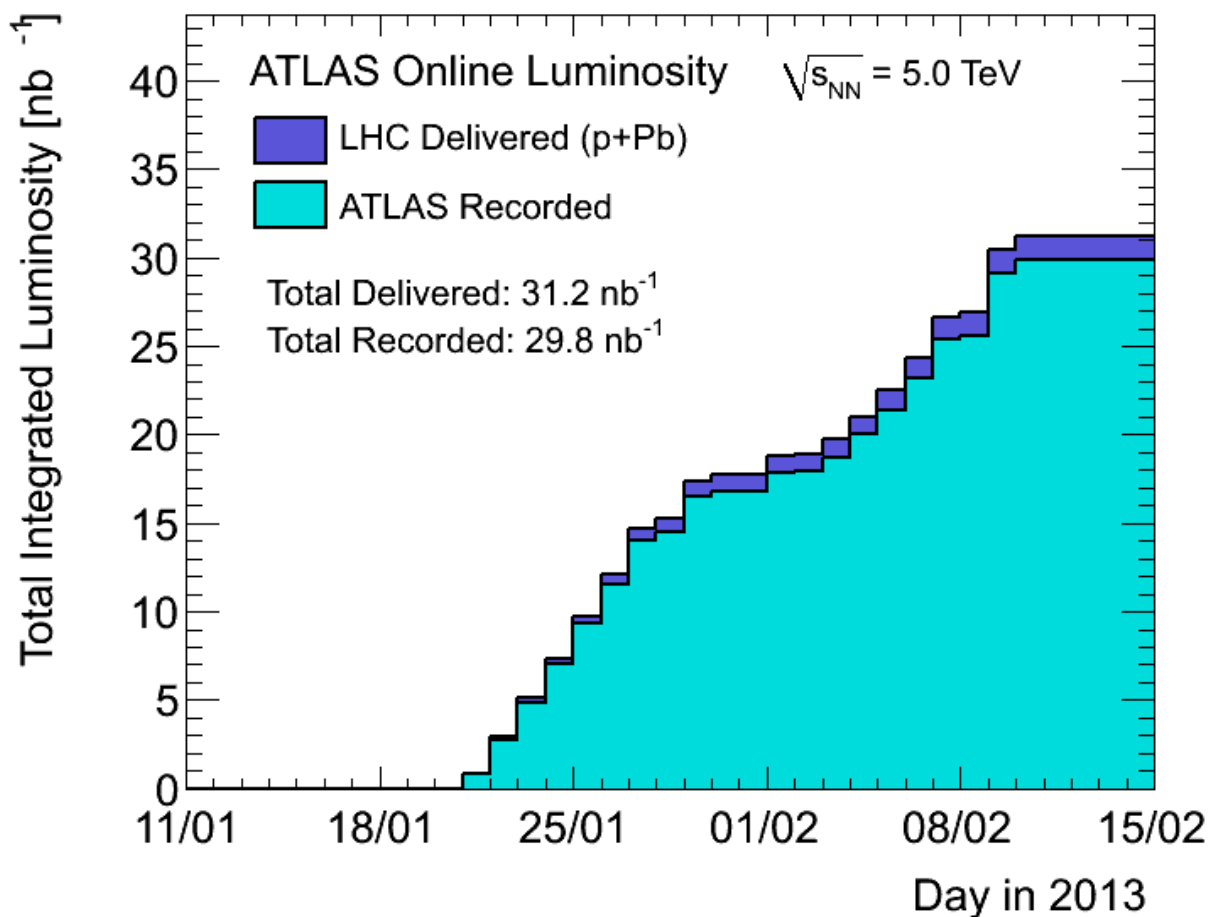
Short, but successful p+Pb run $\sqrt{s_{NN}}=5$ TeV in early 2013

Peak luminosity:
 $1.12 \times 10^{29} \text{ cm}^{-2} \text{ s}^{-1}$

Best fill: 1.9 nb^{-1}

Data-taking
efficiency: 95.5%

Also recorded
 4.4 pb^{-1} out of 5.5 pb^{-1}
pp data at $\sqrt{s}=2.76$ TeV



Van der Meer scans done for both samples
to allow precise determination of luminosity

Recorded p+Pb Data

Short, but successful p+Pb run $\sqrt{s_{NN}}=5$ TeV in early 2013

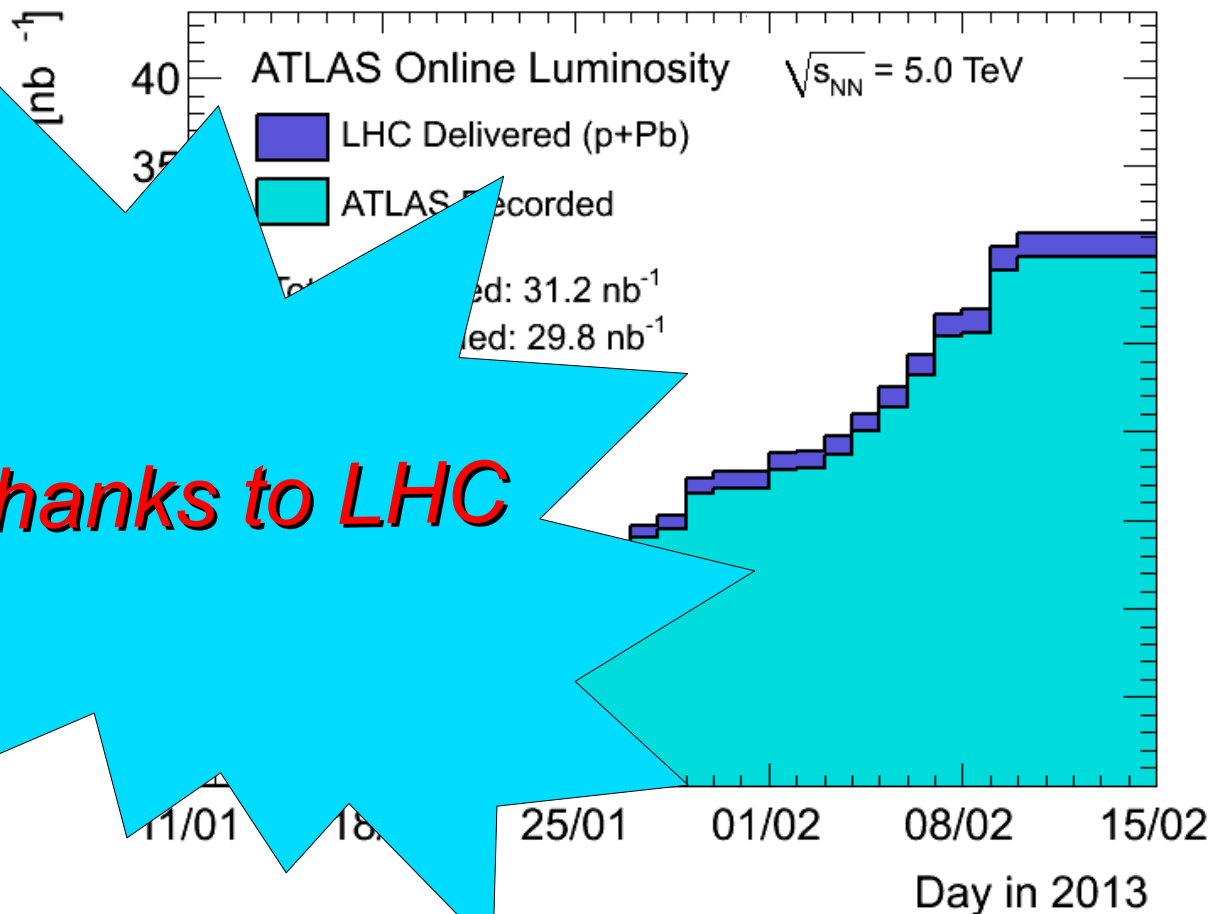
Peak luminosity:
 $1.12 \times 10^{29} \text{ cm}^{-2} \text{ s}^{-1}$

Best fill: 1.9 nb^{-1}

Data-taking
efficiency: 95.5%

Also recorded
 4.4 pb^{-1} out of 5.5 pb^{-1}
pp data at $\sqrt{s}=2.76$ TeV

Thanks to LHC



Van der Meer scans done for both samples
to allow precise determination of luminosity

p+Pb Data

ATLAS p-Pb run: January-February 2013

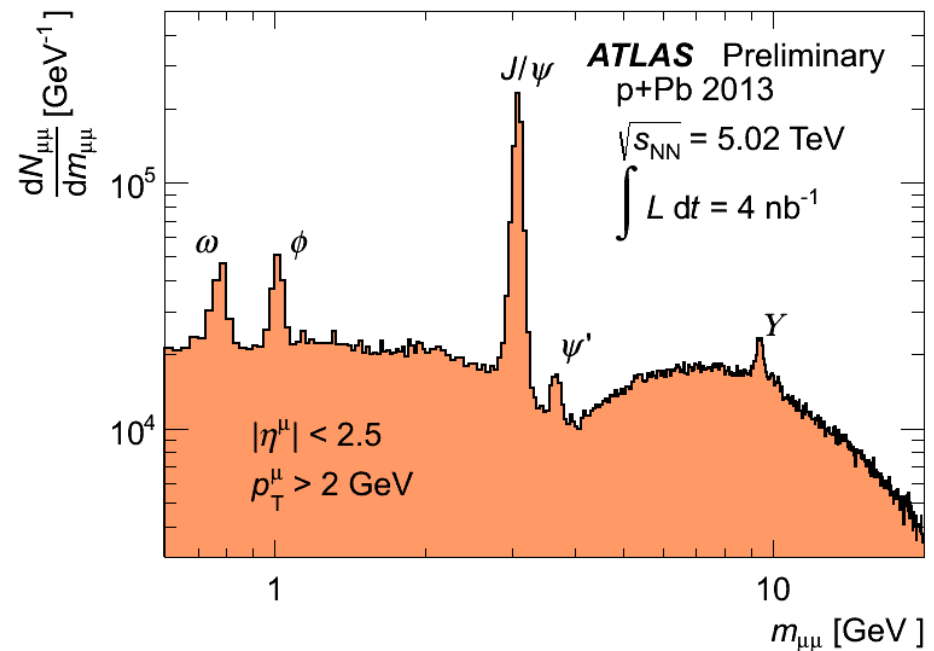
Inner Tracker			Calorimeters		Muon Spectrometer				Magnets	
Pixel	SCT	TRT	LAr	Tile	MDT	RPC	CSC	TGC	Solenoid	Toroid
98.6	99.7	99.9	98.6	99.1	100.	100.	91.9	99.6	100.	100.

All good for physics: 86.9%

Good for physics without CSC requirement: 94.8%

Luminosity weighted relative detector uptime and good quality data delivery during 2013 stable beams in p-Pb collisions at $\sqrt{s_{NN}}=5$ TeV between January 20th and February 10th (in %) – corresponding to 29.9 nb⁻¹ of recorded data.

Analysis of 2013
p+Pb data underway

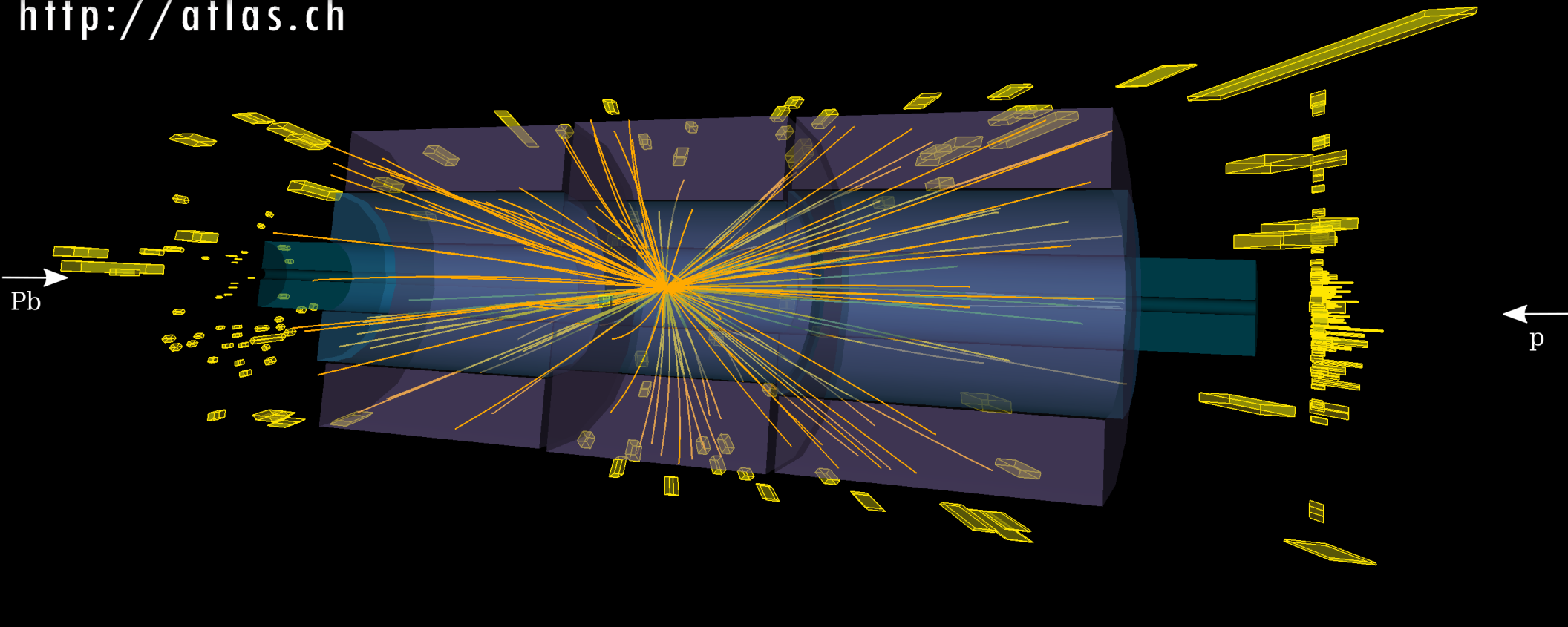


High Track Multiplicity Event



High multiplicity p+Pb event

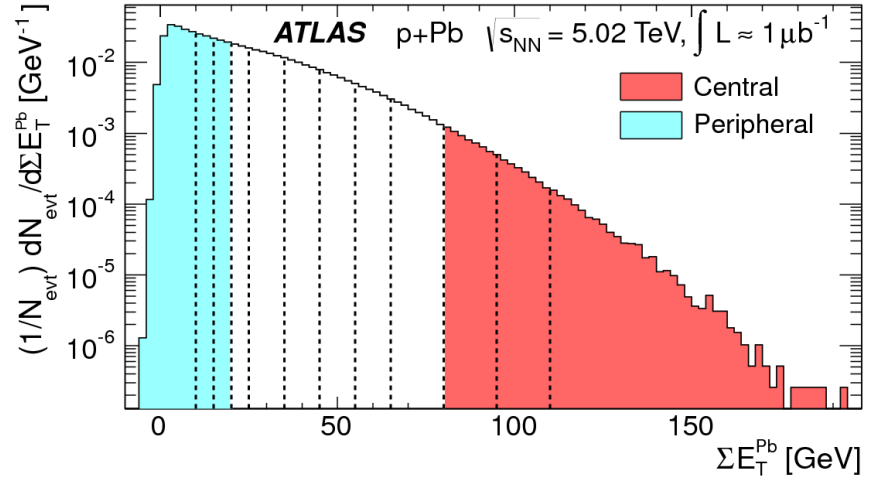
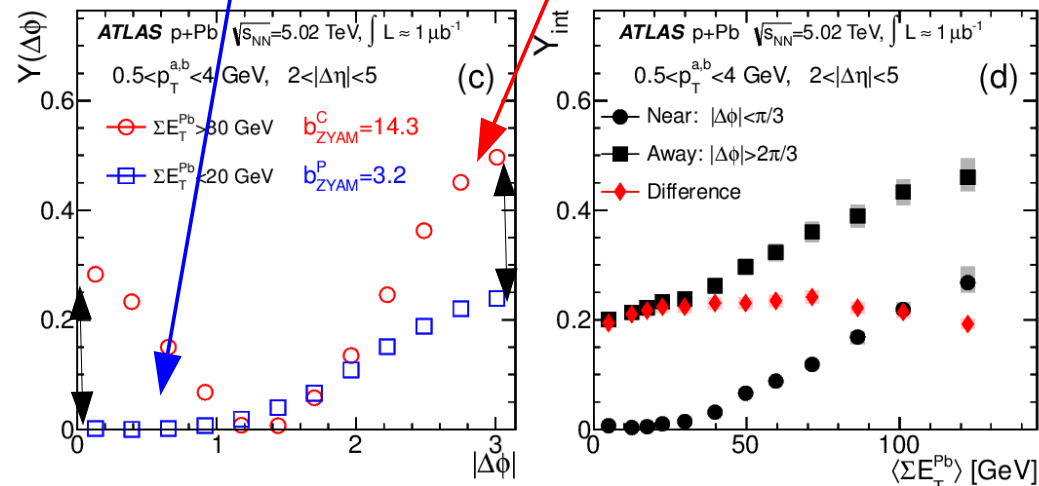
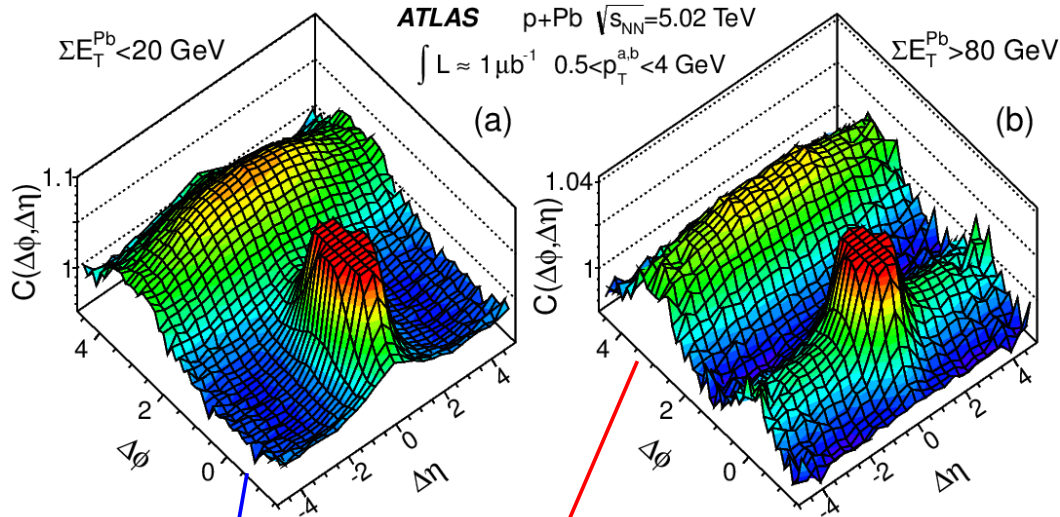
Run: 217946 $N_{\text{Trk}}(p_T > 0.4 \text{ GeV}) = 273,$
Event: 32291041 $N_{\text{Trk}}(p_T > 1.0 \text{ GeV}) = 106$ (shown)
Date: 2013-01-20 FCal A (Pb going side) $\Sigma E_T = 139 \text{ GeV}$



Two Particle Correlations in p+Pb

Study two particle correlations in 2012 p+Pb pilot run ($1 \mu\text{b}^{-1}$)

- Confirm near-side ridge in high-mult. pPb events first reported by CMS



Split events by centrality measured by forward energy

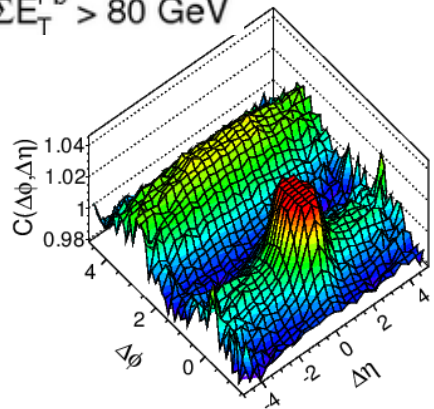
Define “per-trigger yield”
~ number of correlated particles

$$Y(\Delta\phi) = \left(\frac{\int B(\Delta\phi) d\Delta\phi}{\pi N_a} \right) C(\Delta\phi) - b_{ZYAM}$$

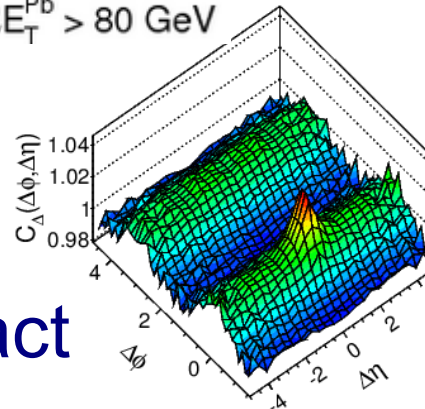
Difference between yield on near-side ($\Delta\phi \sim 0$) and far-side ($\Delta\phi \sim \pi$) almost independent of ΣE_T

Subtraction of Recoil Contribution

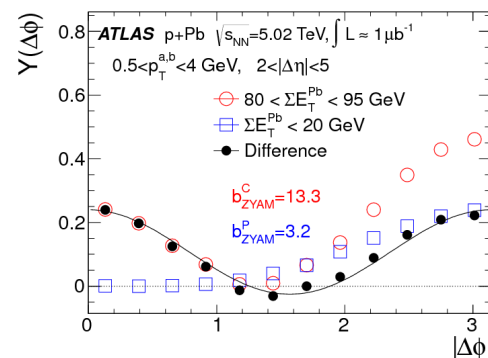
$\Sigma E_T^{Pb} > 80 \text{ GeV}$



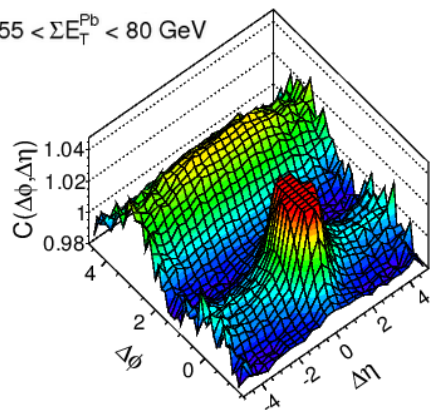
$\Sigma E_T^{Pb} > 80 \text{ GeV}$



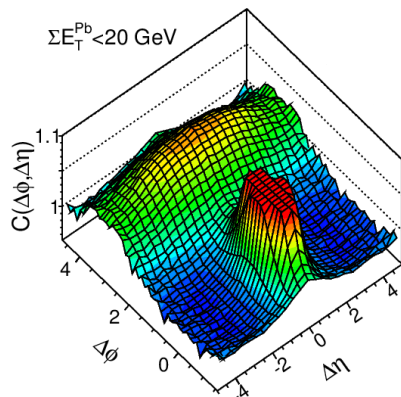
Use peripheral collisions to subtract recoil contribution



$55 < \Sigma E_T^{Pb} < 80 \text{ GeV}$

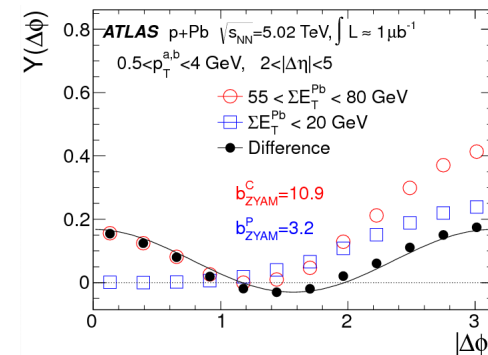
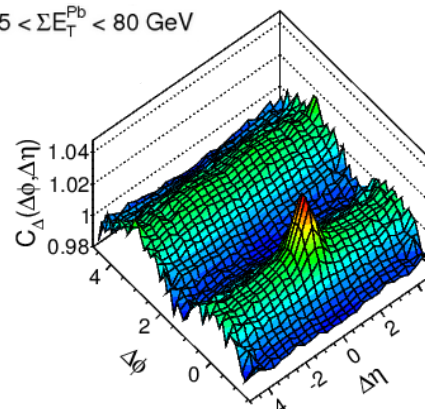


$\Sigma E_T^{Pb} < 20 \text{ GeV}$

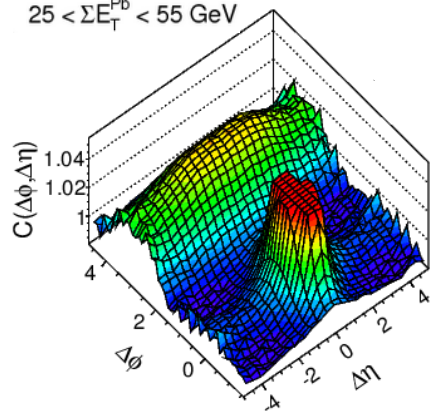


=

$55 < \Sigma E_T^{Pb} < 80 \text{ GeV}$

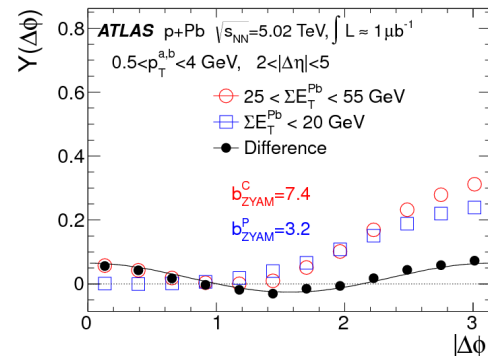
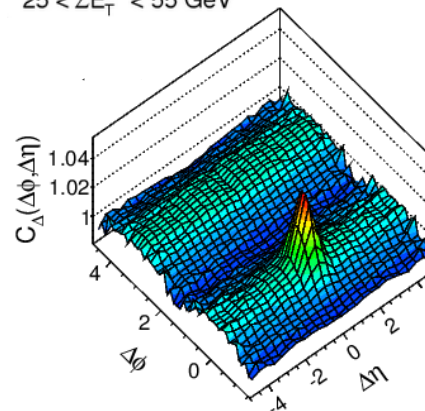


$25 < \Sigma E_T^{Pb} < 55 \text{ GeV}$

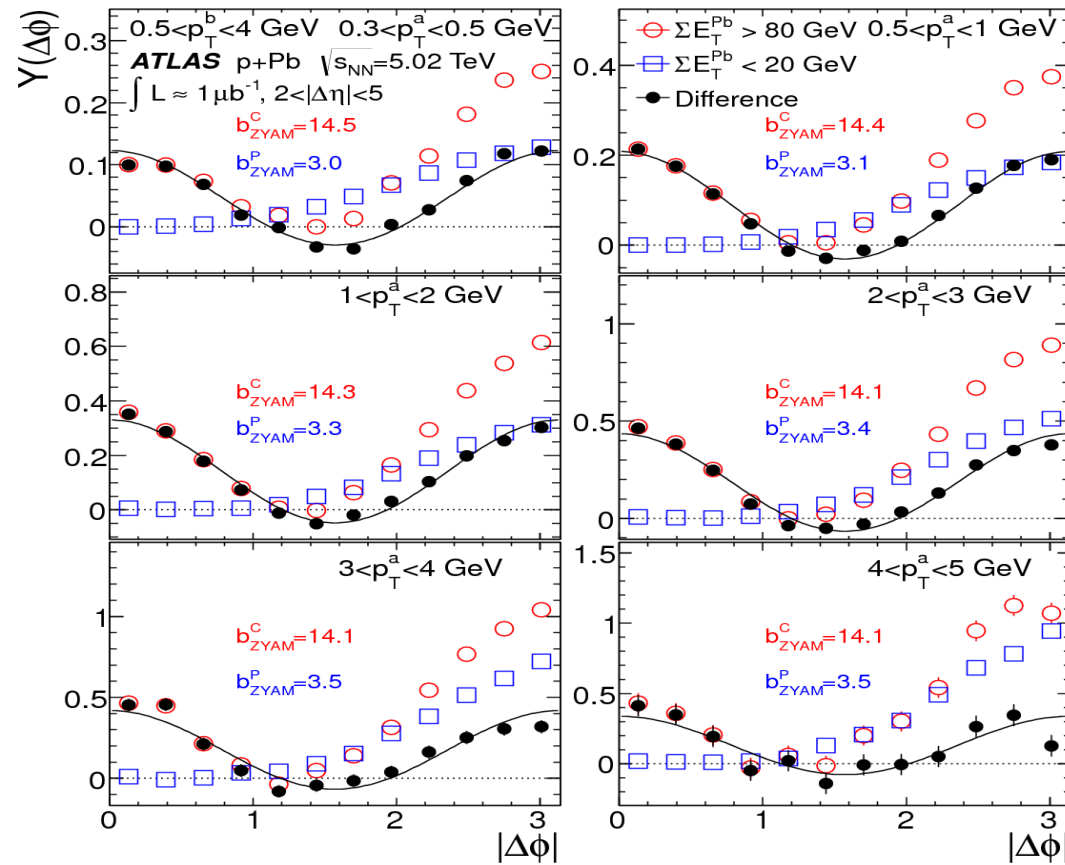


Reveals $\cos(2\Delta\phi)$ contribution in central collisions

$25 < \Sigma E_T^{Pb} < 55 \text{ GeV}$



Two Particle Correlations in p+Pb



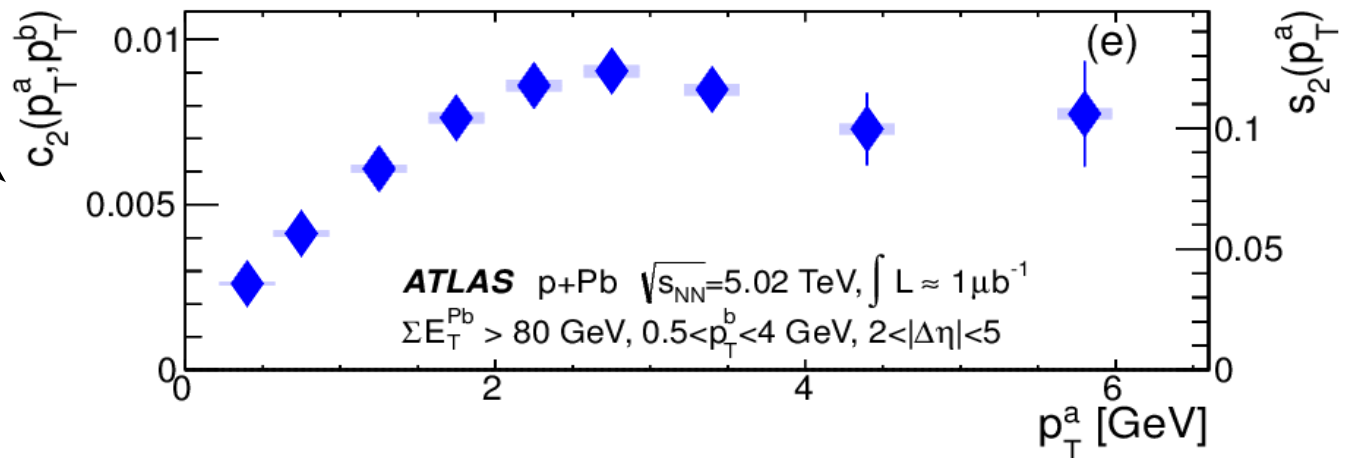
$\cos(2\Delta\phi)$ modulation seen for all values of track p_T

Behavior very similar to those measured in PbPb

Suggest flow-like effects in high-multiplicity collisions

Confirmed in analysis using four-particle cumulants

Extract normalized $\cos(2\Delta\phi)$ amplitude



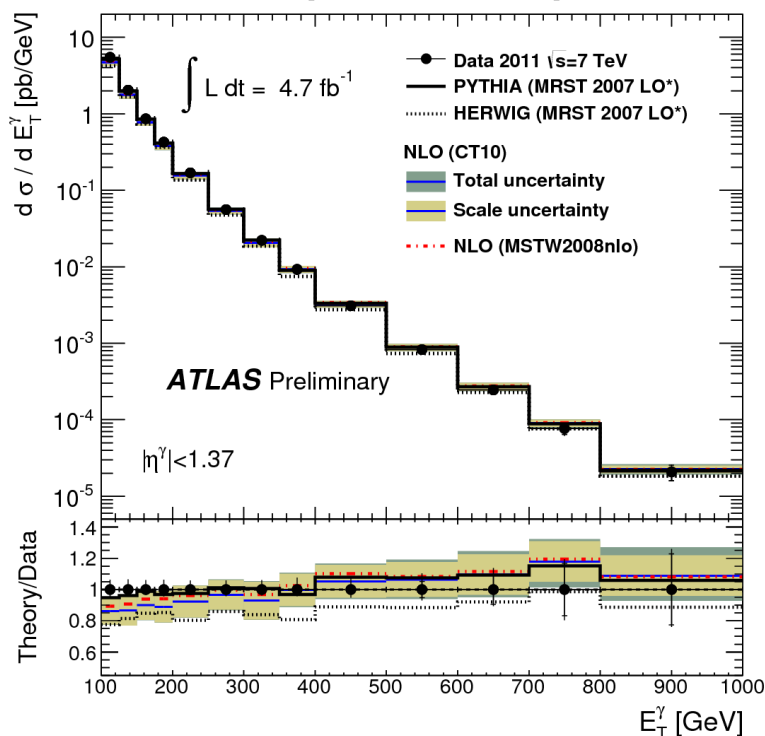
Standard Model Measurements

Standard Model Measurements

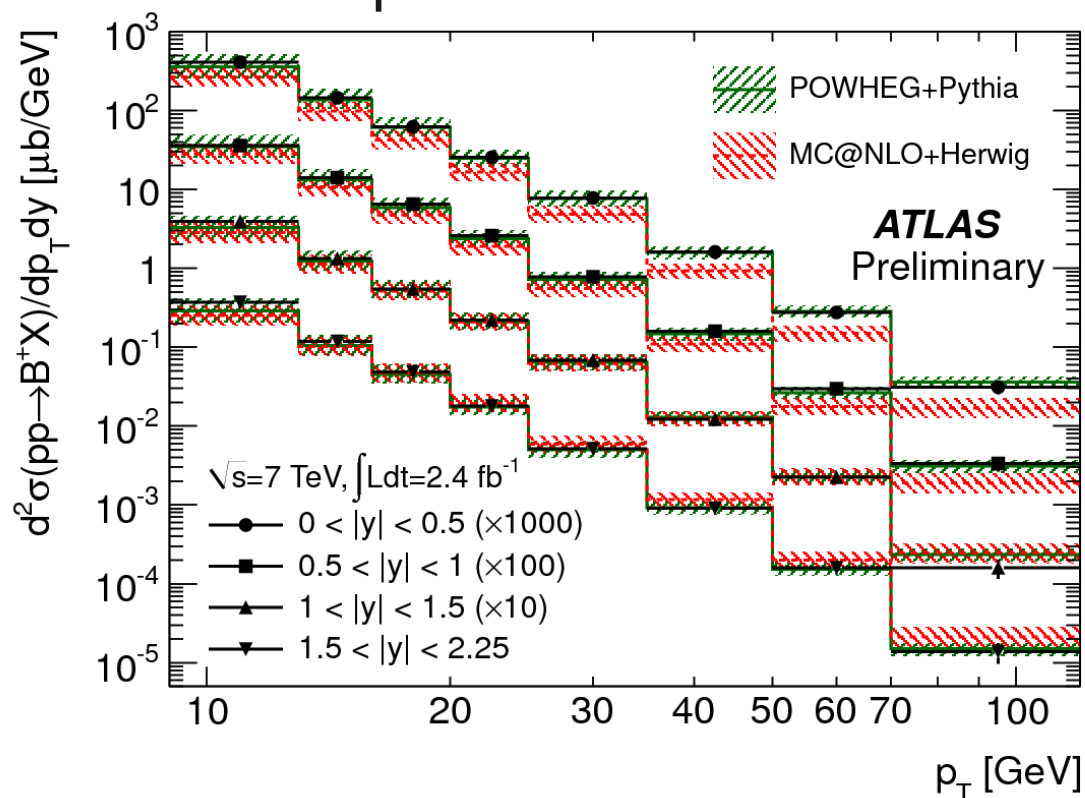
Wide range of precision measurements using high-statistics samples

- Tests (perturbative) QCD predictions
- Validity of MC generators
- Constrain parton distribution functions
- ...

Inclusive photon spectrum



B^+ production

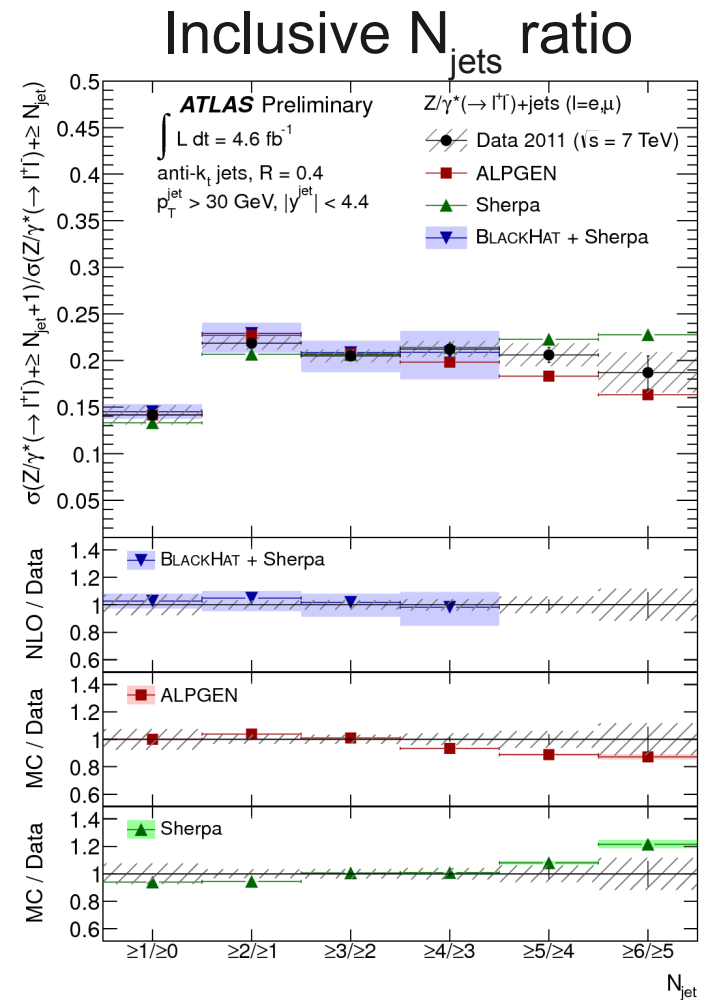
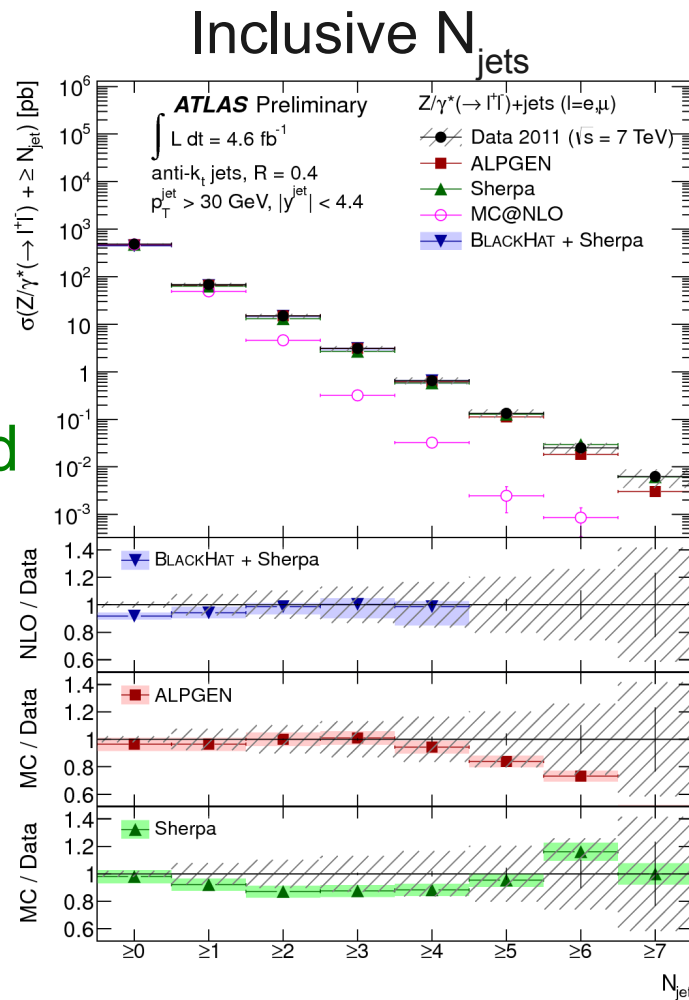


Study of Z+Jets Production

Detailed measurements of jets in association with Z

- Study jets up to $p_T=500$ GeV, $|y|<4.4$ and more than 7 jets
- Unfold distributions to particle level for comparison to MC and NLO calculations
- Multiple measurements for cross sections for jet p_T , rapidity, multiplicities, etc.
- Also measurements with asymmetric jet p_T selections and VBF-like selection

Generally observe good agreement between data and MC generators and NLO calculations

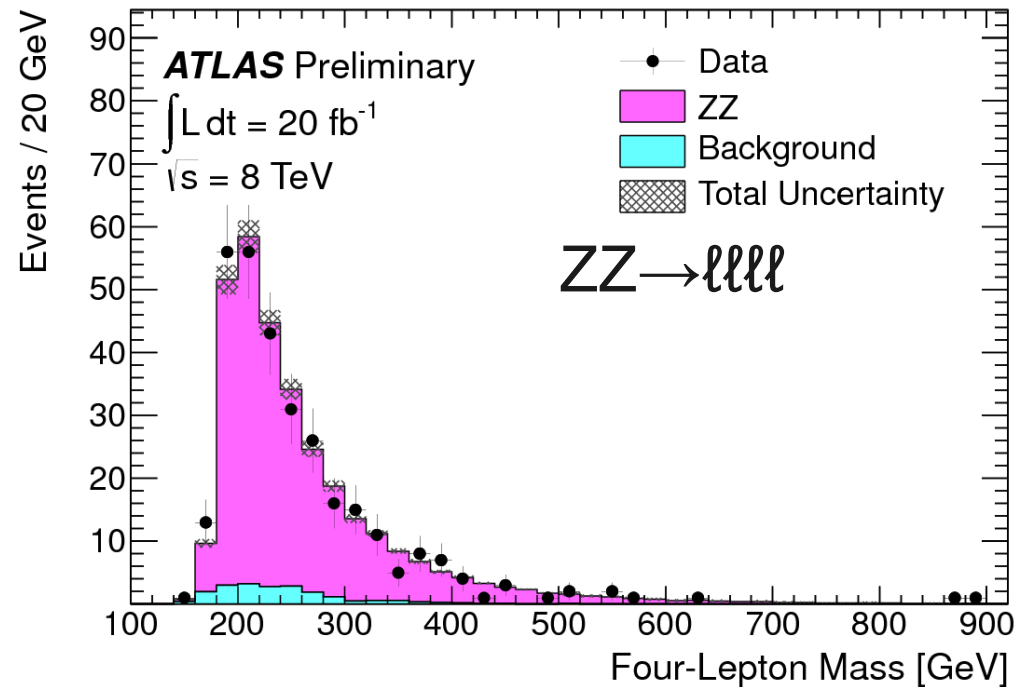
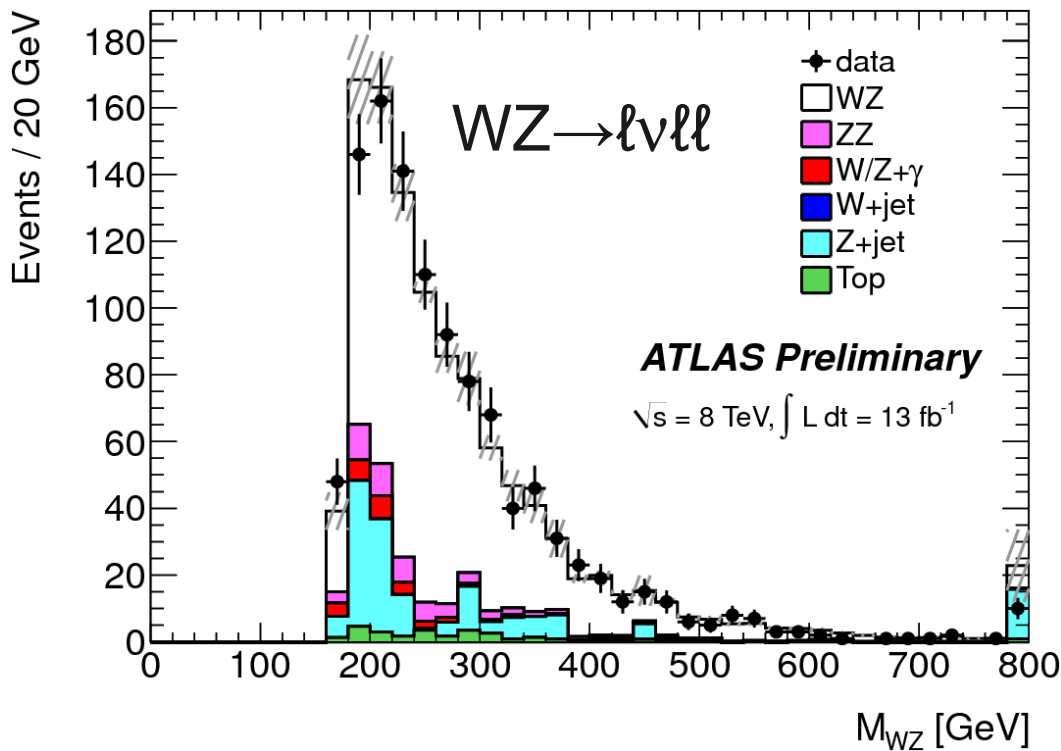
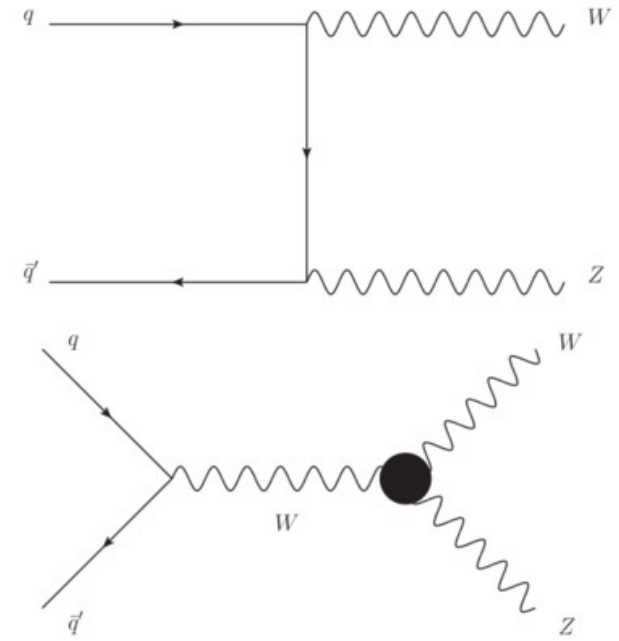


Diboson Cross Sections

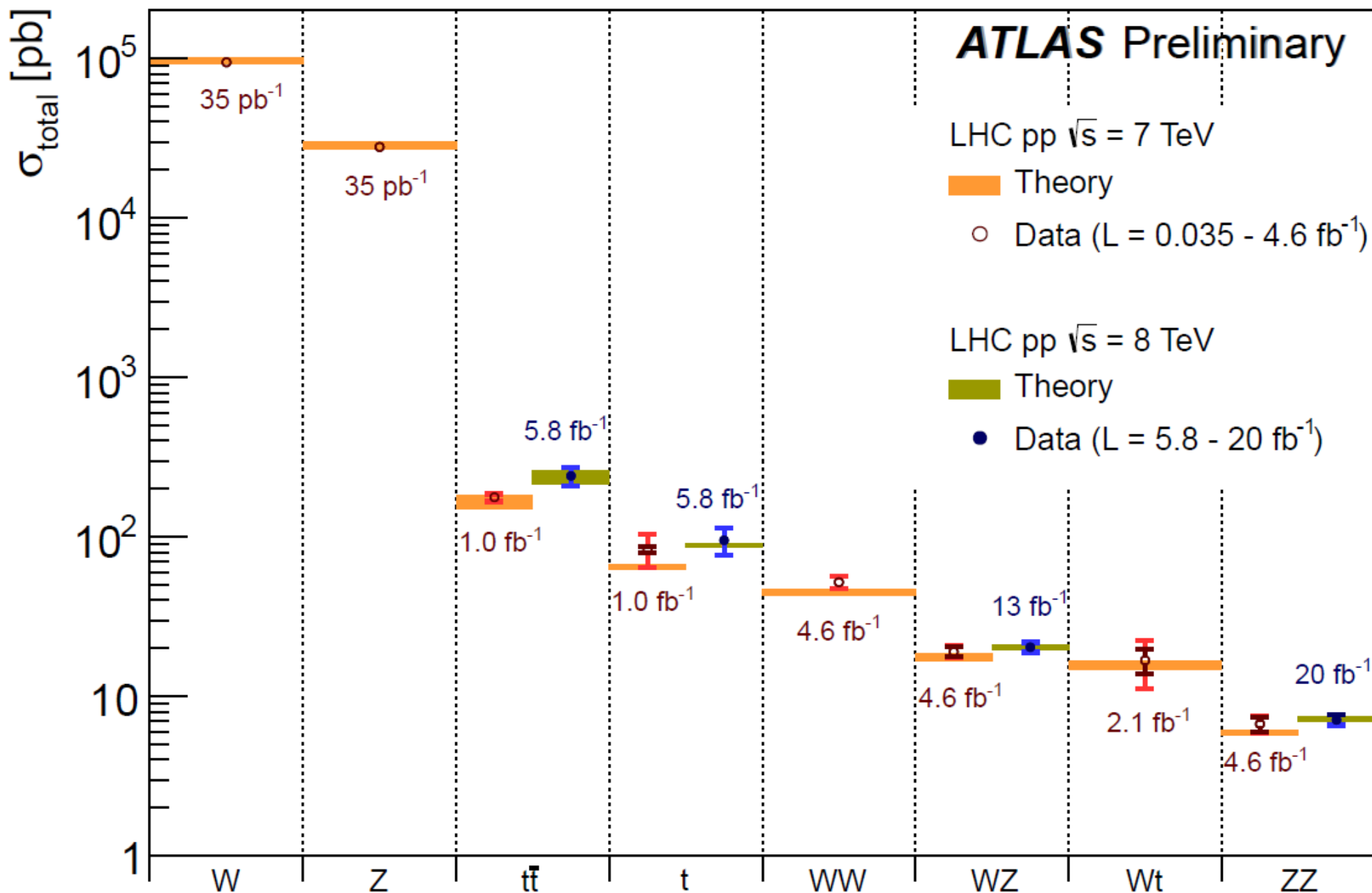
Updated WZ and ZZ measurements

- Tests SM electroweak predictions
- Important background for Higgs and many new physics searches

Measured cross sections are in excellent agreement with NLO predictions (next slide)



Summary of EW and top Cross Sections



The New Boson

H \rightarrow $\gamma\gamma$

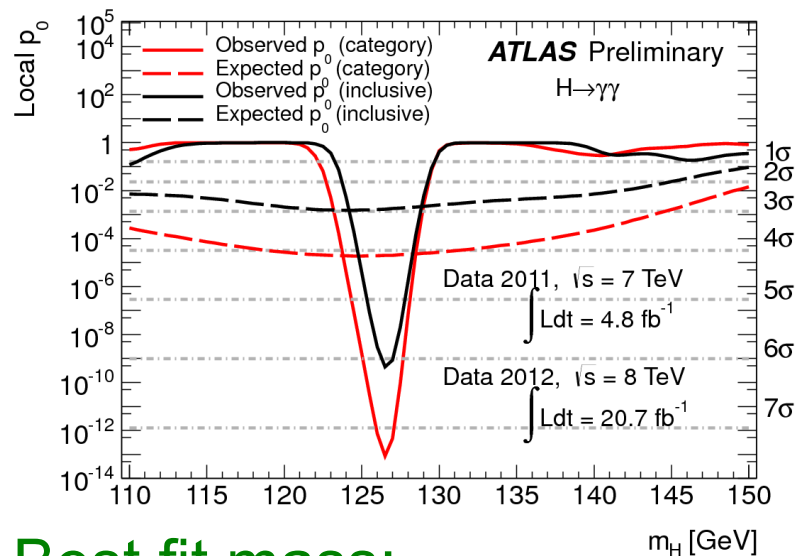
Updated to full 2011+2012 data sets

Re-optimized event categorization to improve coupling measurements

- New categories for associated production
- Multi-variate selection for VBF categories

Observed significance: 7.4σ

(Expected: 4.1σ for SM Higgs)



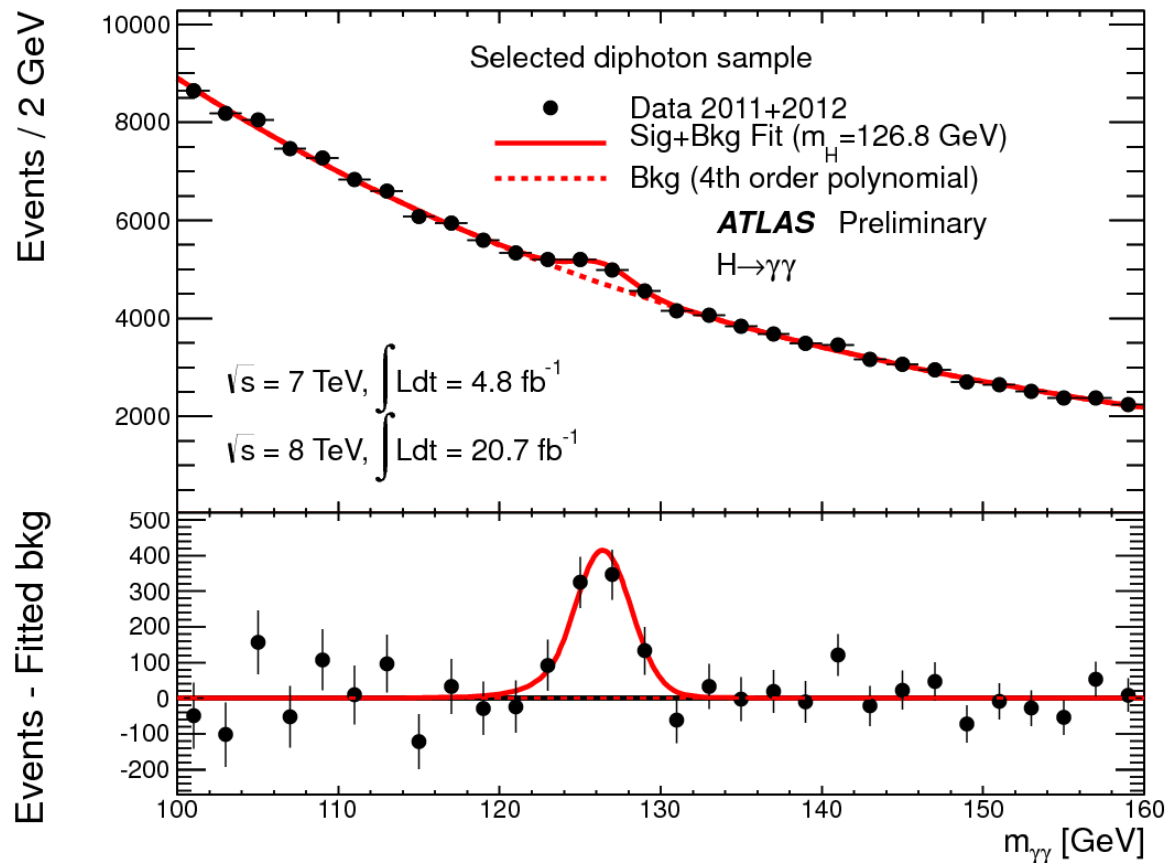
Best fit mass:

$126.8 \pm 0.2(\text{stat}) \pm 0.7(\text{syst}) \text{ GeV}$

Signal strength:

$\mu = 1.65 \pm 0.24(\text{stat})_{-0.18}^{+0.25}(\text{syst})$ (2.3σ above SM Higgs prediction)

Fiducial cross section: $\sigma_{\text{fid}} \times BR = 56.2 \pm 10.5(\text{stat}) \pm 6.5(\text{syst}) \pm 2.0(\text{lumi}) \text{ fb}$



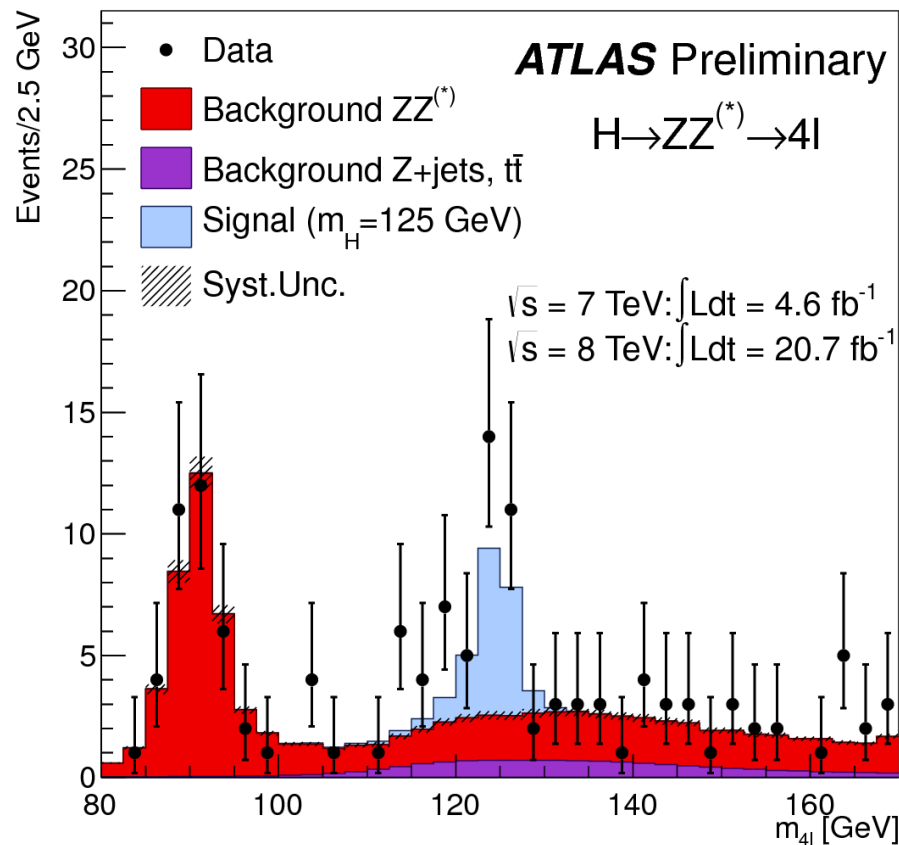
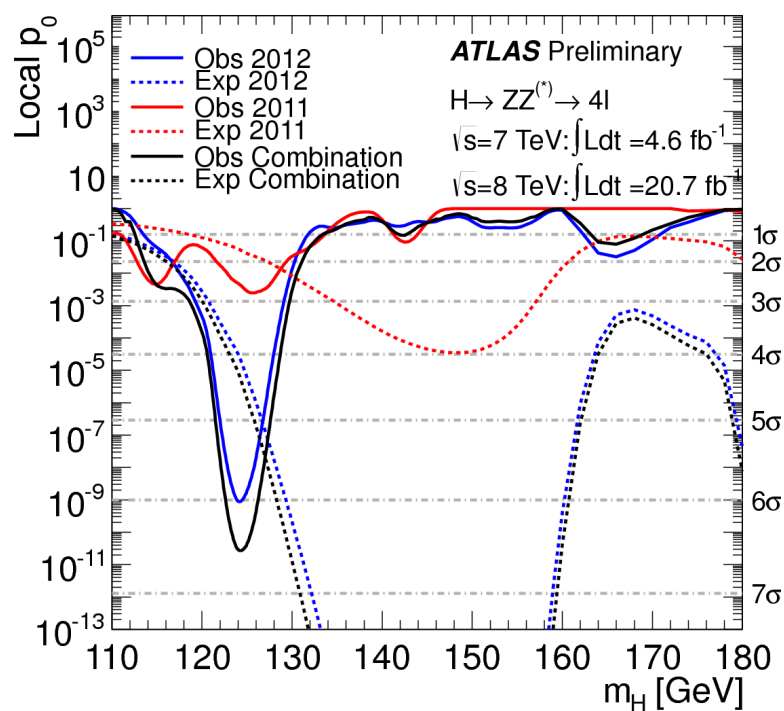
H → ZZ

Analysis reoptimized for full 2011+2012 data set

- Tighter electron identification for low mass ee pair
- Improved mass-pairing and lower mass cut
- Z mass constraint and new FSR recovery procedure

Observed significance: 6.6σ

(Expected: 4.4σ for SM Higgs)



Best fit mass: $124.3^{+0.6}_{-0.5} \text{ (stat)}^{+0.5}_{-0.3} \text{ (syst) GeV}$

Signal strength: $\mu = 1.7^{+0.5}_{-0.4}$

Combined Boson Mass

Combined mass measurements with profile likelihood

- $\mu_{\gamma\gamma}$ and $\mu_{4\ell}$ treated independently
- Common e/ γ energy scale shifts $m_{\gamma\gamma}$ down by 350 MeV

Combined mass fit:

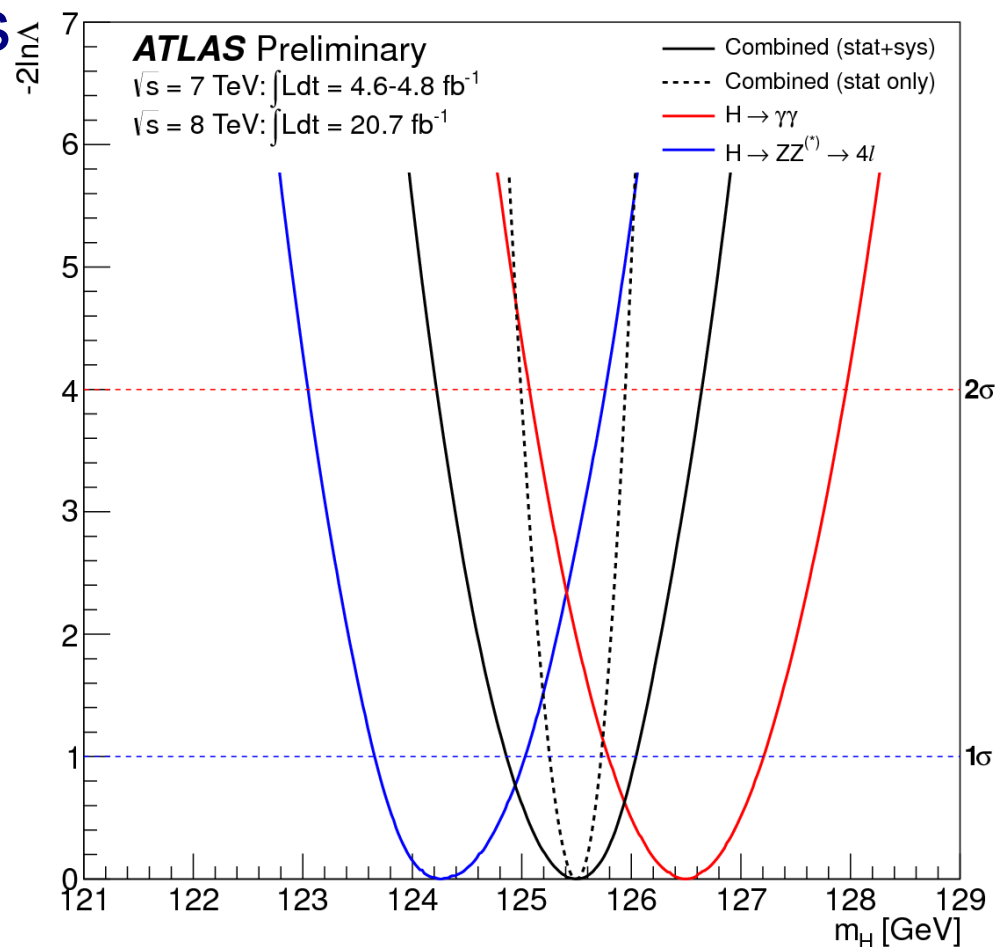
$$m_H = 125.5 \pm 0.2 \text{ (stat)}^{+0.5}_{-0.6} \text{ (sys)} \text{ GeV}$$

Difference between the two measured masses:

$$\Delta\hat{m}_H = \hat{m}_H^{\gamma\gamma} - \hat{m}_H^{4\ell} = 2.3^{+0.6}_{-0.7} \text{ (stat)} \pm 0.6 \text{ (sys)} \text{ GeV}$$

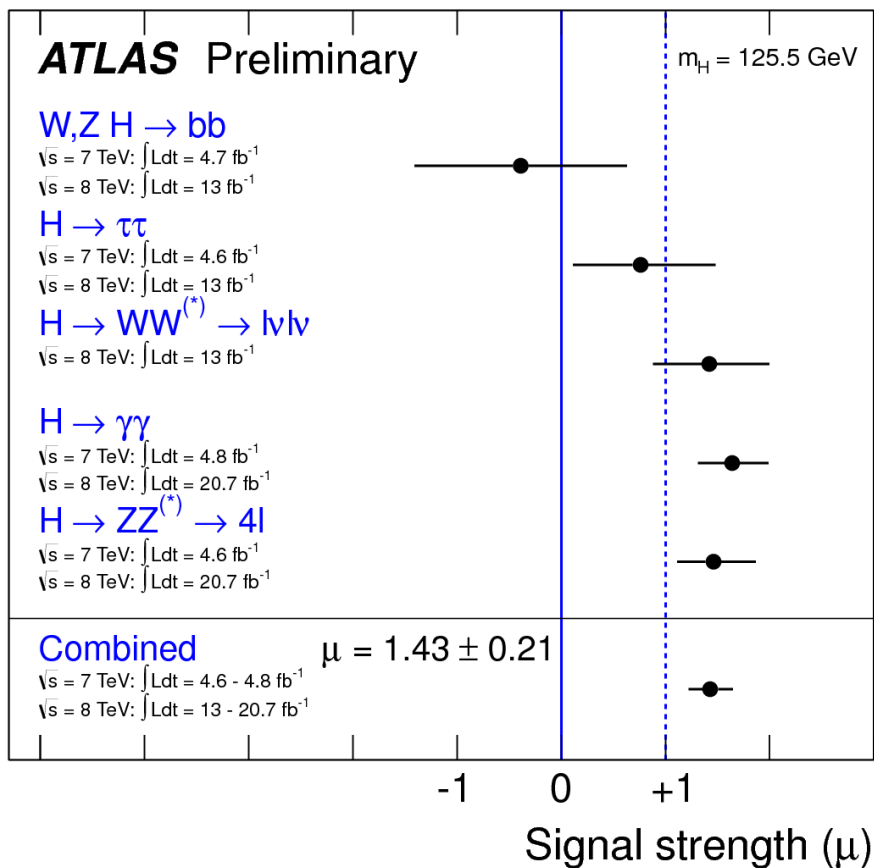
Consistency of mass measurements:

2.4 σ (was 2.8 σ in December)

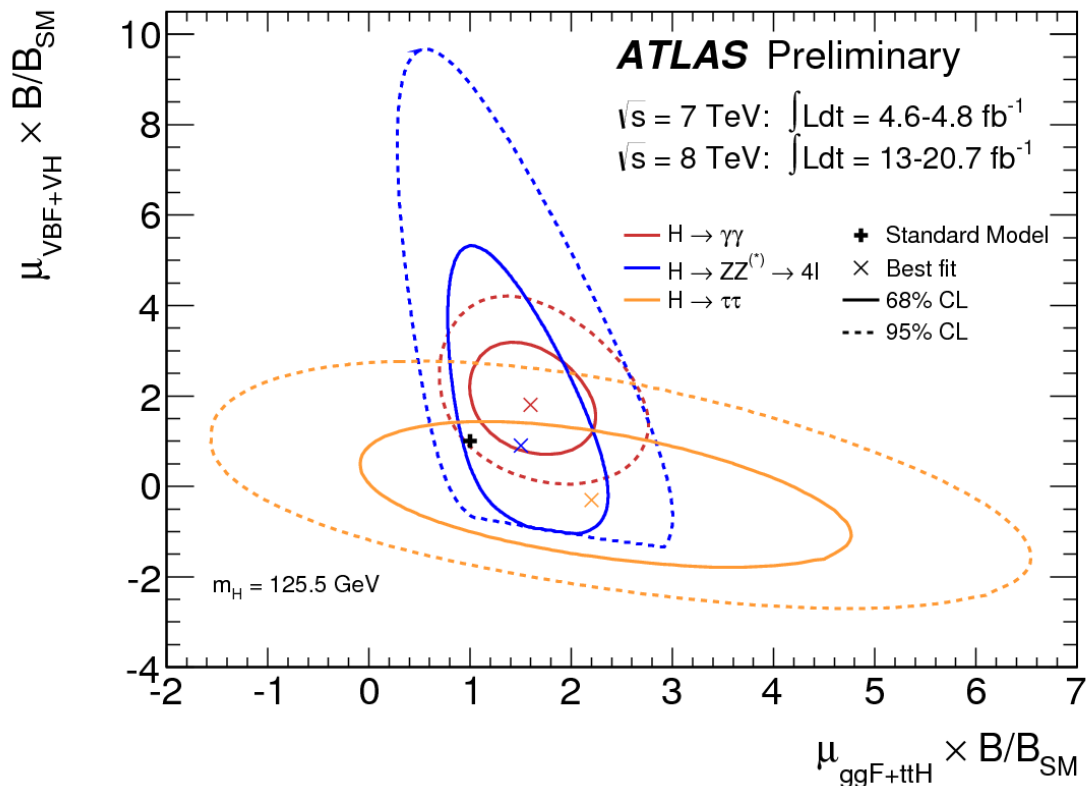


Signal Strengths and Couplings

Combine new $\gamma\gamma$ and ZZ results with previous 13(+5) fb⁻¹ results for global signal strength



Split by production mode



VBF signal in $\gamma\gamma$ at 2σ significance

Ratio: $\mu_{VBF+VH} / \mu_{ggF+ttH} = 0.9^{+0.7}_{-0.4}$

More detailed coupling results to be released in the next days

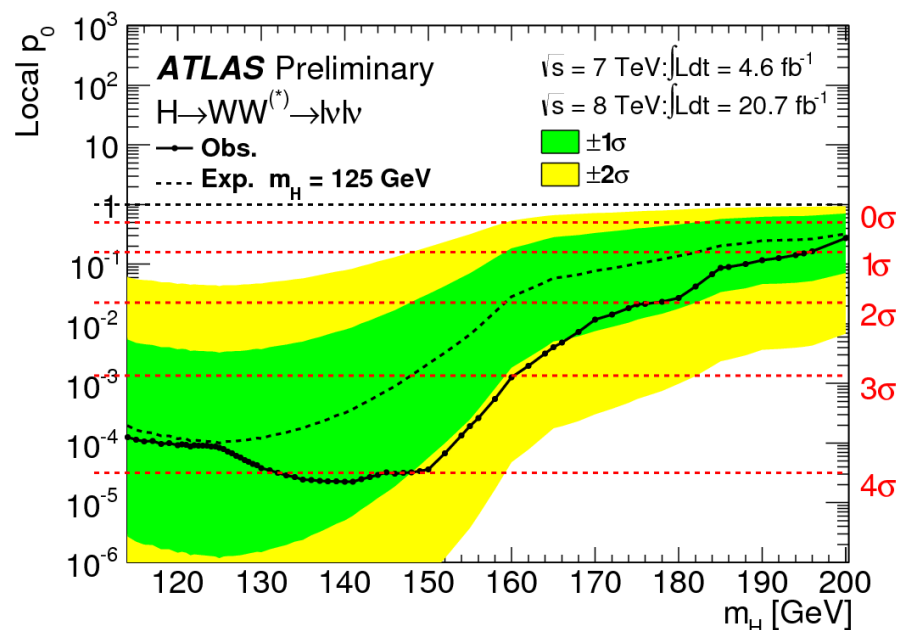
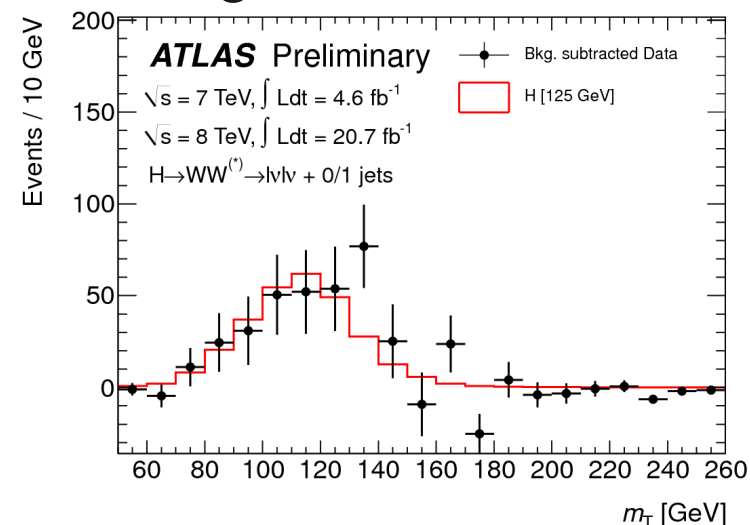
H → WW

Updated to full data sample Improved & expanded analysis

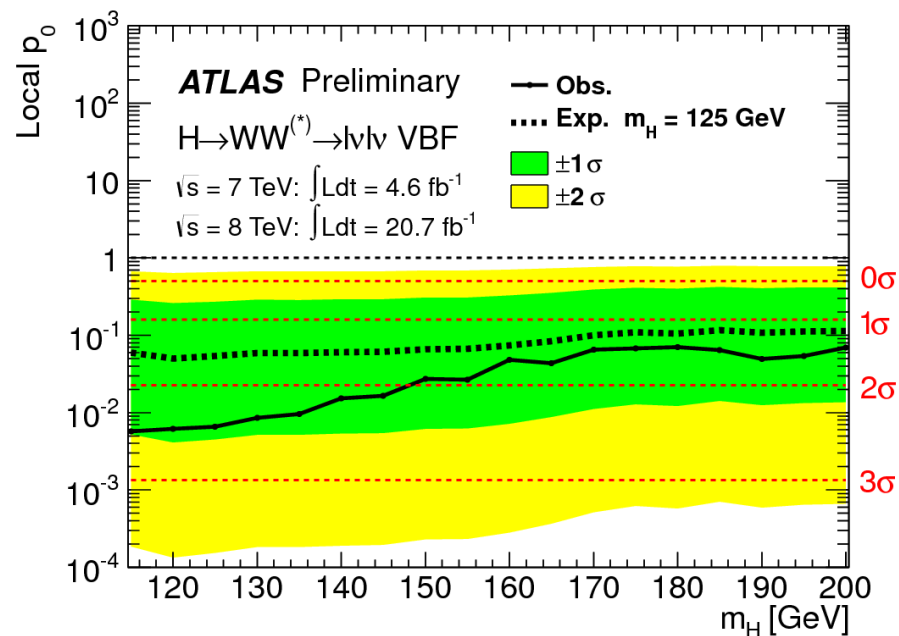
- Included same-flavor modes
- Added 2-jet category for VBF channel
- Optimized for $m_H = 125$ GeV

Observed Significance: 3.8σ
(Expected: 3.7σ for SM Higgs)

Background subtracted



Fitted signal strength:
 $\mu = 1.01 \pm 0.31$ for $m_H = 125$ GeV

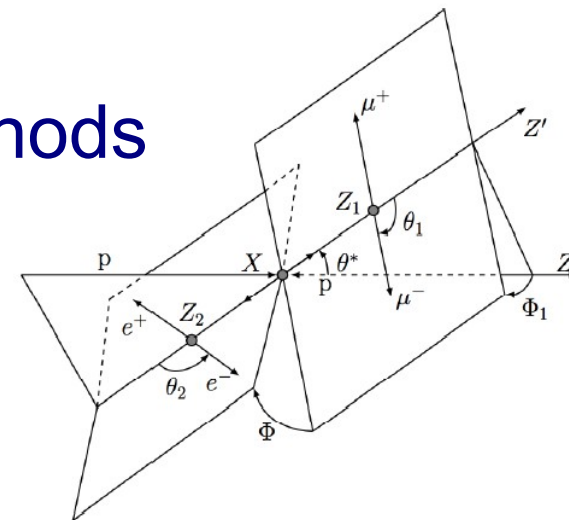


Obs. Significance for VBF: 2.5σ
(Expected: 1.6σ for SM Higgs)

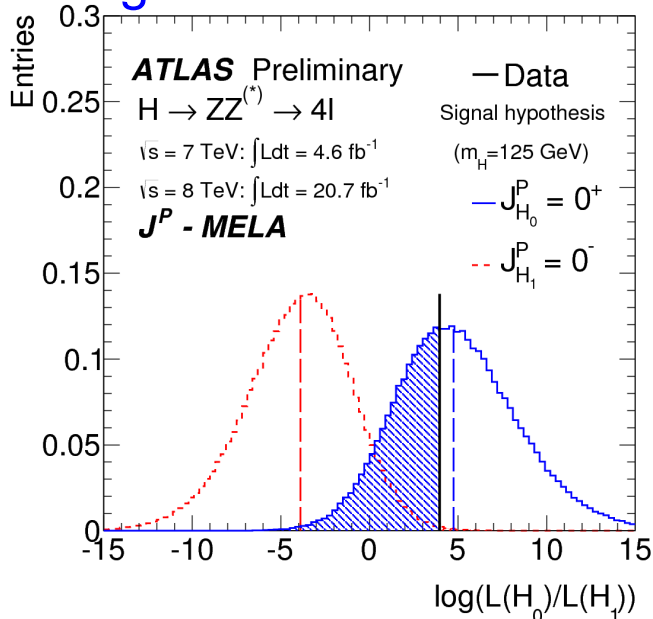
Spin and Parity in 4ℓ

Critical to establish J^P of the new boson
Compare J^P hypothesis in 4ℓ with two methods

- Boostered decision tree (BDT)
- Matrix element based likelihood ratio (MELA)
- Both use up to 5 decay angles and m_{12}, m_{34}
- For spin-2 hypothesis consider only graviton-like minimal coupling, but vary gg vs $q\bar{q}$ prod. fraction

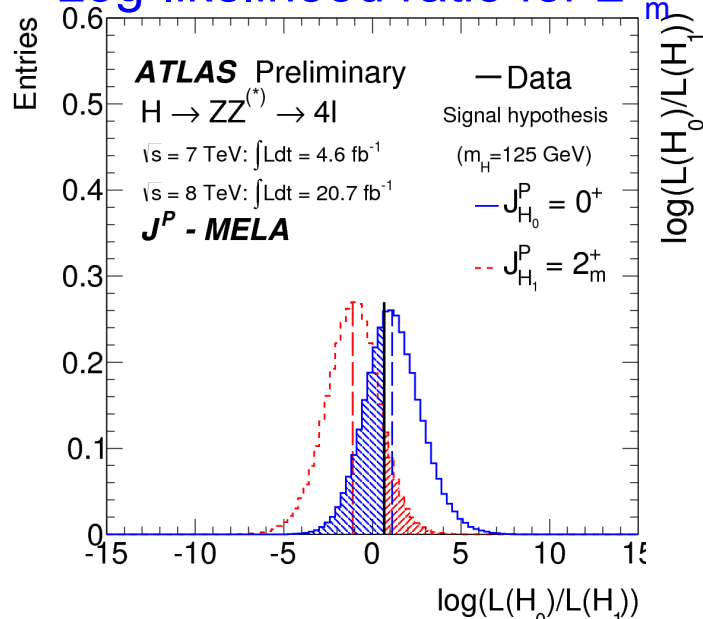


Log-likelihood ratio for 0^-



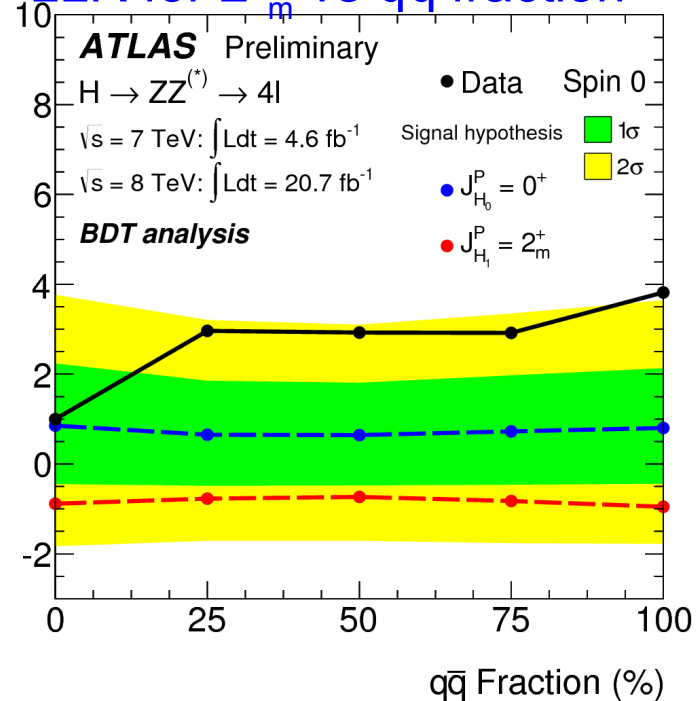
Disfavor $0^-, 1^+$ and 1^- hypotheses at $>2\sigma$

Log-likelihood ratio for 2^+



Inconclusive for spin-2 hypotheses

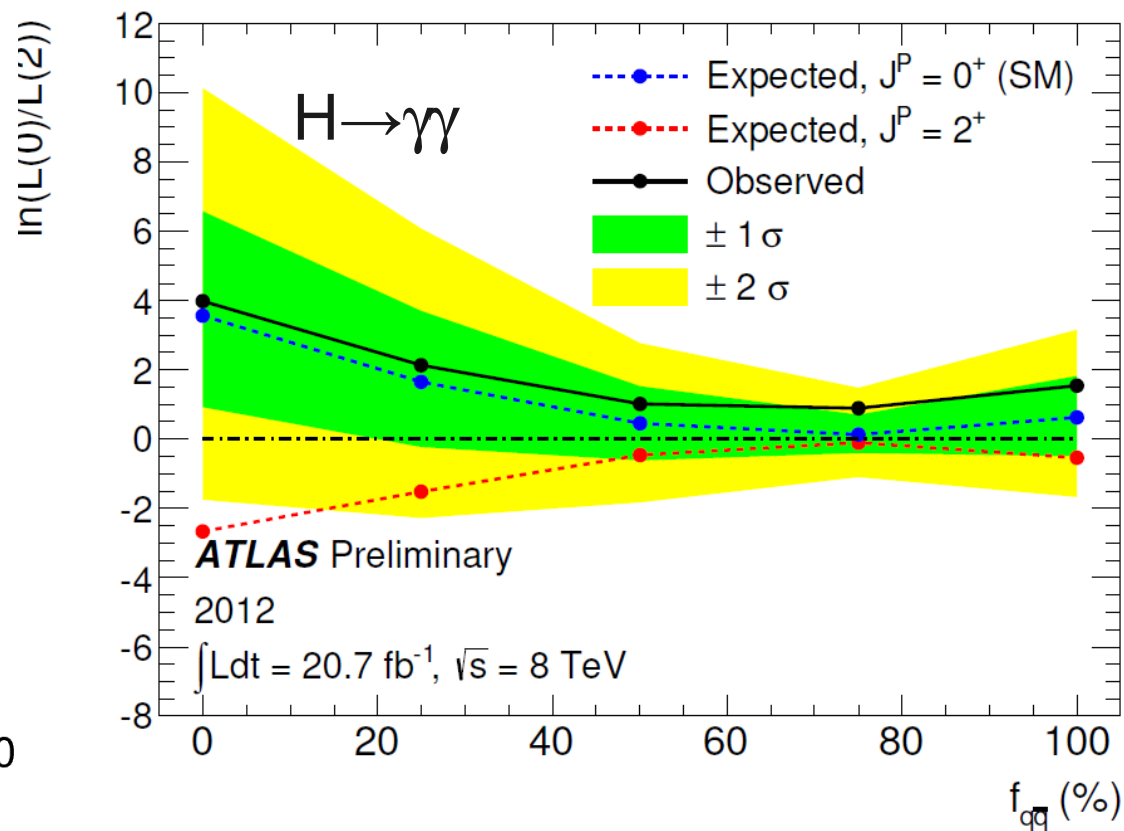
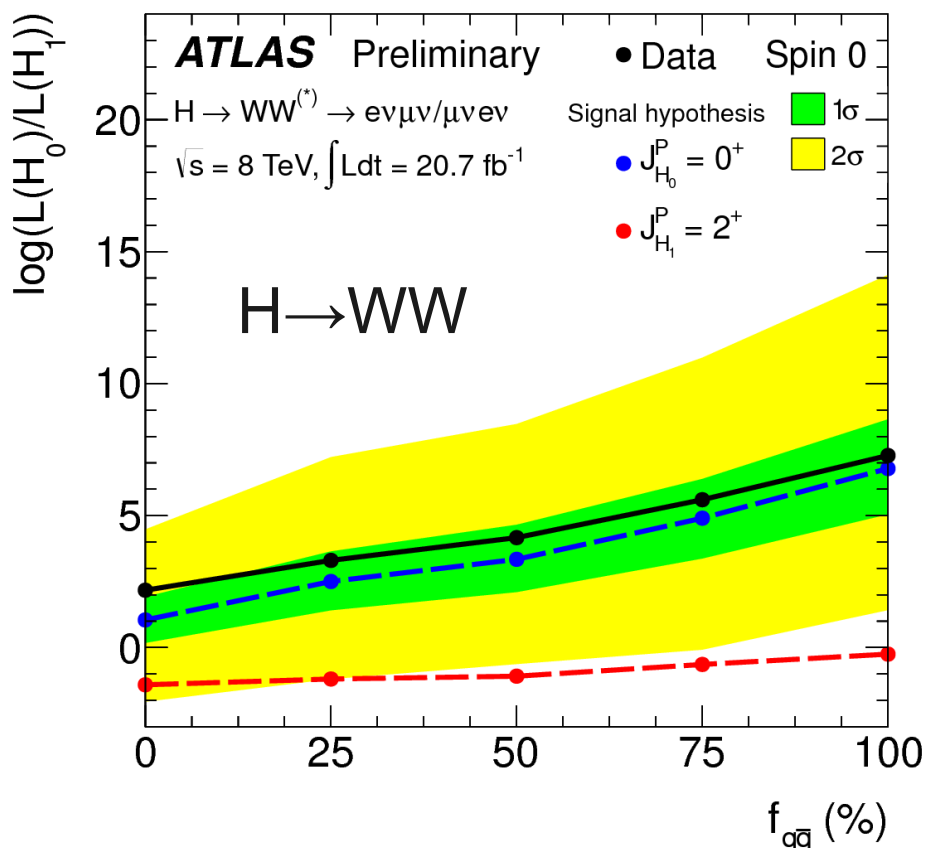
LLR for 2^+ vs $q\bar{q}$ fraction



Spin and Parity – $\gamma\gamma$ and WW

Also discriminate between spin 0 and 2 in $\gamma\gamma$ and WW

- In $\gamma\gamma$, use a fit to $|\cos\theta^*|$ distribution
- In WW, use BDT with inputs $m_{\ell\ell}$, $p_{T,\ell\ell}$, $\Delta\phi_{\ell\ell}$, and m_T
- For both analyses selection reoptimized – WW only uses $e\nu\mu\nu$ (0-jet)
- Testing only against minimal coupling scenario



Disfavor minimal coupling graviton-like spin-2 hypotheses at $>2\sigma$

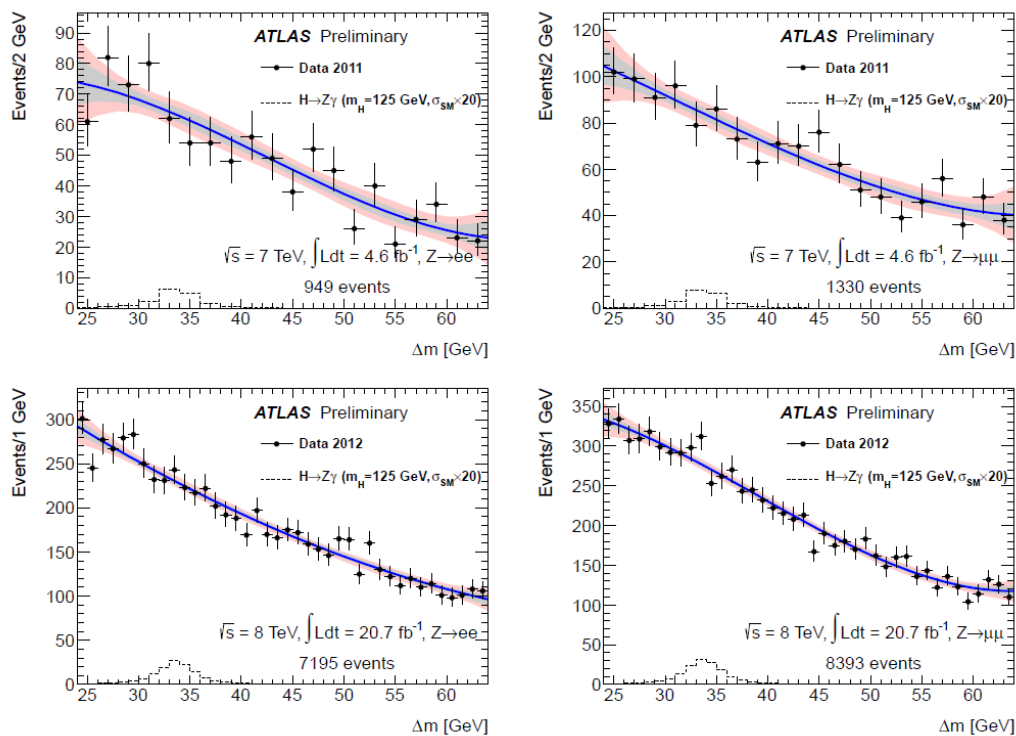
H \rightarrow Z γ Search

Possible new physics in rare/forbidden Higgs decays

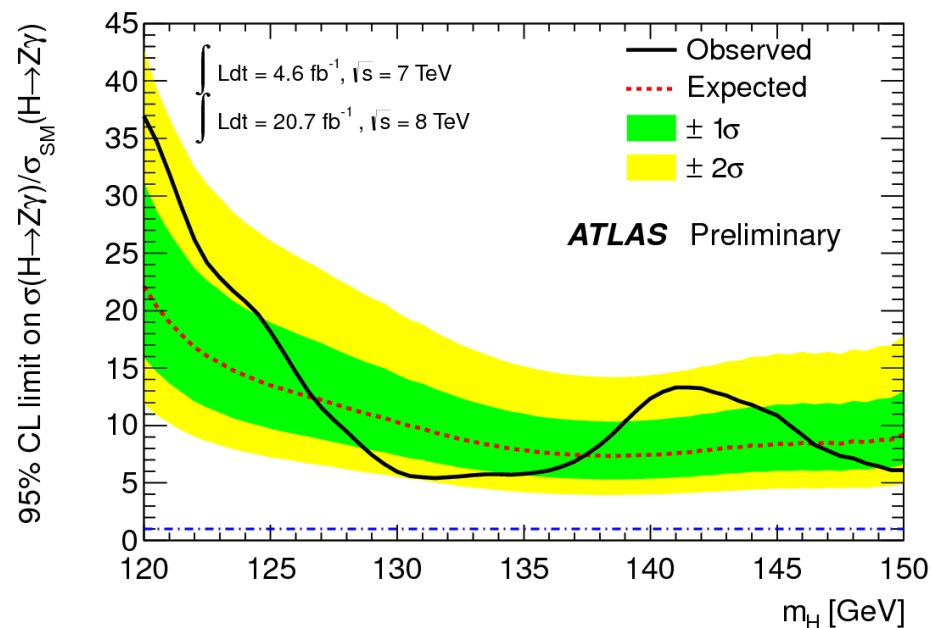
Search for H \rightarrow Z γ (Z \rightarrow $\ell\ell$)

- $\sigma \cdot B$ similar to H \rightarrow ZZ \rightarrow 4 ℓ , but much worse S/B
- Main backgrounds are Z+ γ and Z+jets

Use full 2011+2012 data set



No significant signal



For $m_H = 125$ GeV @ 95%CL:

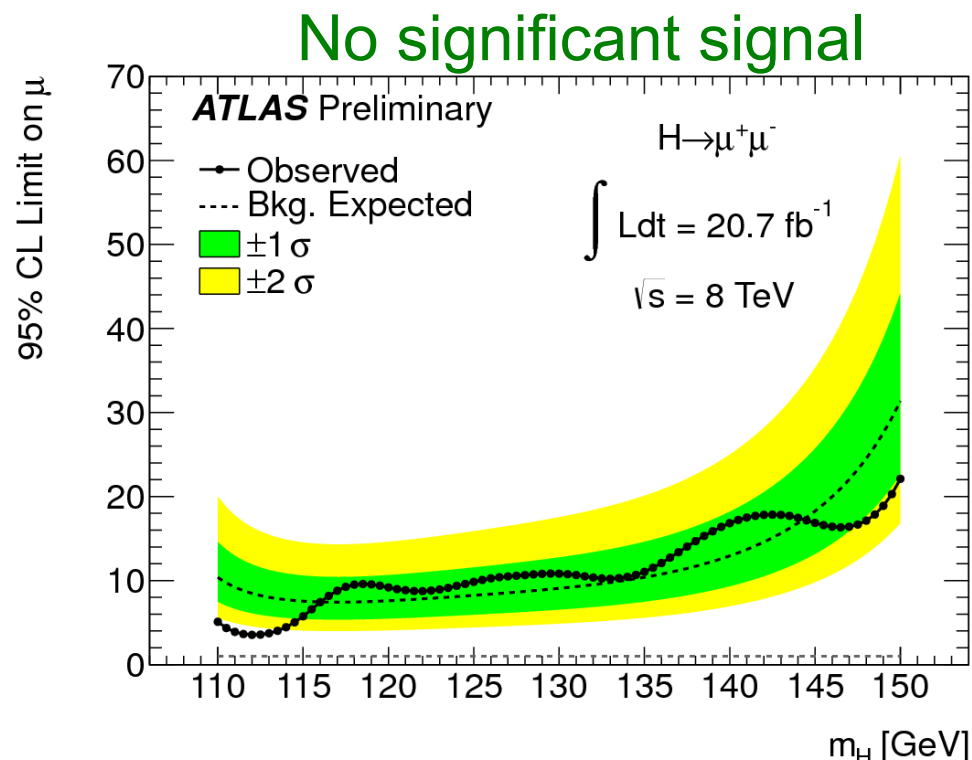
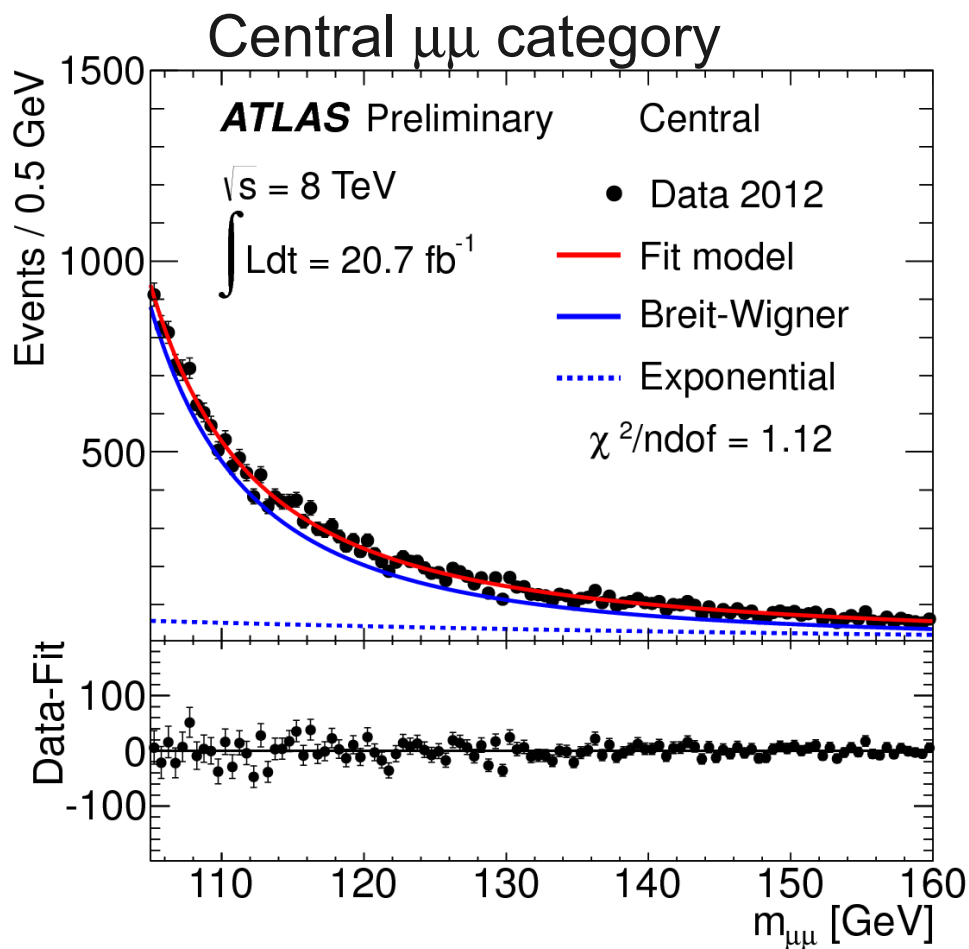
$\sigma(H \rightarrow Z\gamma) < 18.2 \cdot \sigma(H \rightarrow Z\gamma)_{SM}$
(Expected 13.5)

Fit for signal in $\Delta m = m_{\ell\ell\gamma} - m_{\ell\ell}$

$H \rightarrow \mu\mu$ Search

Search for small resonance on top of Drell-Yan background

- Enhance S/B by req. $p_T(\mu\mu) > 15$ GeV & splitting in central/non-central $\mu\mu$
- Background modeled with Breit-Wigner+exponential



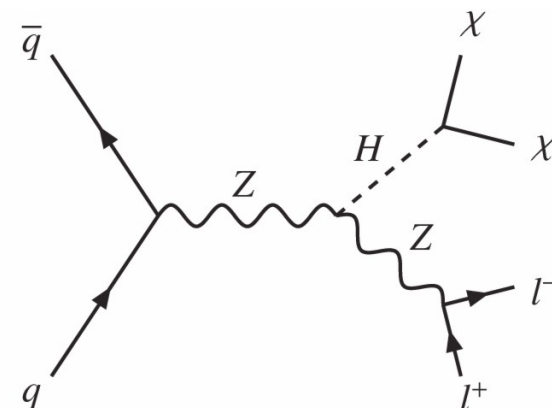
For $m_H = 125$ GeV @ 95% CL:

$\sigma(H \rightarrow \mu\mu) < 9.8 \cdot \sigma(H \rightarrow \mu\mu)_{\text{SM}}$
 (Expected 8.2)

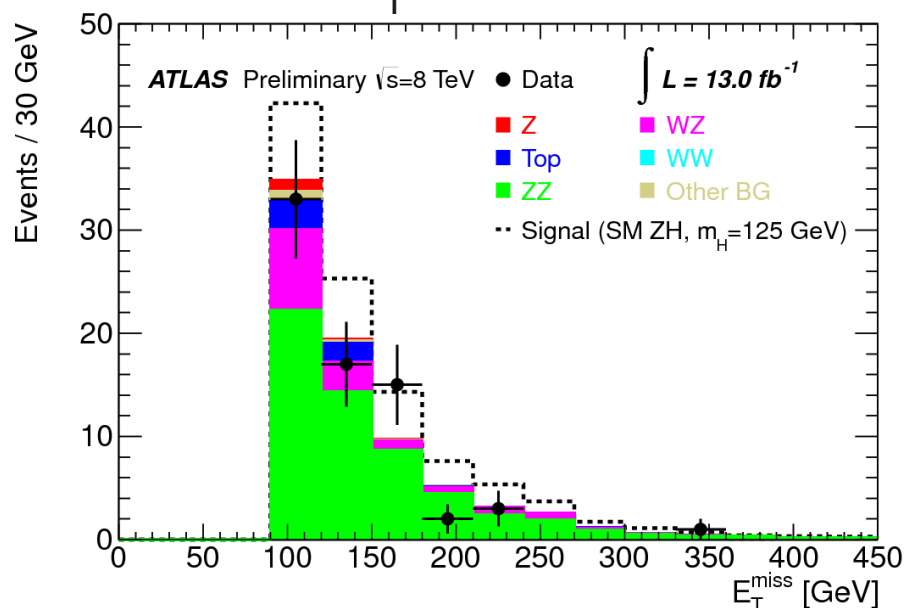
Invisible Higgs Search

Search for invisible decays in ZH prod.

- Suppress Z background with $E_T^{\text{miss}} > 90$ GeV
- Require boosted Z and back-to-back with E_T^{miss}
- Veto events with jets
- Main backgrounds: ZZ, WZ and WW

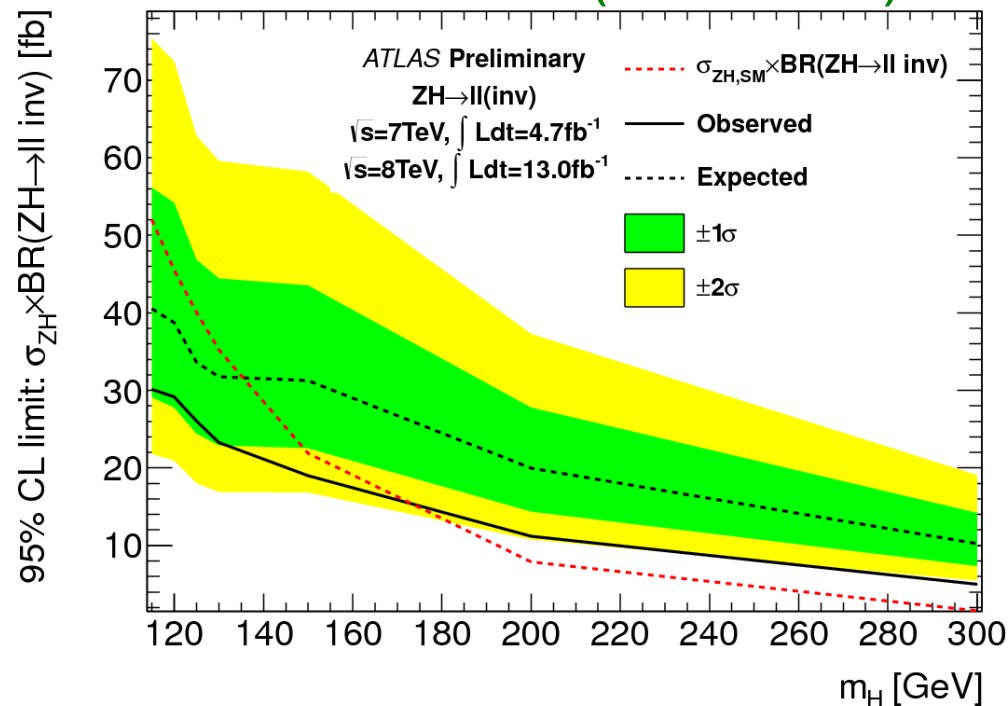


Final E_T^{miss} distribution



For $m_H = 125$ GeV and SM $\sigma(\text{ZH})$:
 $B(H \rightarrow \text{invisible}) < 65\%$ @ 95%CL
 (Expected: 84%)

Limit on $\sigma \cdot B(\text{ZH} \rightarrow \ell\ell \text{inv})$



BSM Searches

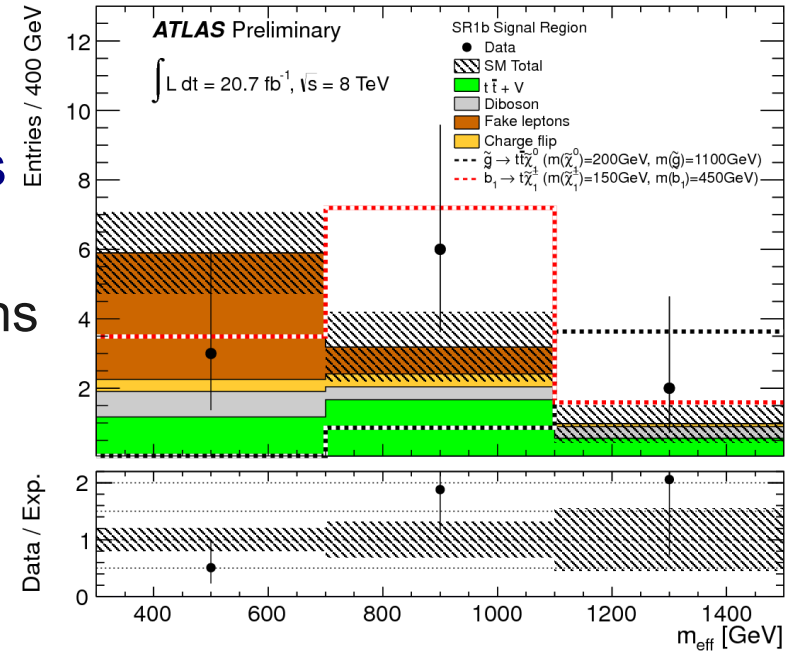
SUSY – Same-sign Leptons

“Natural SUSY” is major focus area

Same-sign leptons sensitive in many channels

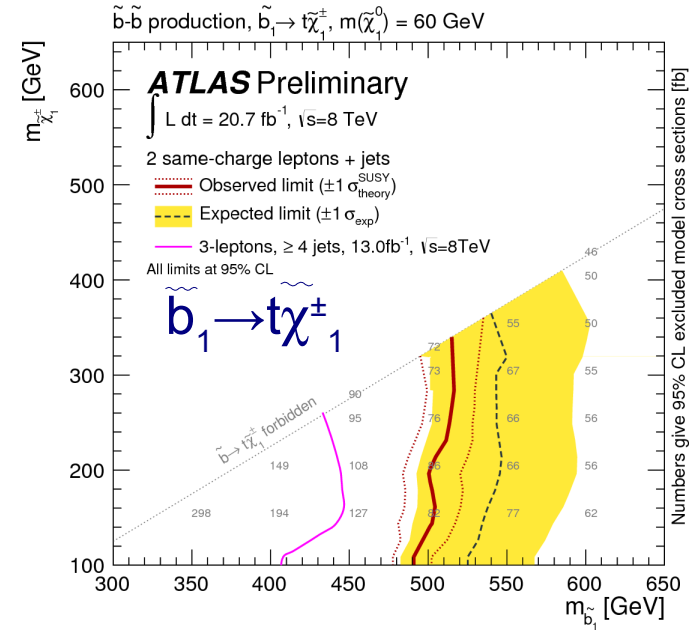
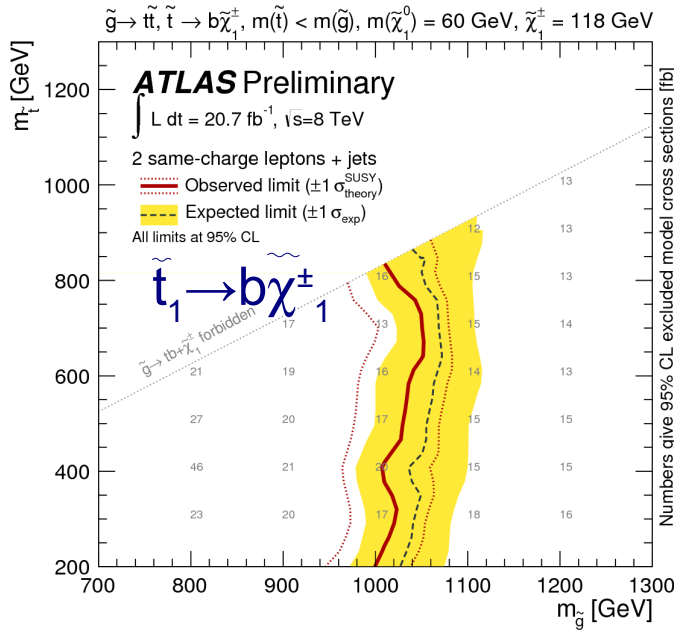
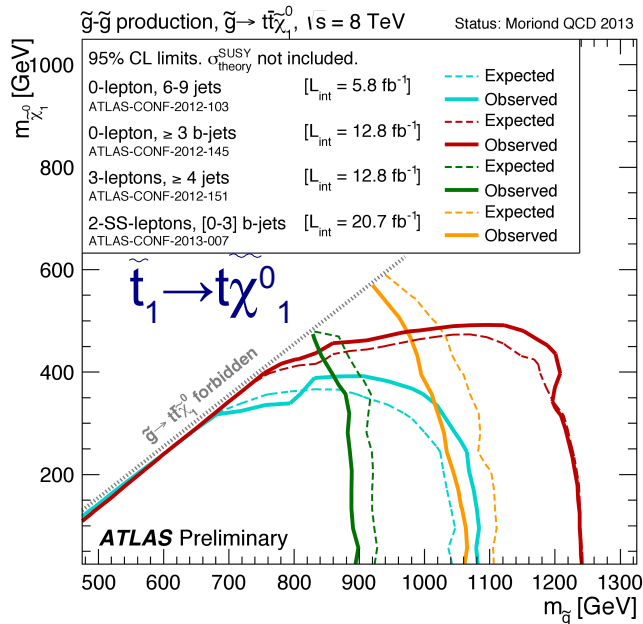
- $\ell^\pm \ell'^\pm$, E_T^{miss} , 3-5 jets and 0-3 b-jets
- Main bkgds: $t\bar{t}$ (+W/Z), WZ/ZZ and fake leptons
- Simultaneous fit to three signal regions in b-jet multiplicity for exclusion limits

No excess observed
Interpreted in multiple SUSY models



Glauino-mediated stop production

Direct sbottom production



Direct stop Search

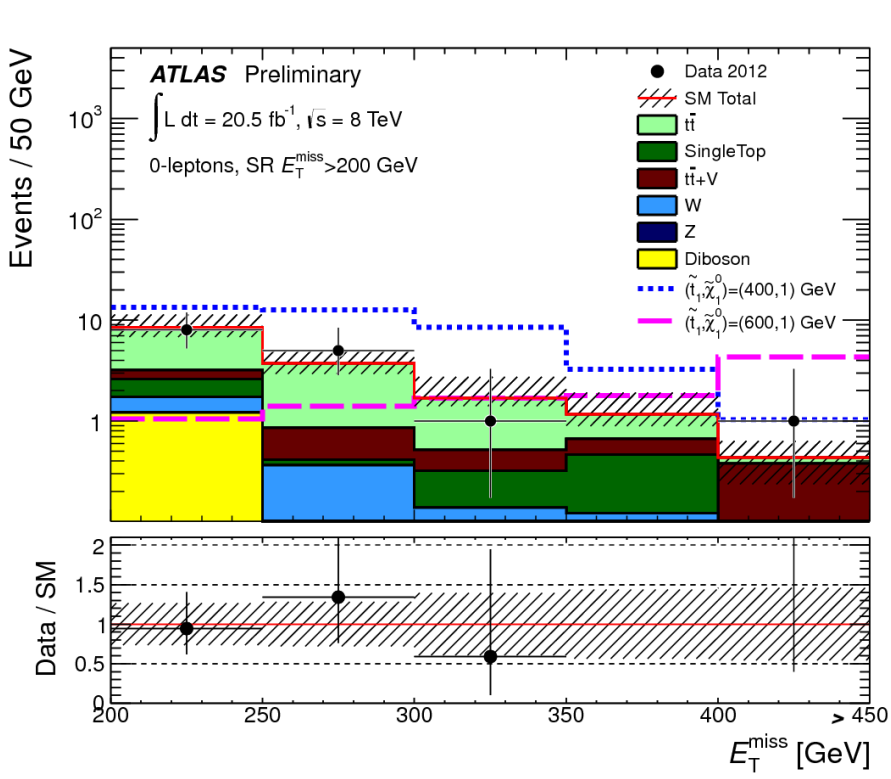
Direct stop in many channels – two new results with 20 fb⁻¹

$\tilde{t}_1 \rightarrow t\tilde{\chi}_1^0$ with all hadronic top decays

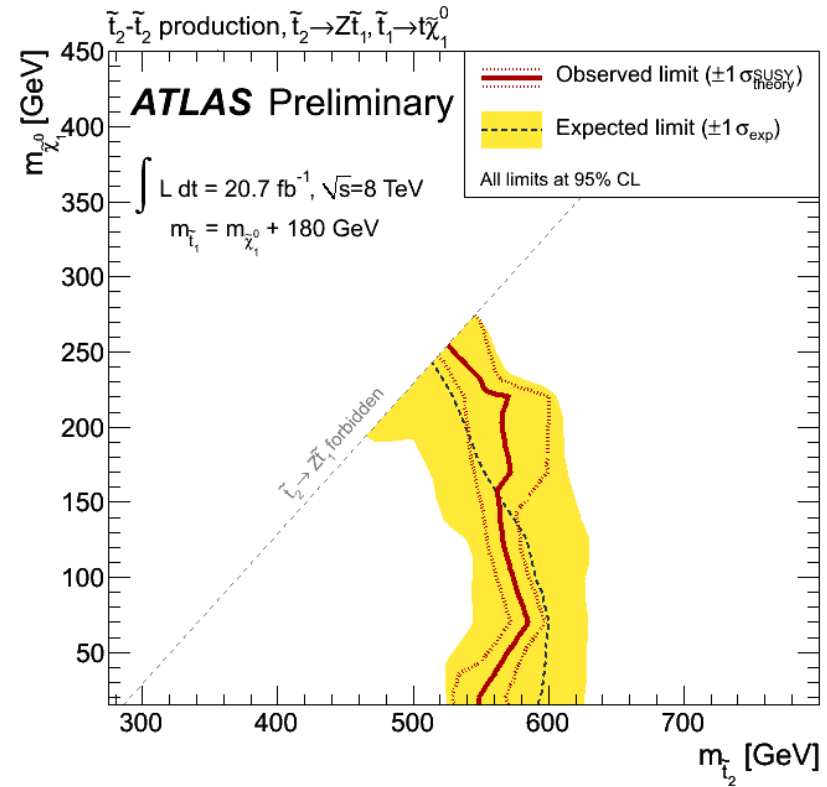
- Six jets (2 b-jets) and E_T^{miss}
- Main bkgds: $t\bar{t}$ and $Z(\rightarrow \nu\nu)+\text{jets}$

$\tilde{t}_2 \rightarrow \tilde{t}_1 Z$ (new decay mode)

- $Z(\rightarrow \ell\ell)+\text{b-jet}$ (+3rd ℓ)
- Main bkgds: $t\bar{t}$ (+W/Z)

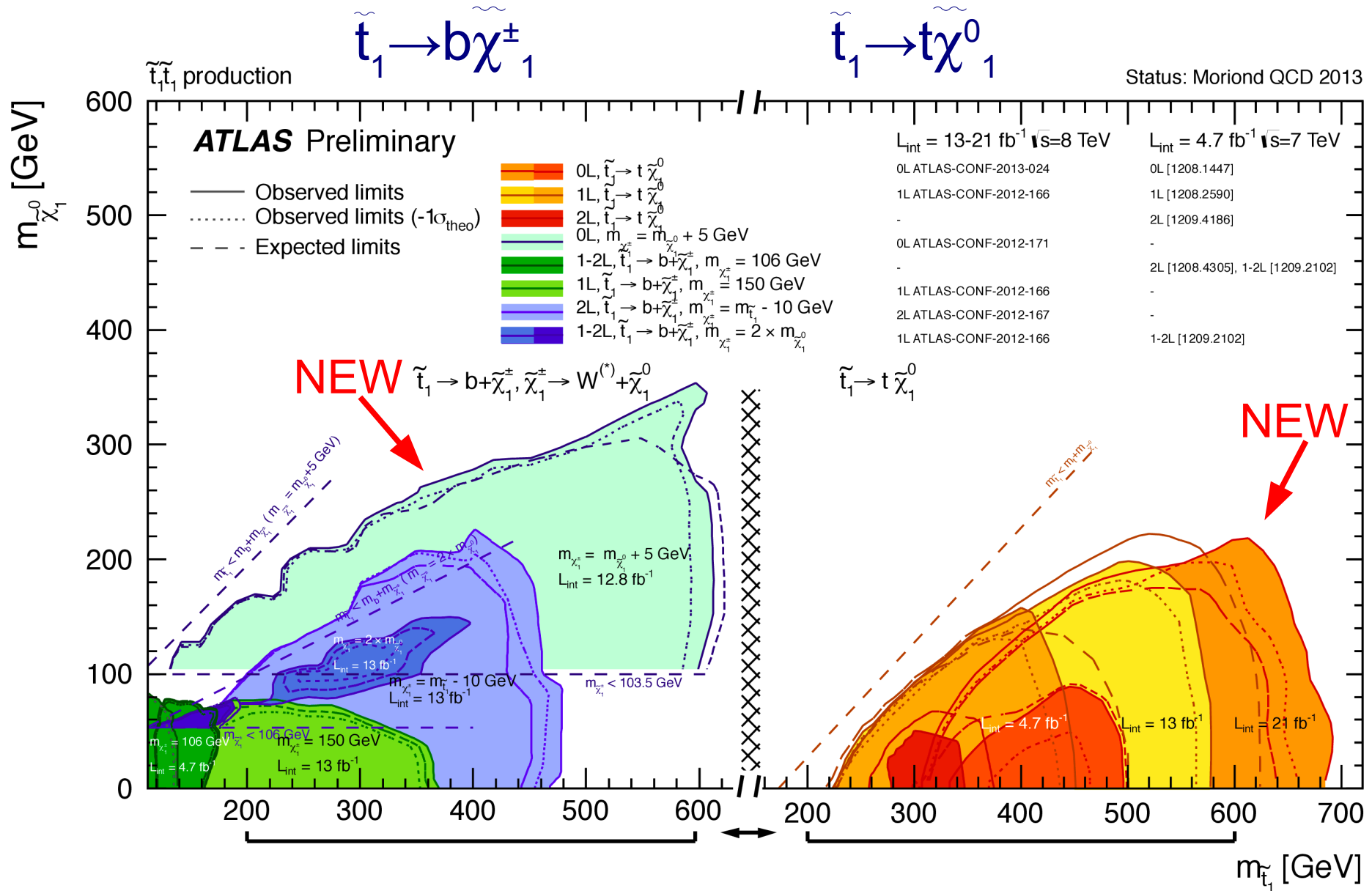


Excludes \tilde{t}_1 up to 660 GeV
 depending on LSP (next slide)



Also limits on $\tilde{t}_1 \rightarrow t\tilde{\chi}_1^0, \tilde{\chi}_1^0 \rightarrow Z\tilde{G}$

Summary of Direct Stop



Sensitivity up to large stop masses (660 GeV)

● Note that limits are calculated in specific simplified models

Direct Gaugino Search

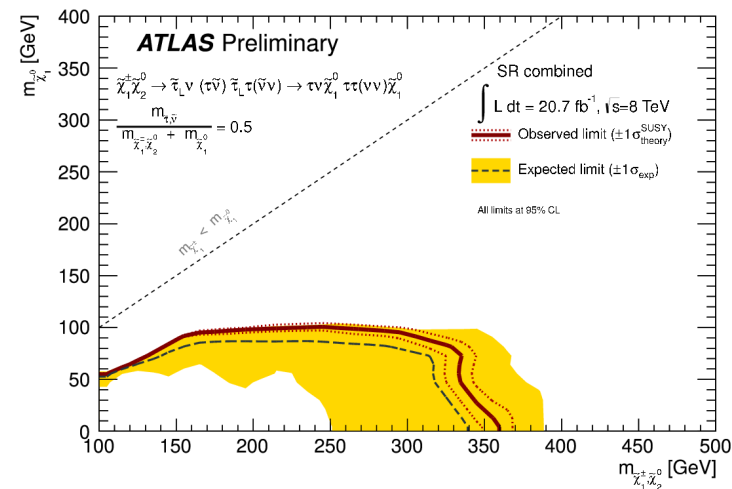
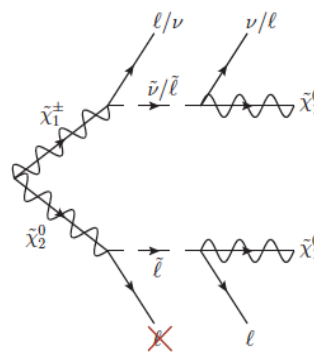
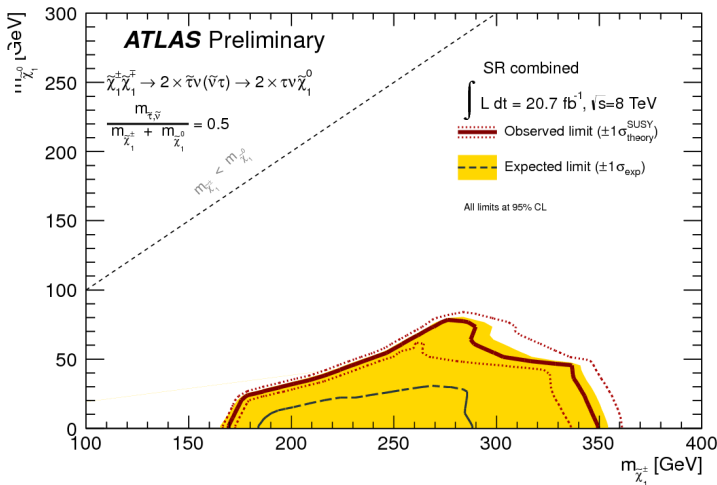
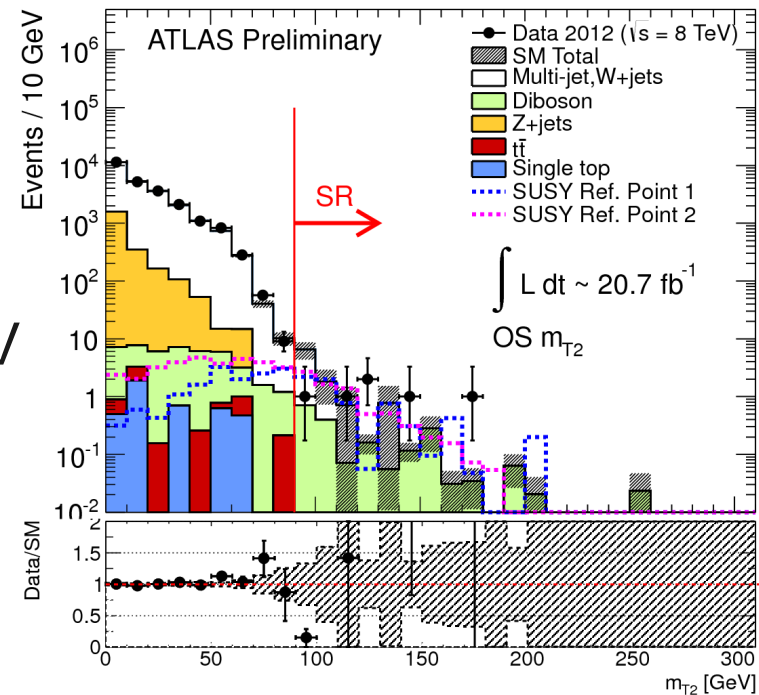
Natural SUSY requires light $\tilde{\chi}_1^\pm, \tilde{\chi}_1^0$

$\tilde{\chi}_1^0$ good candidate for dark matter

Search for decays in to τ 's and E_T^{miss}

- $\geq 2 \tau_{\text{had}}$, no e/μ , no (b-)jet, no Z, $E_T^{\text{miss}} > 40$ GeV
- Discriminate using transverse mass, m_{T2}
- Data-driven estimate of multi-jets & W+jets

Limits are set in scenarios with light $\tilde{\tau}$

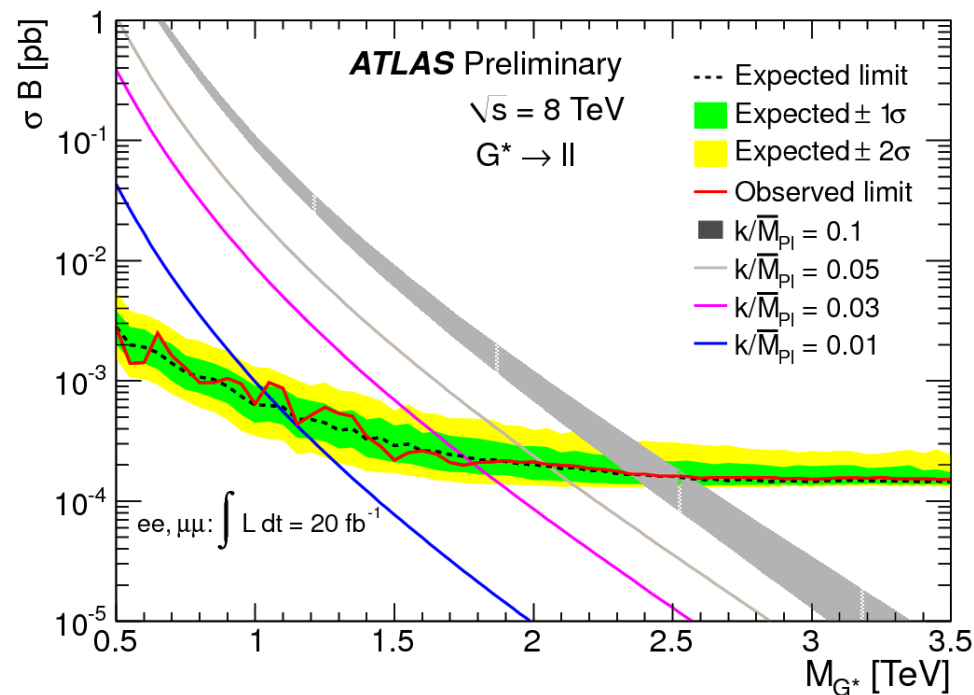
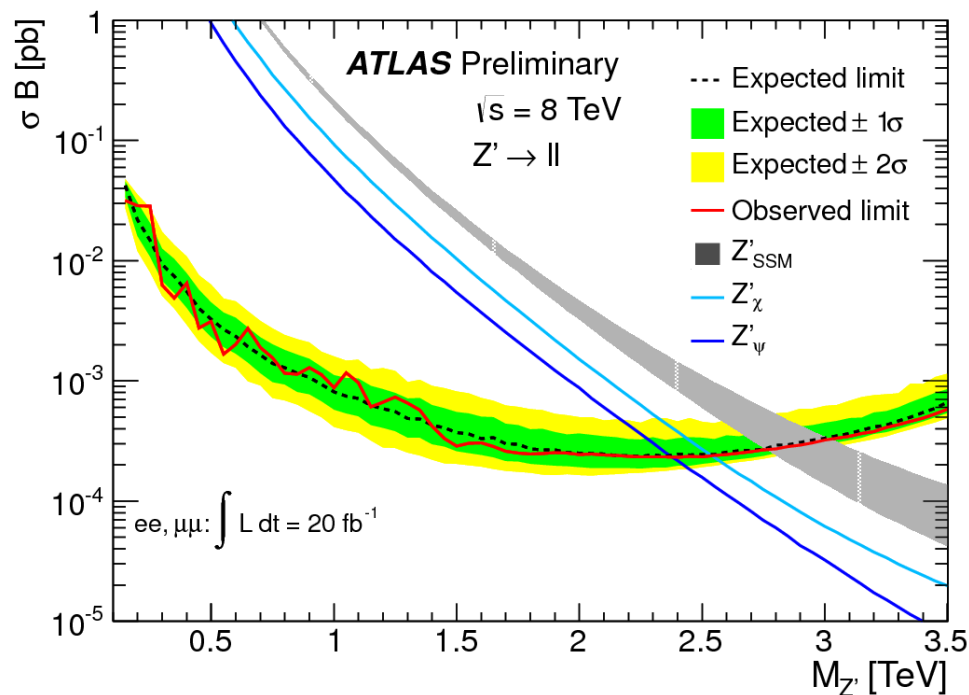
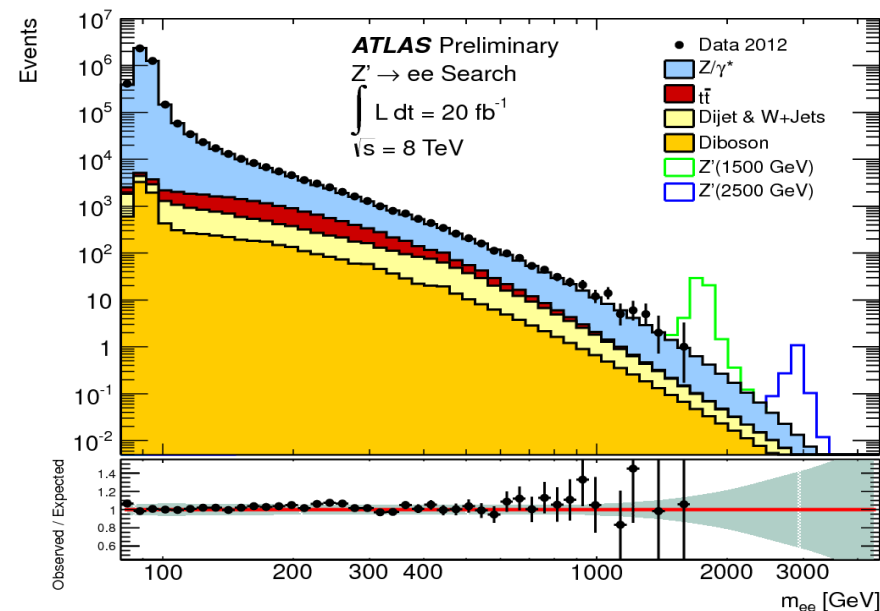


Di-lepton Resonance Search

$ee/\mu\mu$ resonance search
updated to full 2012 data set

- Improved lepton identification

Limits on SSM Z' , E6-motivated Z'
and spin-2 RS graviton ($k/M_{\text{PL}}=0.1$)
between 2.38 and 2.86 TeV

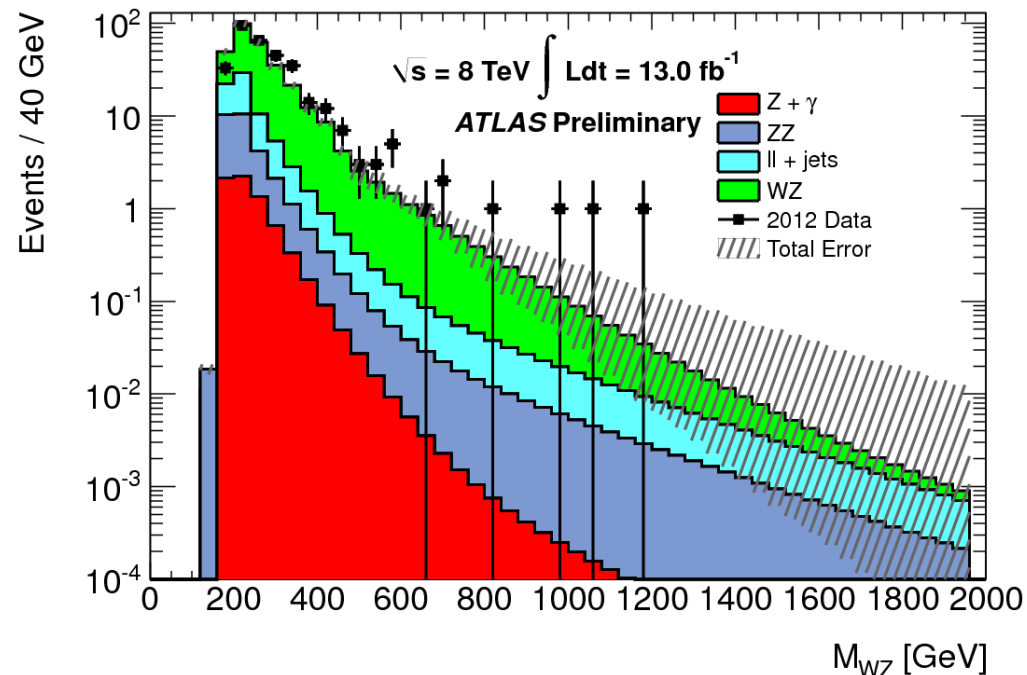


WZ Resonance Search

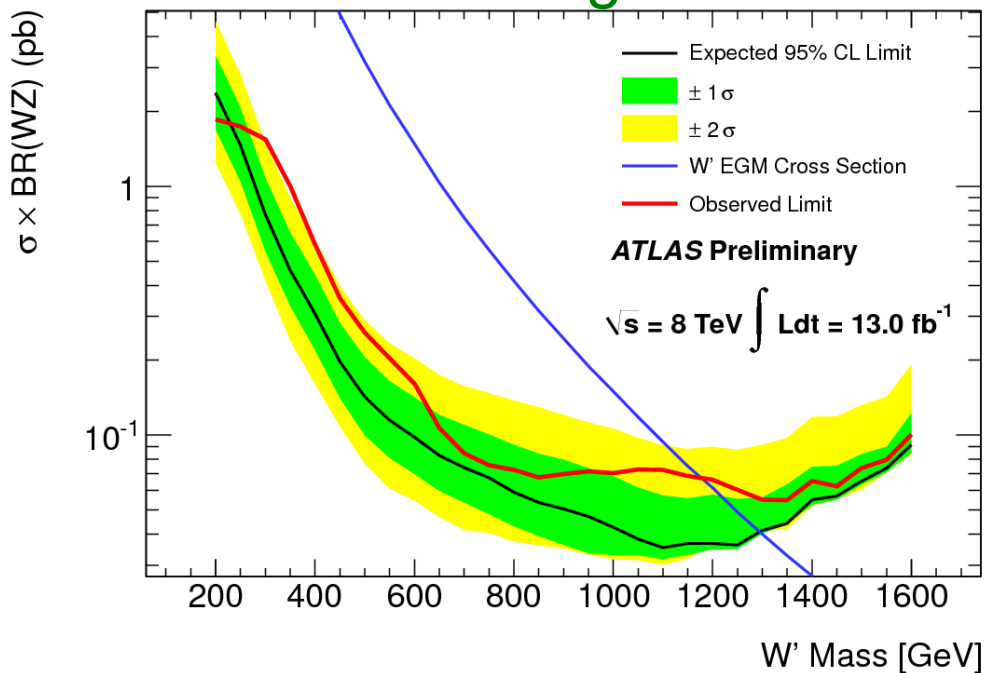
Search for resonant WZ

- 3 leptons and E_T^{miss}
- Very clean signal

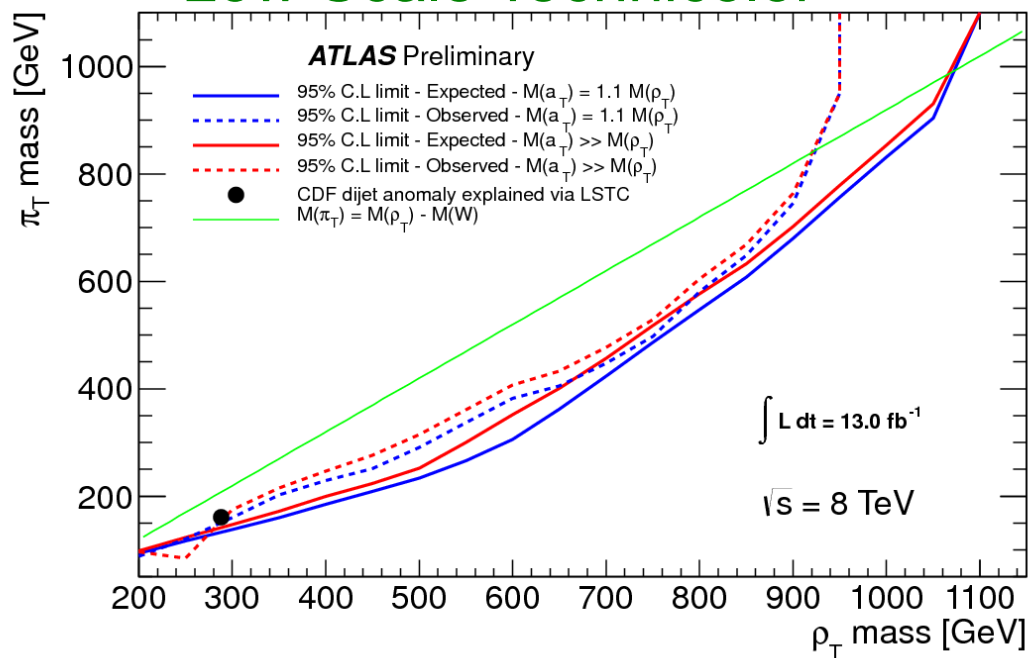
No significant signal
Limits set in two models



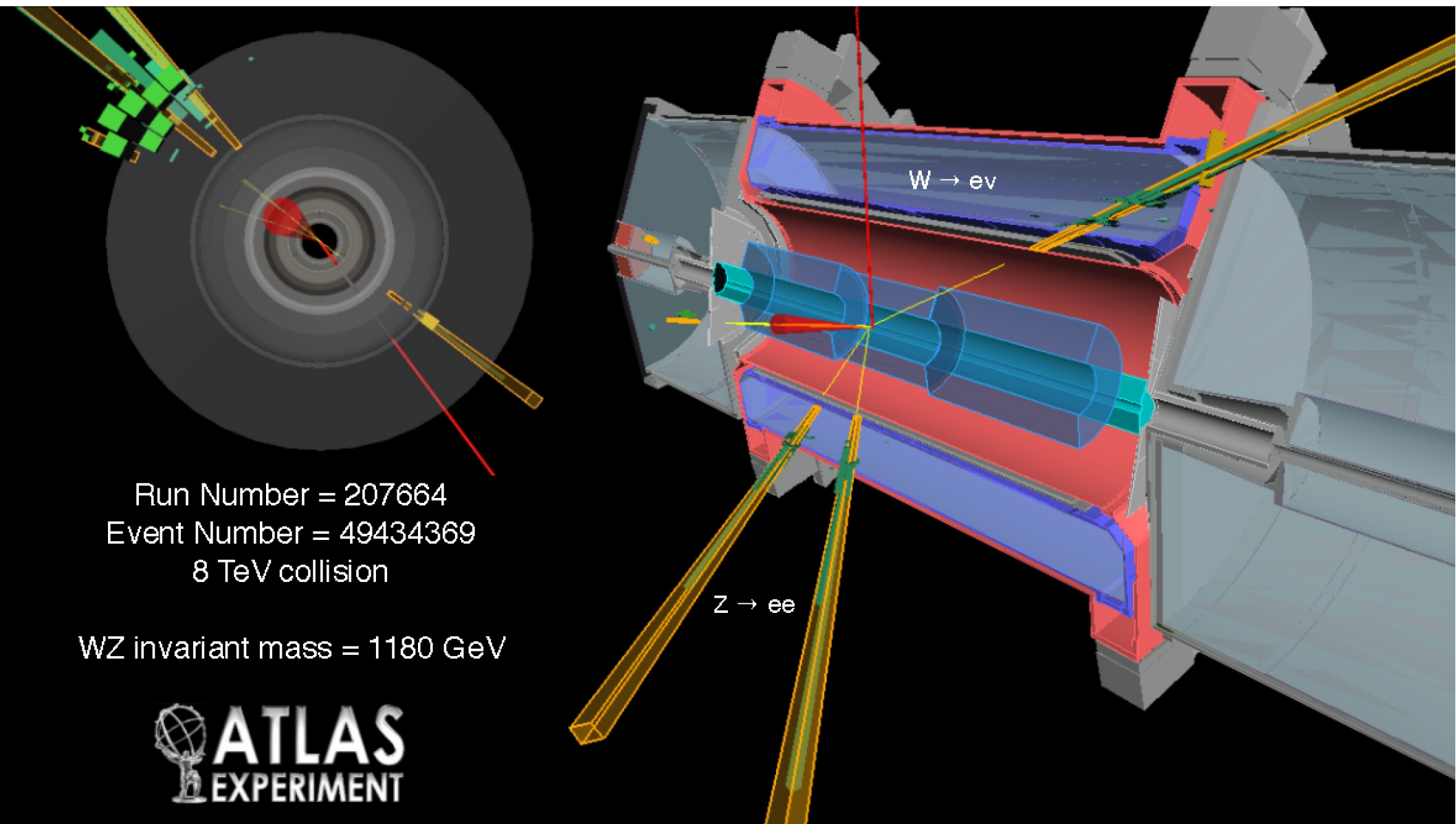
Extended Gauge Model W'



Low Scale Technicolor



WZ Resonance Search

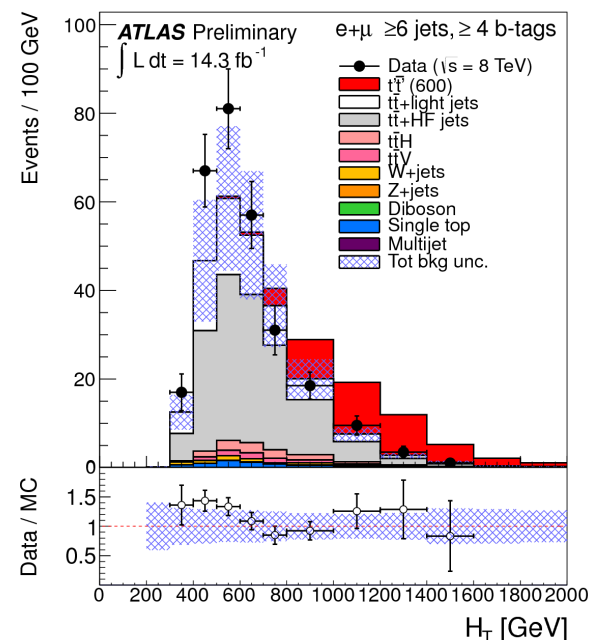


Search for $t't' \rightarrow tH+X$

Search for pair produced vector-like quark
 $t't' \rightarrow Ht, Zt, Wb$: First search for Ht modes

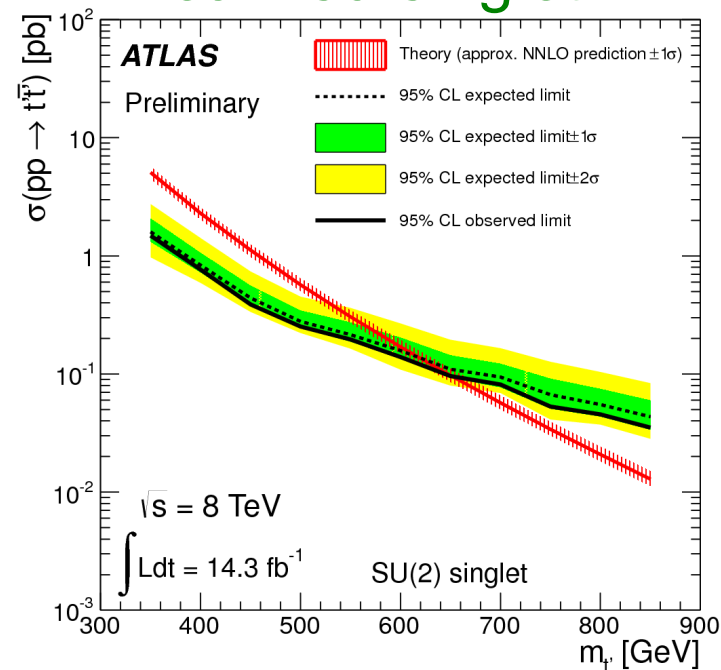
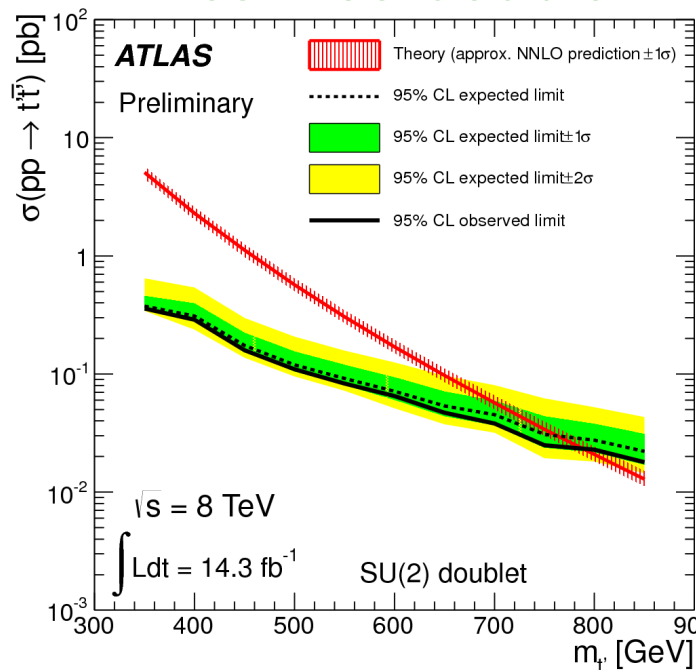
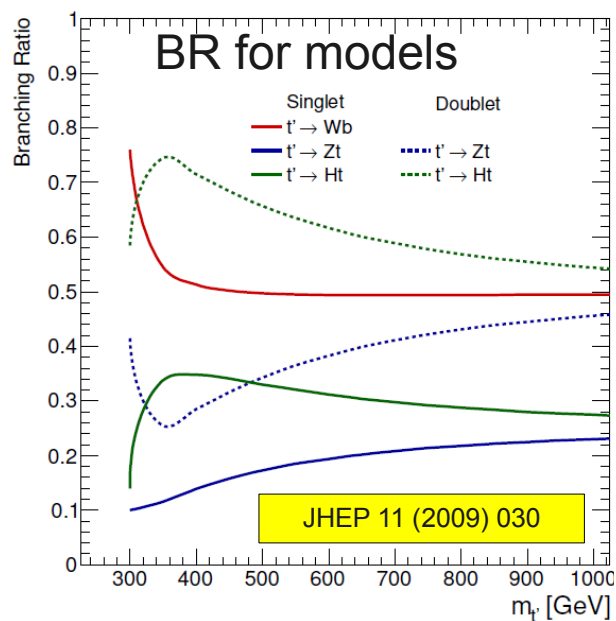
- Lepton+ E_T^{miss} +6 jets (2-4 b-jets)
- $t\bar{t}$ +jets is main background
- Use H_T as discriminating variable
- Sensitive to several decay modes:
 $t't' \rightarrow HtHt, ZtHt, WbHt$

Limits set on $BR(t' \rightarrow Wb)$ vs $BR(t' \rightarrow tH)$ vs $m(t')$
 and on two specific benchmark models



Weak Iso-doublet

Weak Iso-singlet



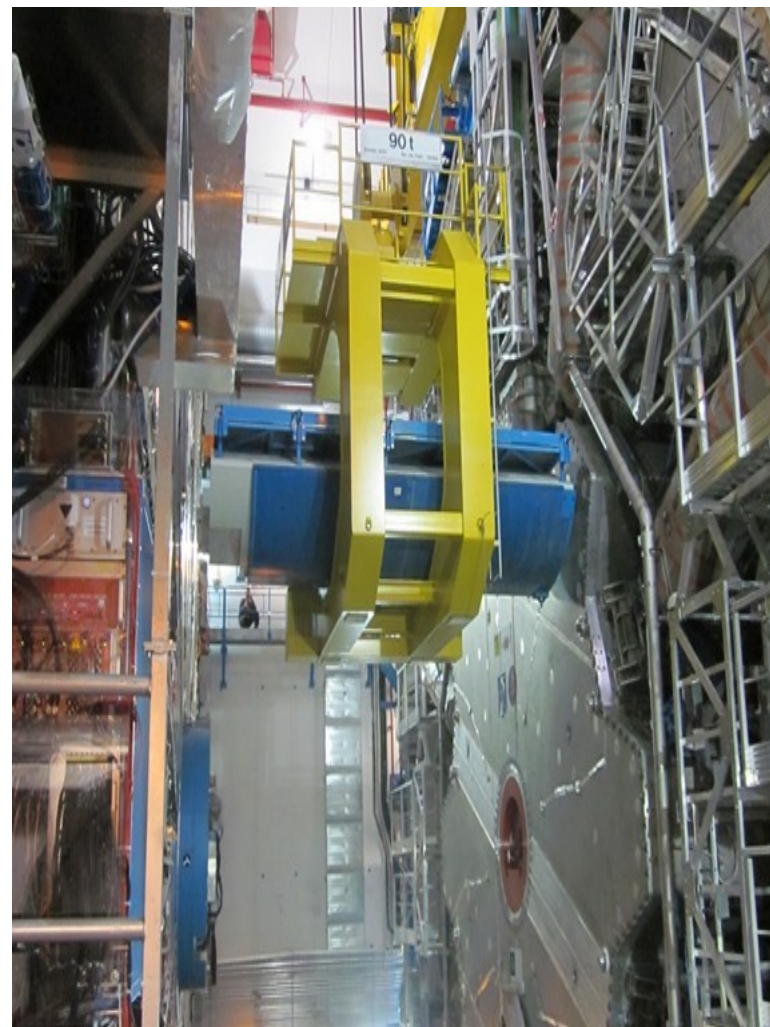
Shutdown Activities

Point 1 Activities

Long list of consolidation and upgrade work for shutdown

- New insertable pixel B-layer
- New pixel service quarter panels
- New evaporative cooling plant for inner detector
- Completion/addition of muon spectrometer chambers
- New AI forward beam pipe
- New calorimeter LVPS
- Additional shielding for muons
- Upgrade of magnet cryogenics
- Consolidation of infrastructure
- Detector readout for 100 kHz L1 Rate

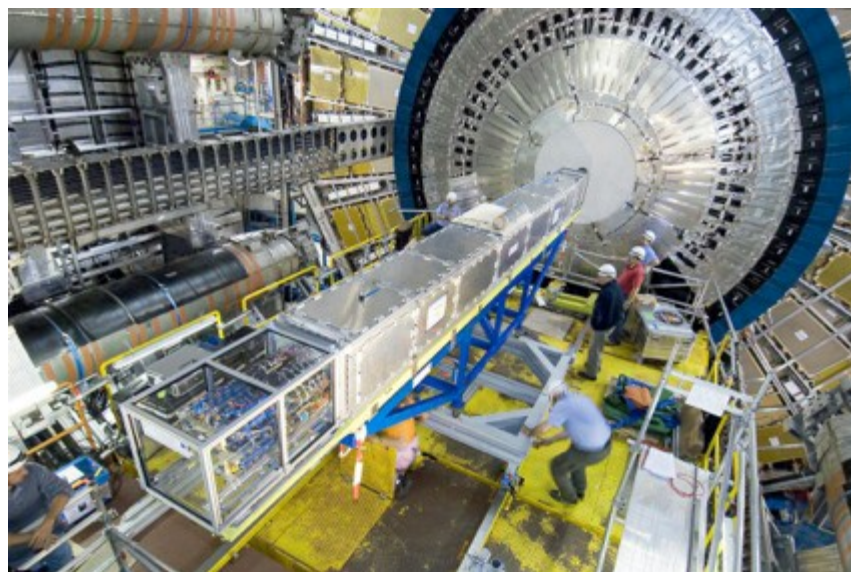
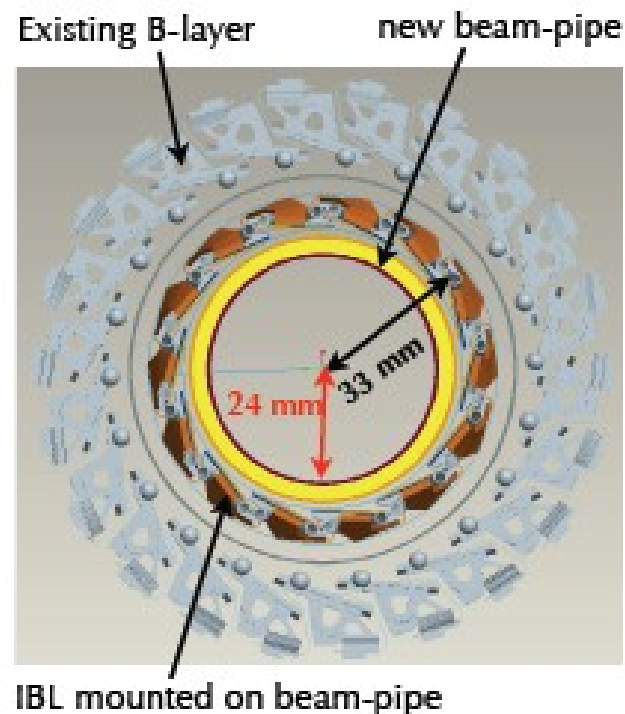
Will have very busy schedule
at Point 1 for most of shutdown



New Pixel Layer

Installation of new pixel layer moved forward due to late, but long shutdown

- New inner layer with 14 staves at $r=3.3$ cm
- Provides better resolution and performance in high pileup than existing b-layers
- Improved radiation hardness
- Requires new cooling plant and new Be beam pipe



Decided to extract pixel detector to insert support tube on surface

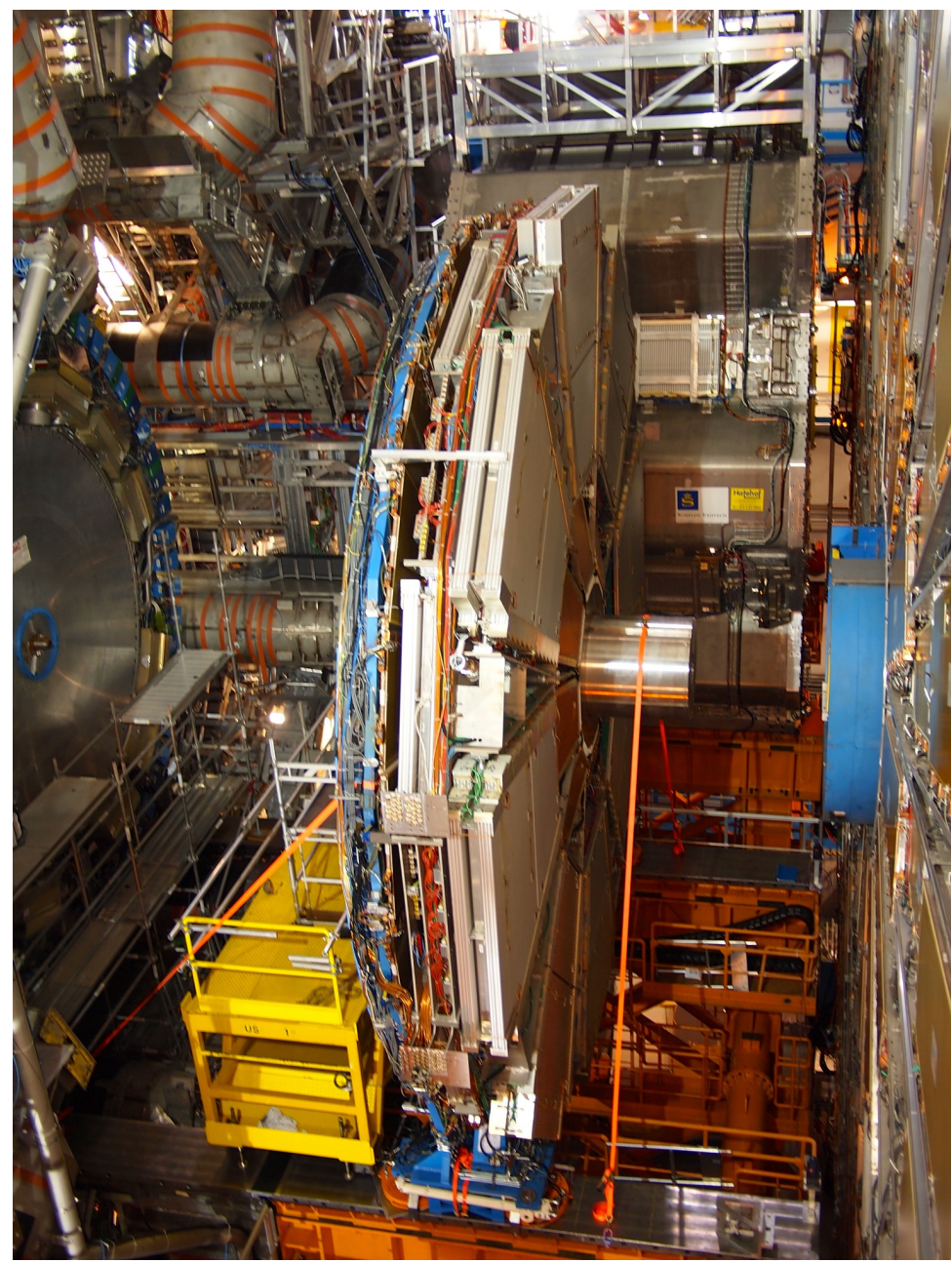
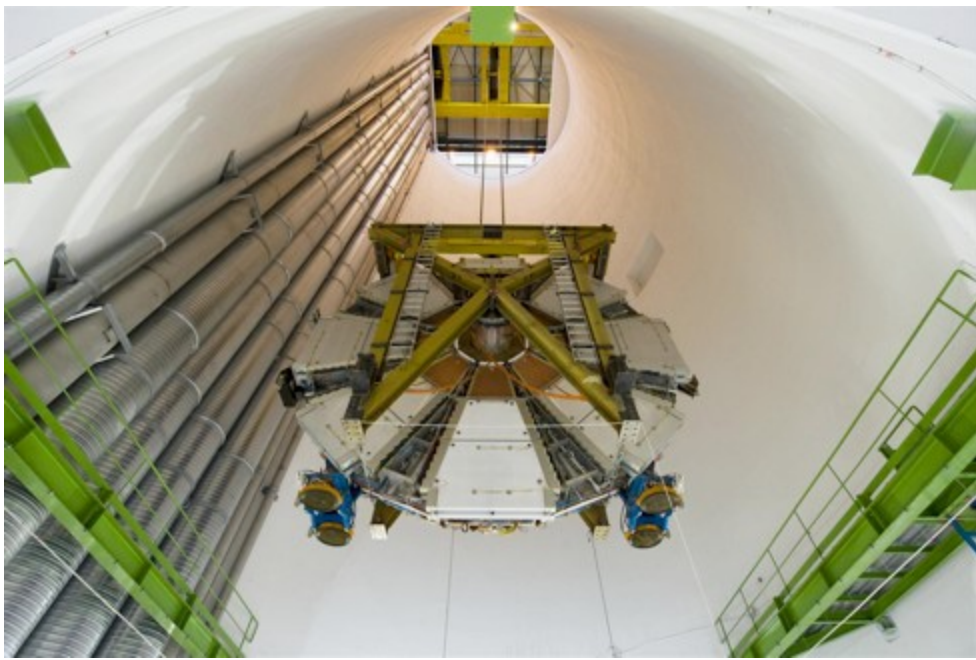
- Evaluated to be safest option
- Allows replacement of service quarter panels and repair of readout channels

Extraction of Small Wheel

To allow pixel extraction and insertion, muon small wheel on side C will be brought to the surface

- Will use opportunity to make some repairs

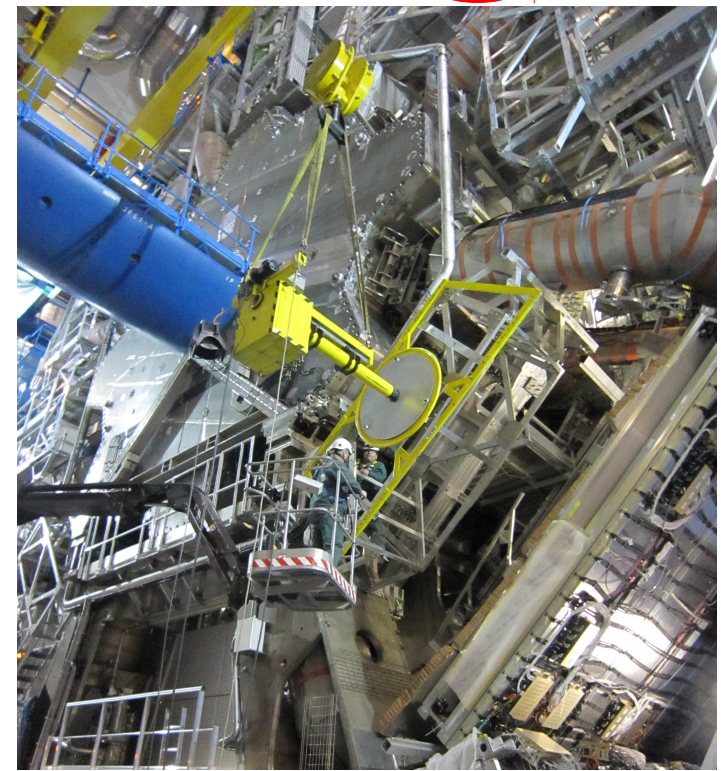
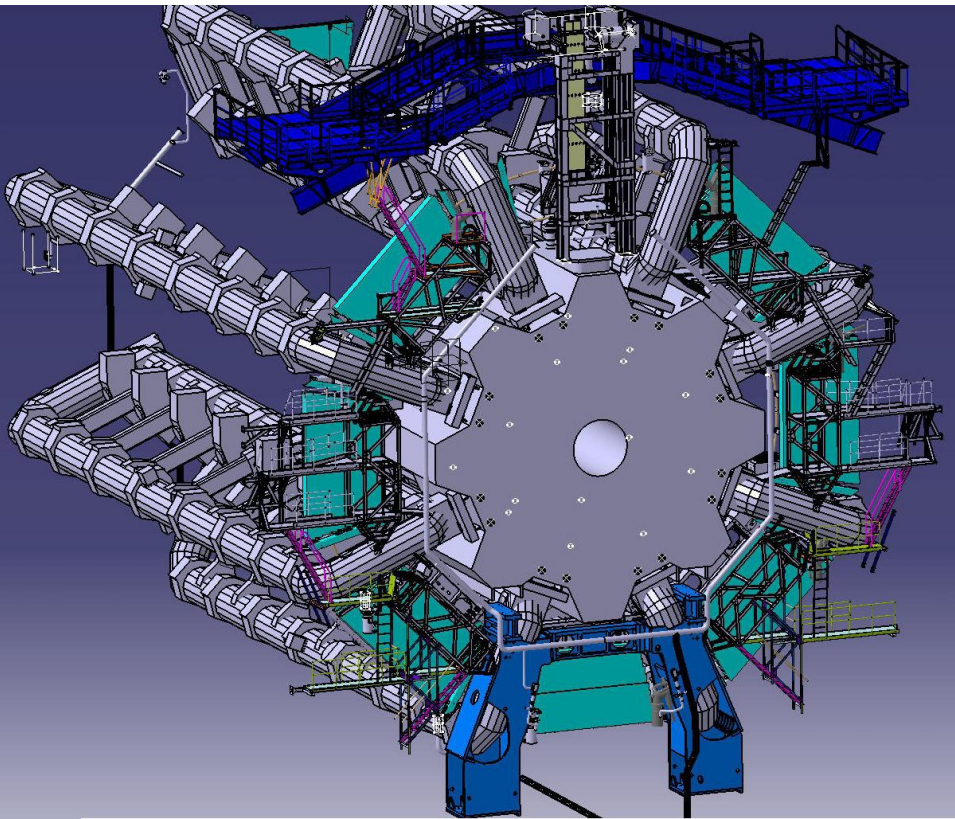
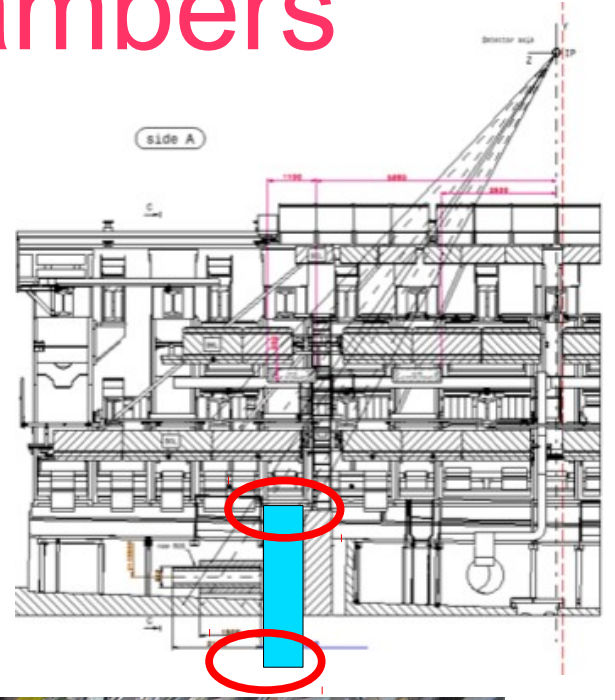
Scheduled for today



Additional Muon Chambers

Installing additional muon chambers

- Upgrade in spectrometer feet region and elevator shafts to increase acceptance
- Complete installation of EE chambers on A-side
First one already installed

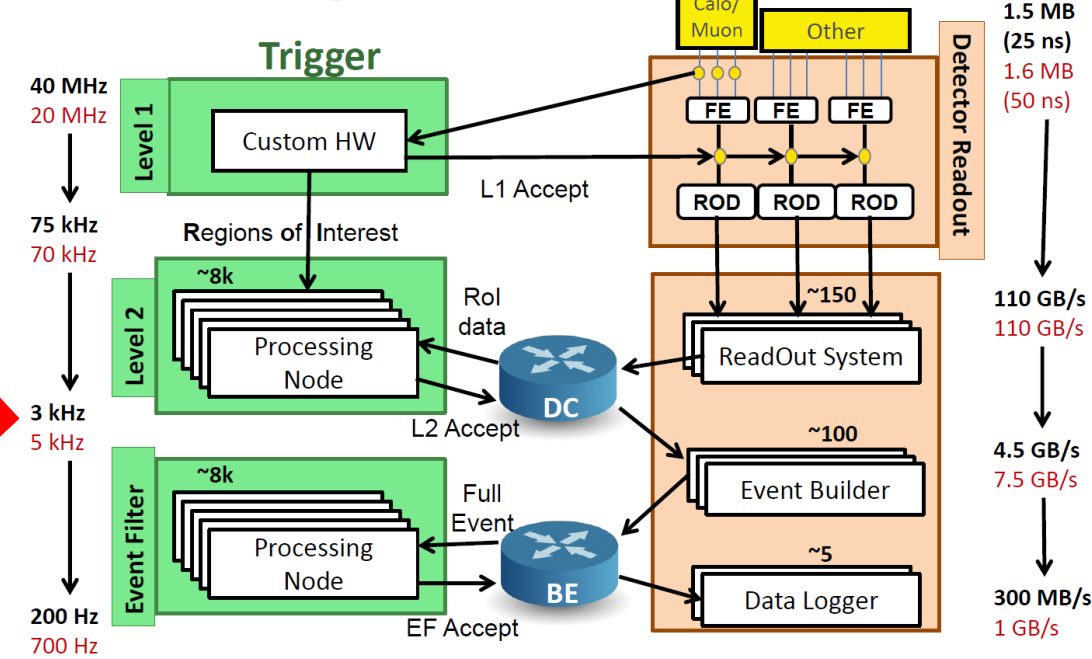


Trigger/DAQ Evolution

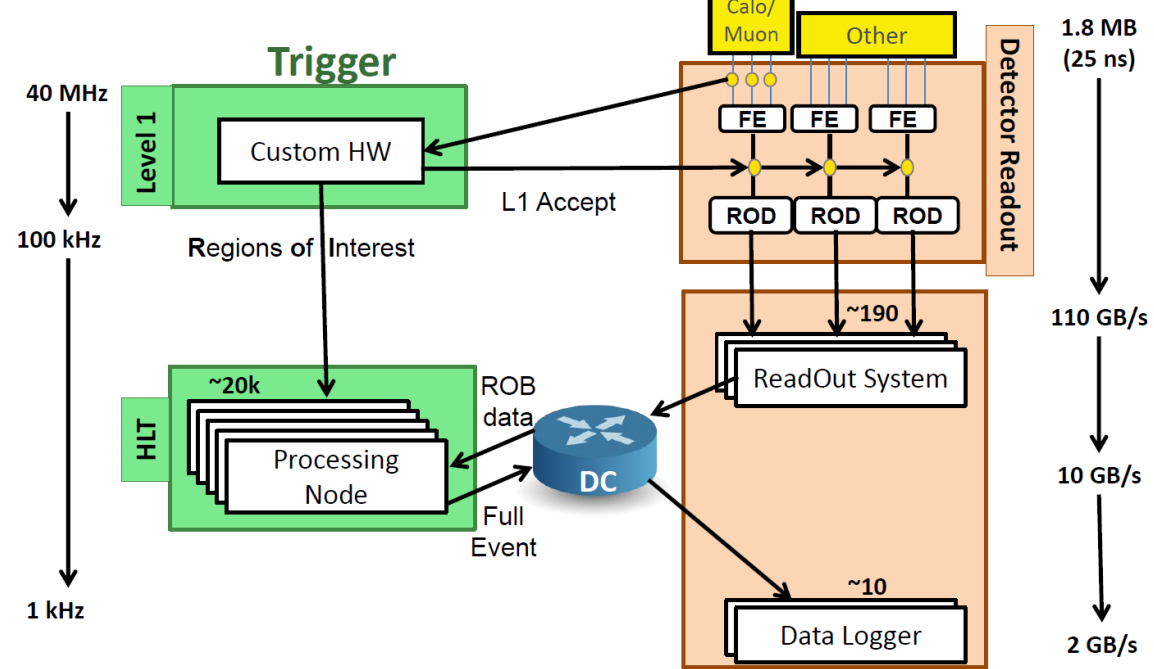
Merging of L2 and EF

- HLT selection and event building to be done in common node, merging three separate farms
- Tighter integration between L2 (custom) and EF (offline-based) algorithms

TDAQ Today



TDAQ After LS1



Advantages

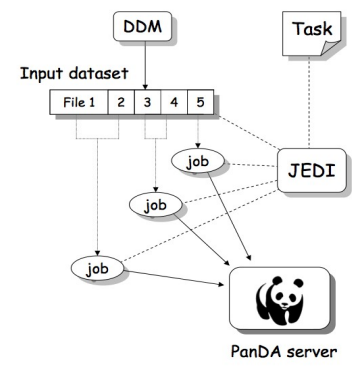
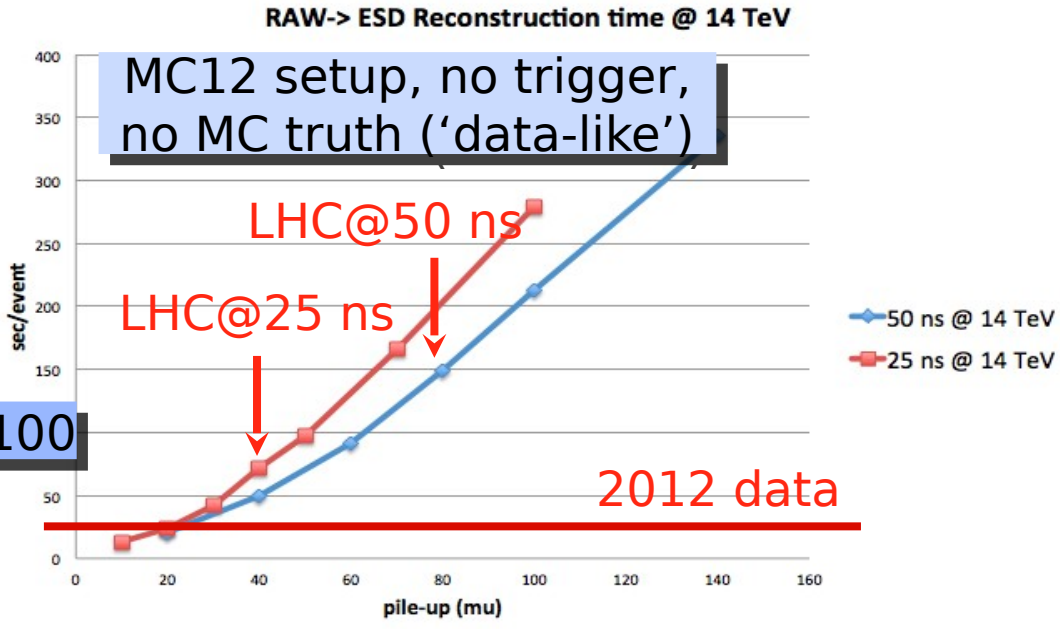
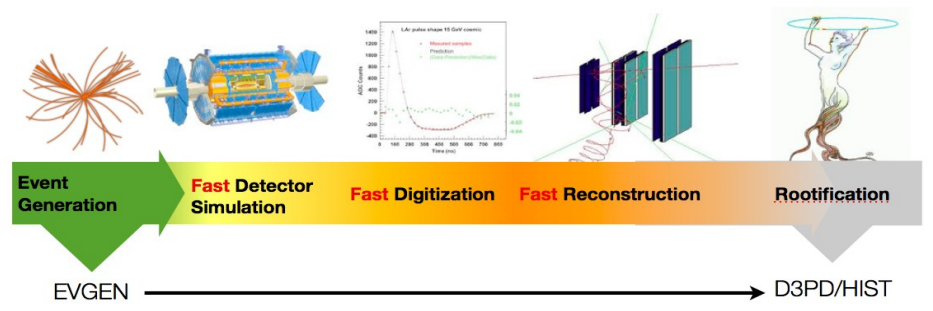
- Simplified architecture
- Single homogeneous farm
- Simpler configuration
- Automatic balancing of CPU
- Increased flexibility in HLT selection

Software & Computing Improvements

Ambitious plans for shutdown

- Software improvements
 - Algorithm speed up, better use of CPUs
 - Reduced memory footprint and event size
 - Event and algorithm level parallelism
 - Flexible simulation framework
- Distributed Computing
 - New distributed data management
 - Upgraded production system
- Revised analysis model for group production and physics users

An all-in-one chain for fast MC



Welcome to Rucio's documentation!

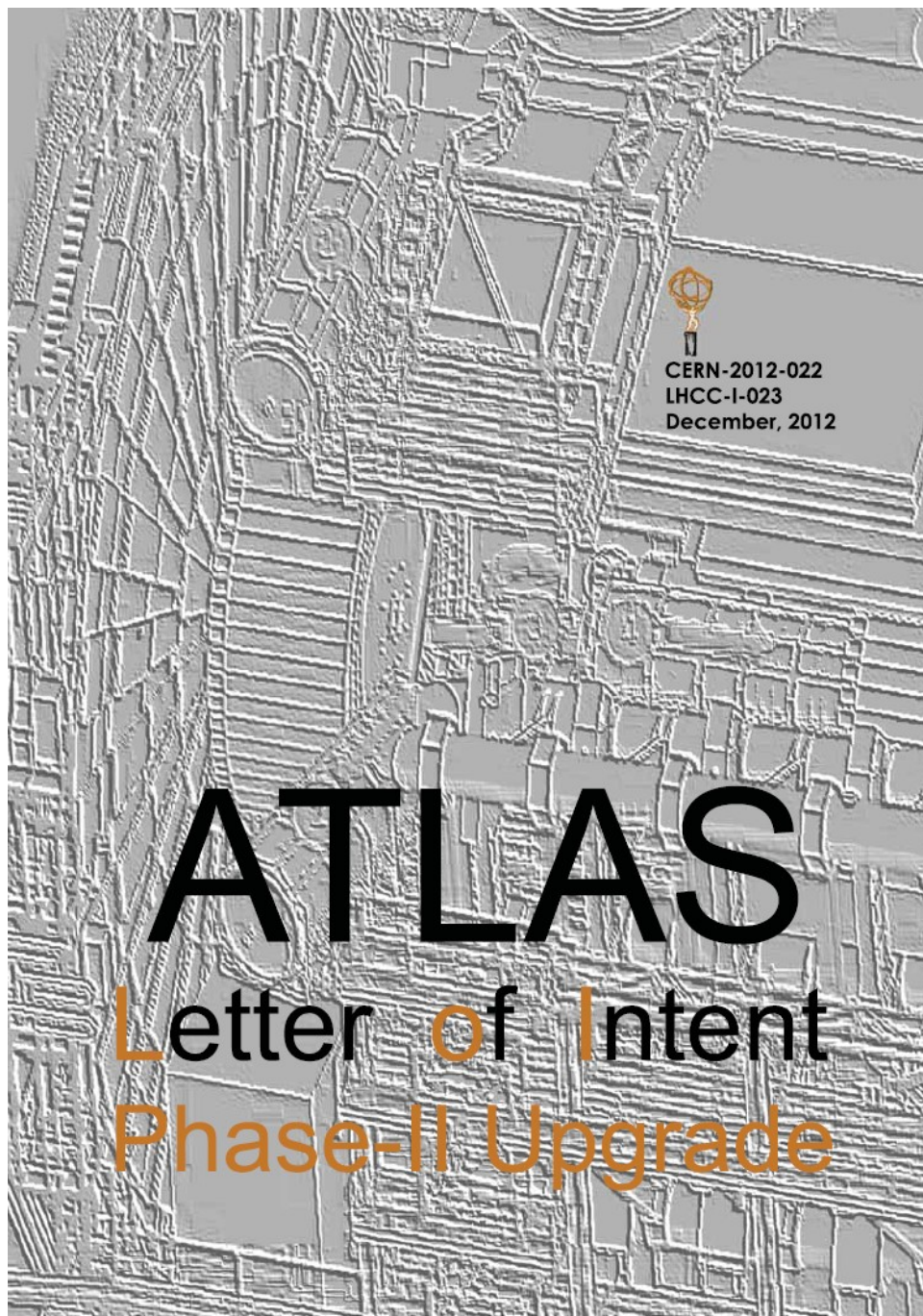
The Rucio project is the new version of ATLAS Distributed Data Management (DDM) system services for allowing the ATLAS collaboration to manage the large volumes of data, both taken by the detector as well as generated or derived, in the ATLAS distributed computing system. Rucio uses to manage accounts, files, datasets and distributed storage systems.

This documentation is generated by the Sphinx toolkit. and lives in the source tree.

Links:

- Documentation - <http://rucio.cern.ch>
- Project tracker - <https://its.cern.ch/jira/browse/RUCIO>

Phase-II Letter of Intent



Contents

- Executive Summary
- Upgrade of Trigger and Dataflow
- Upgrade of Liquid Argon Calorimeter
- Upgrade of Tile Calorimeter
- Upgrade of Muon System
- Upgrade of Inner Tracking System
- Upgrade of Computing and SW
- Physics Goals
- Installation and Commissioning
- Resources

Summary

Summary

Outstanding performance from the LHC team

Huge thanks on behalf of all of ATLAS

- The ATLAS detector has performed extremely well
 - Data-taking efficiency and data quality remains very high
- New analysis possibilities in ATLAS with pPb dataset
 - First surprising results already coming out
- Analysis of full 2011+2012 pp data in full swing
 - Precision measurements testing SM predictions
 - Starting to measure the properties of the new boson
 - So far it is looking like a SM Higgs boson*
 - Searches for wide range of possible new physics signals
- Extensive shutdown effort starting
 - Aim for best possible detector in time for 2015 data taking

Backup

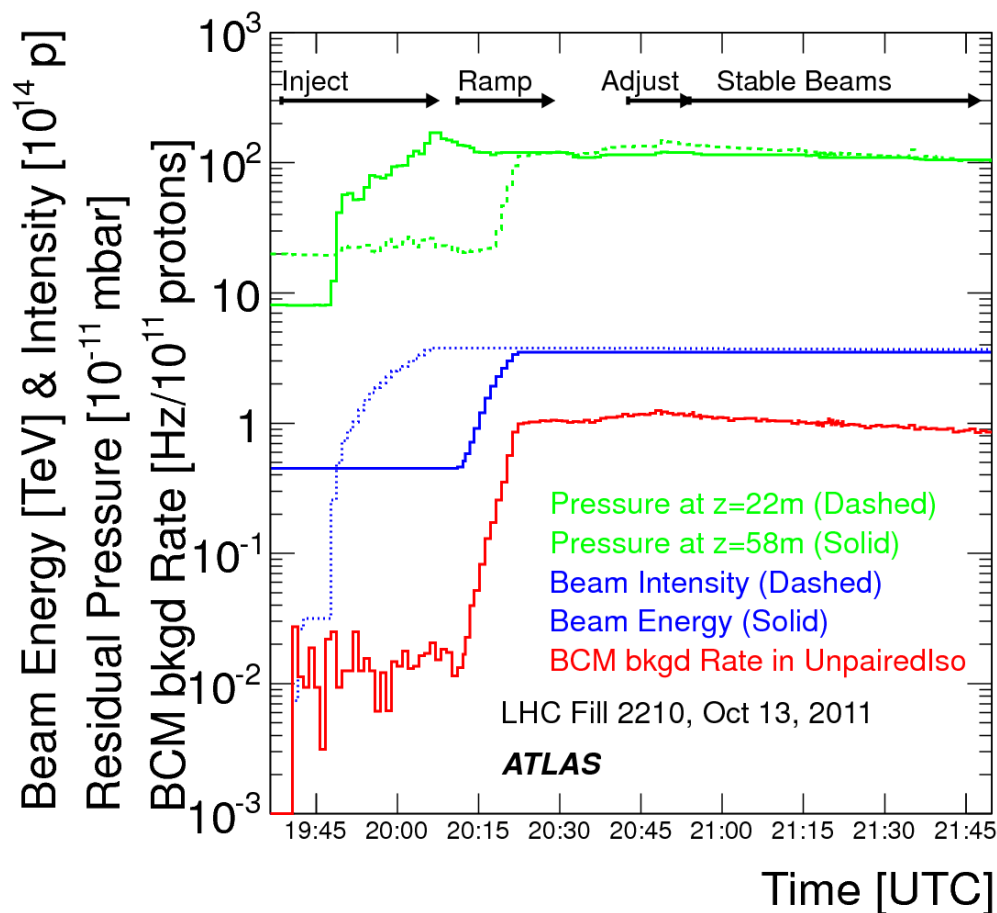
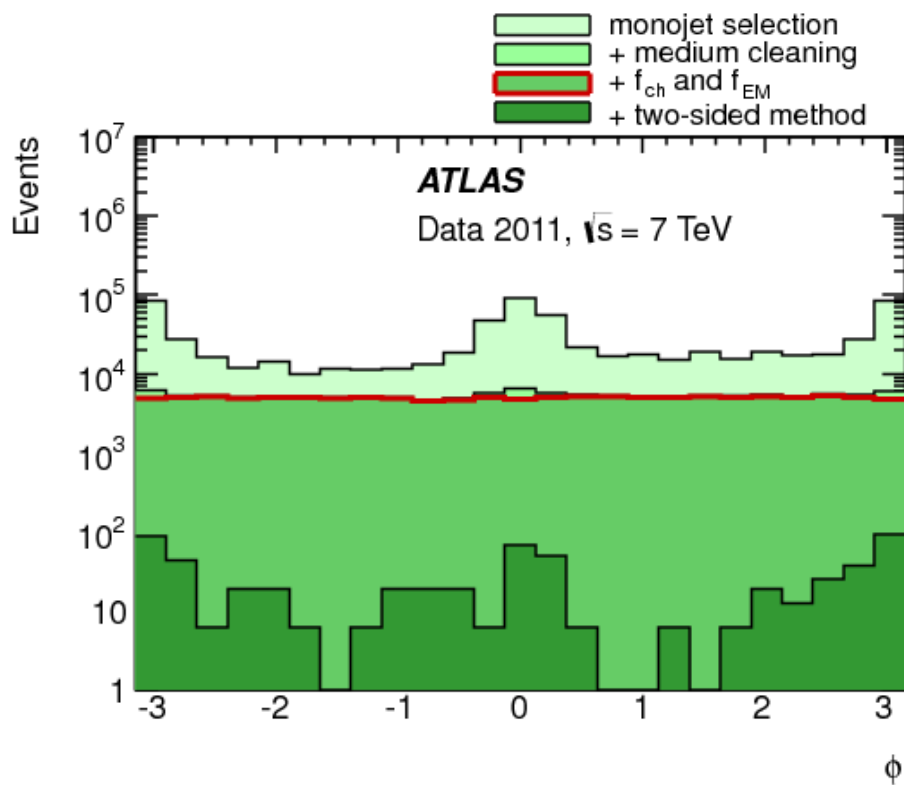
Beam-induced Backgrounds

Beam backgrounds are measured in several sub-detectors, monitored during the year and rejected in the analyses

- Background rates low in 2011 and 2012 with spikes in individual fills

Still searches require rejection of beam backgrounds

- Generic cleaning applied in all analyses
- Tighter cleaning in specific searches, such as mono-jet analysis



2012 Data Reprocessing

For 2013 winter conferences, reprocessed data recorded up until October 2012 – provide the best available conditions for physics results on the full dataset

Improvements included

- A more accurate alignment of the ID and MS sub-systems
- Update of sub-detector conditions to improve DQ efficiency
- Update of derived data content to better suit physics analysis

Reprocessing statistics:

- Luminosity of the reprocessed data periods: $\sim 17 \text{ fb}^{-1}$
- Number of events: $2.0 \cdot 10^9$
- Total CPU Consumption: $\sim 45 \cdot 10^9 \text{ s}$ (~ 1550 CPU years)
- Total size of the primary physics output (AOD): 0.6 PB

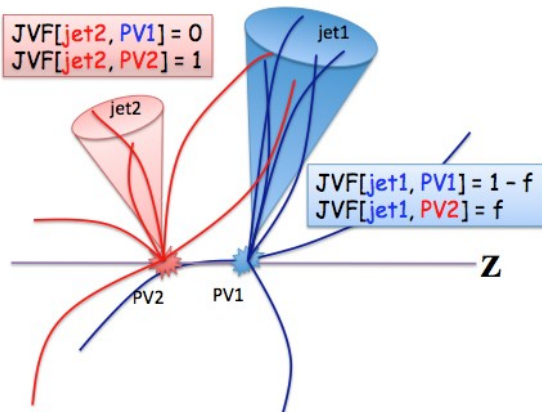
Pile-up Suppression

Pile-up local fluctuations within a same event can lead to fake pile-up jets

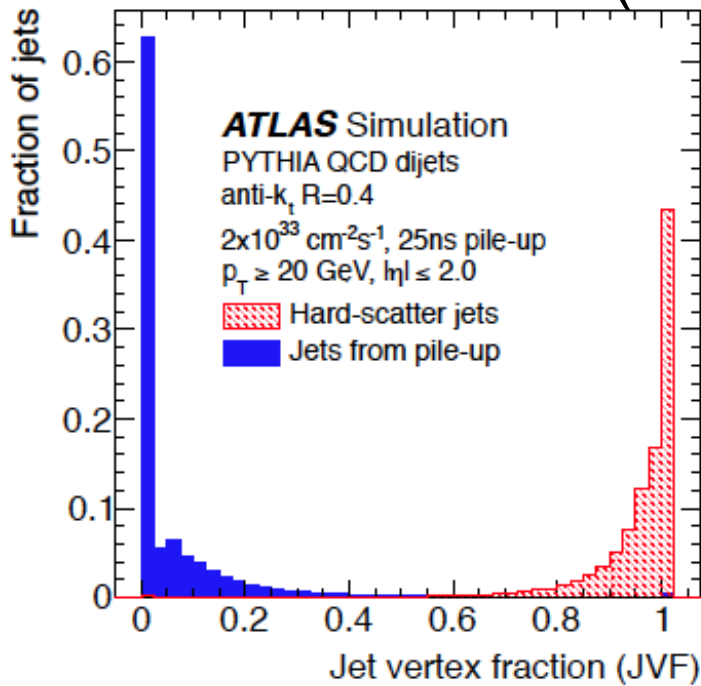
- Uniform distribution of particles from pile-up interactions

Jet Vertex Fraction algorithm

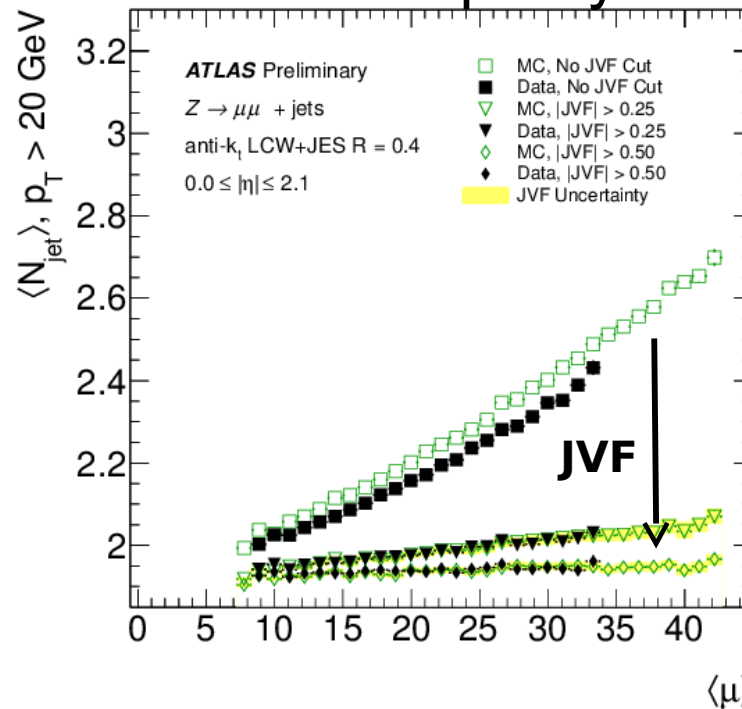
- Reject fake pile-up jets using track and vertex info
- Improve the data/MC agreement



Jet Vertex Fraction (JVF)



Jet multiplicity



E_T^{miss} and Pile-up Suppression

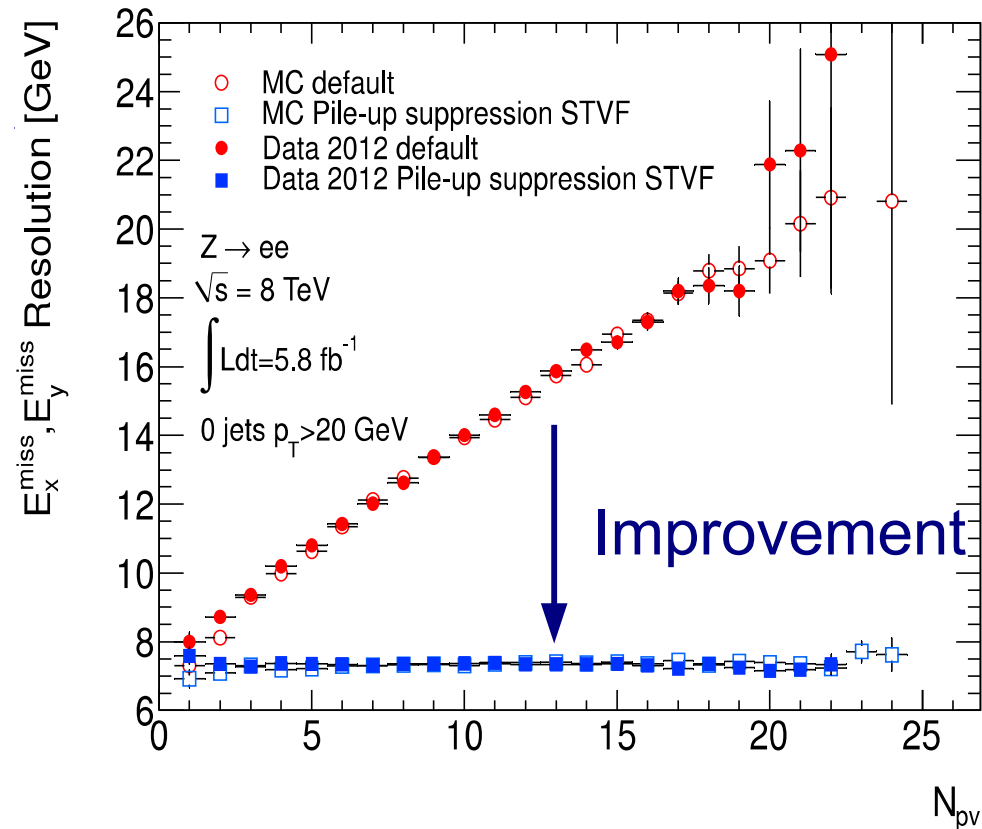
Pile-up is a major challenge for E_T^{miss}

- Very large worsening of the resolution
- Large pile-up contributions to the soft term

Pile-up suppression using tracks

- Soft term vertex fraction (STVF)
- Extension of the JVF concept to the soft component of E_T^{miss}

Missing ET resolution in events with no jets



$$STVF = \left(\frac{\sum p_T^{\text{track}, PV}}{\sum p_T^{\text{track}}} \right)_{\text{unmatched objects}}$$

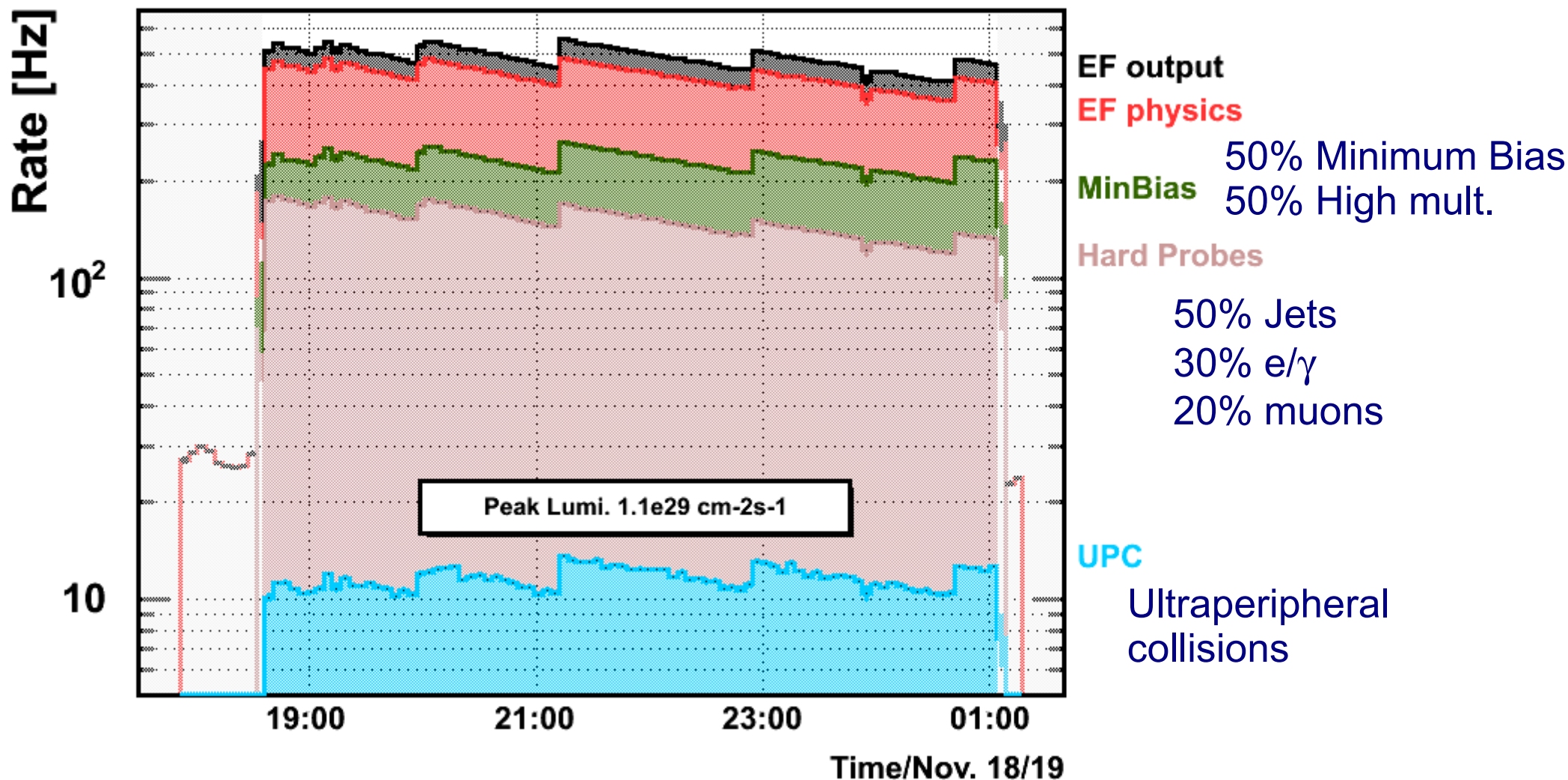
p+Pb Data

Recorded ~400 Hz of physics data (230 million events total)

- Used mainly loose trigger selections with low p_T thresholds

p+Pb 2013, EF rates breakdown

ATLAS Trigger Operation

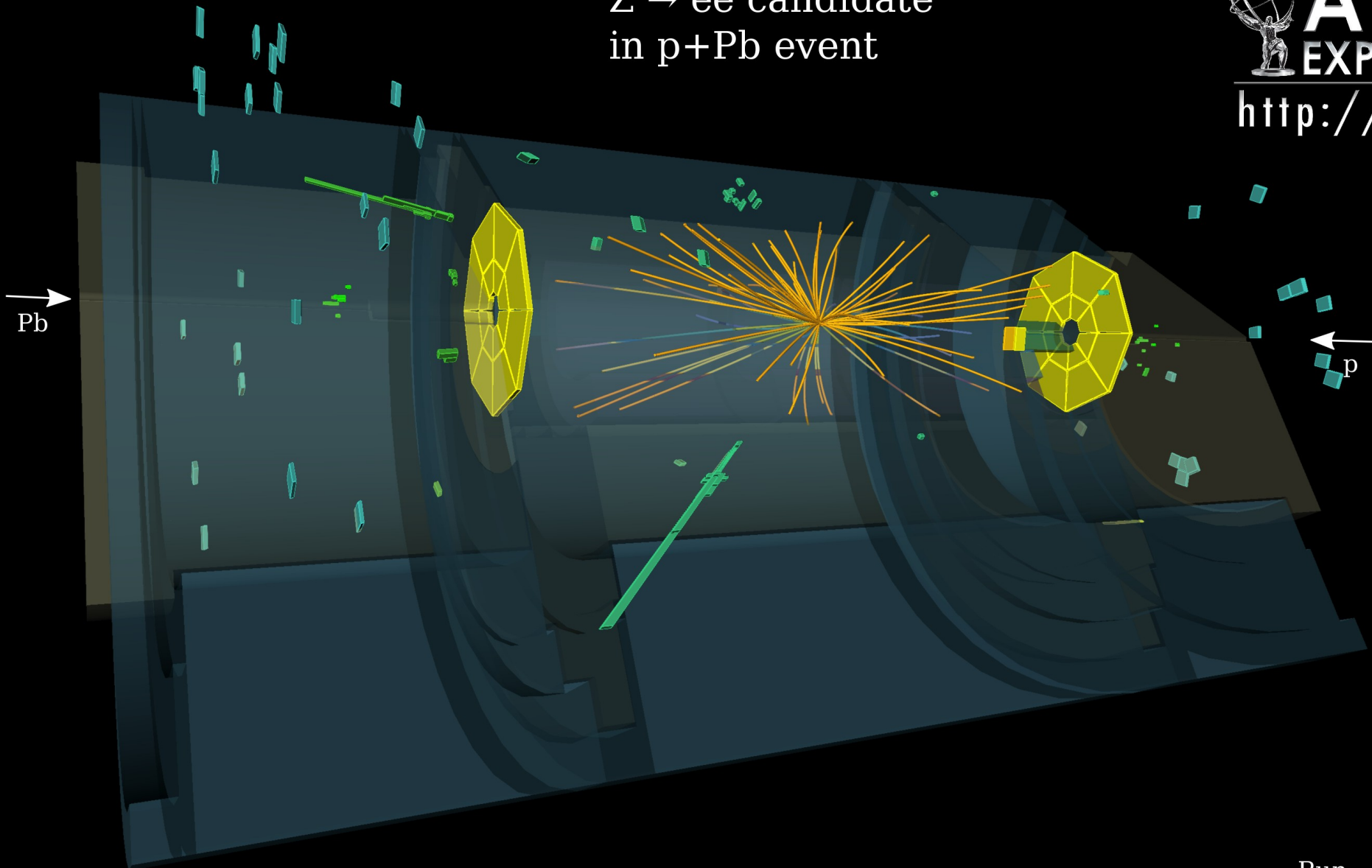


$Z \rightarrow ee$ Candidate Event in p+Pb

58

$Z \rightarrow ee$ candidate
in p+Pb event

 **ATLAS**
EXPERIMENT
<http://atlas.ch>

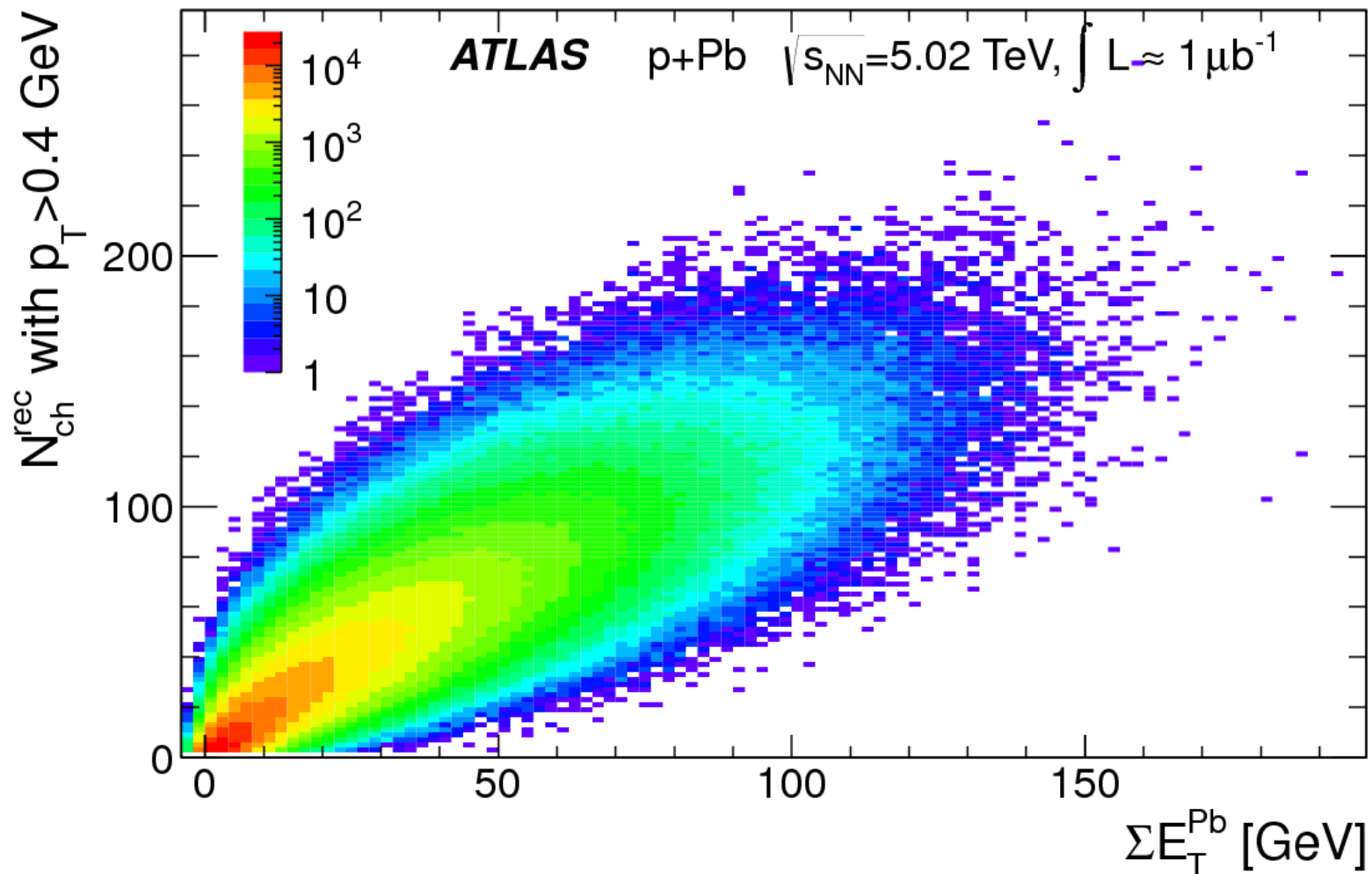


Run: 218048
Event: 212369680
Date: 2013-01-23

Centrality in p+Pb

Define centrality based on summed energy in forward calorimeter $|\eta|>3.2$ in out-going Pb direction

- Avoid systematic effect between multiplicity and correlation study

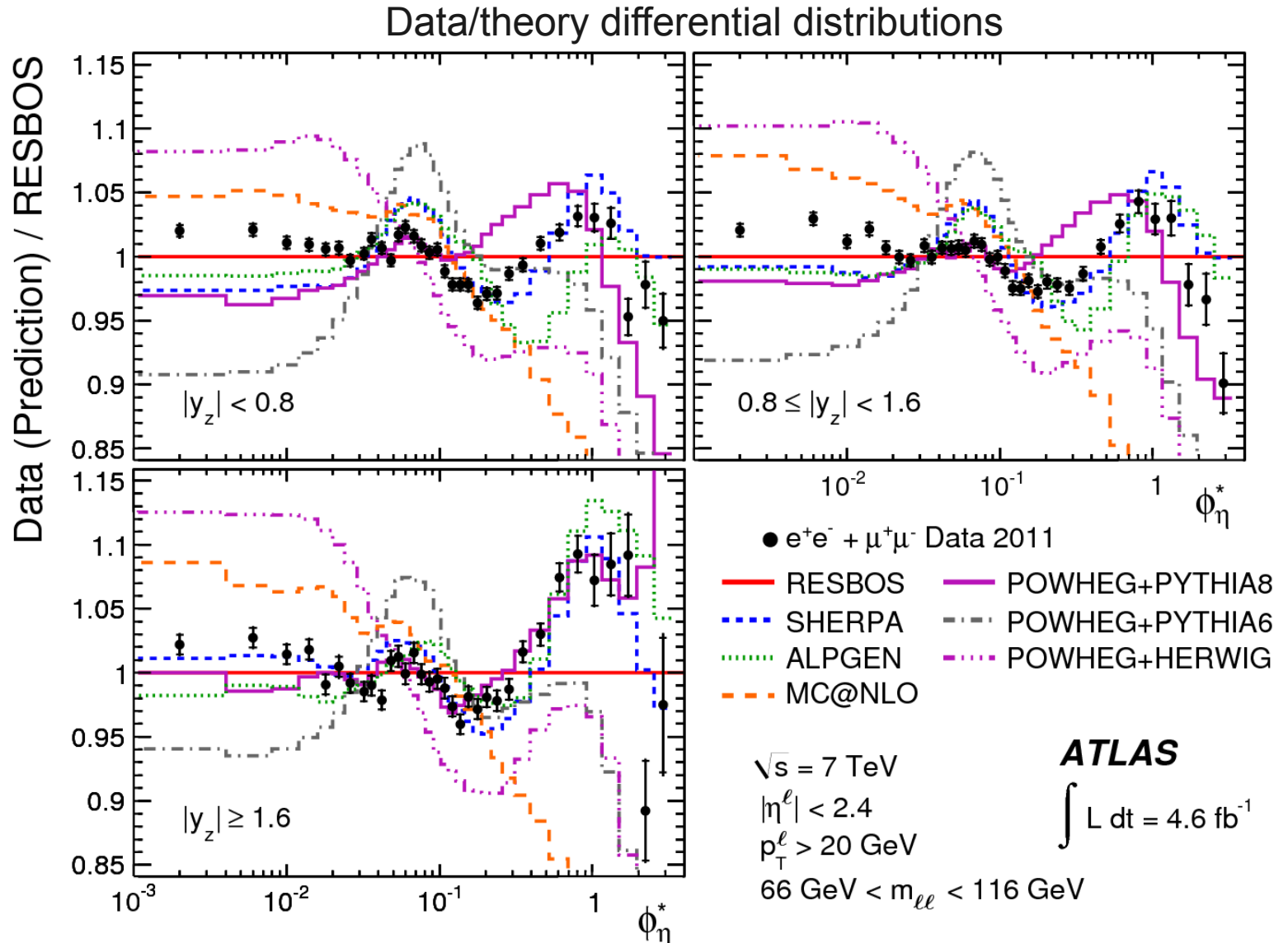


Angular Correlations in Drell-Yan Lepton Pairs

Detailed study of Drell-Yan p_T dependence in rapidity bins

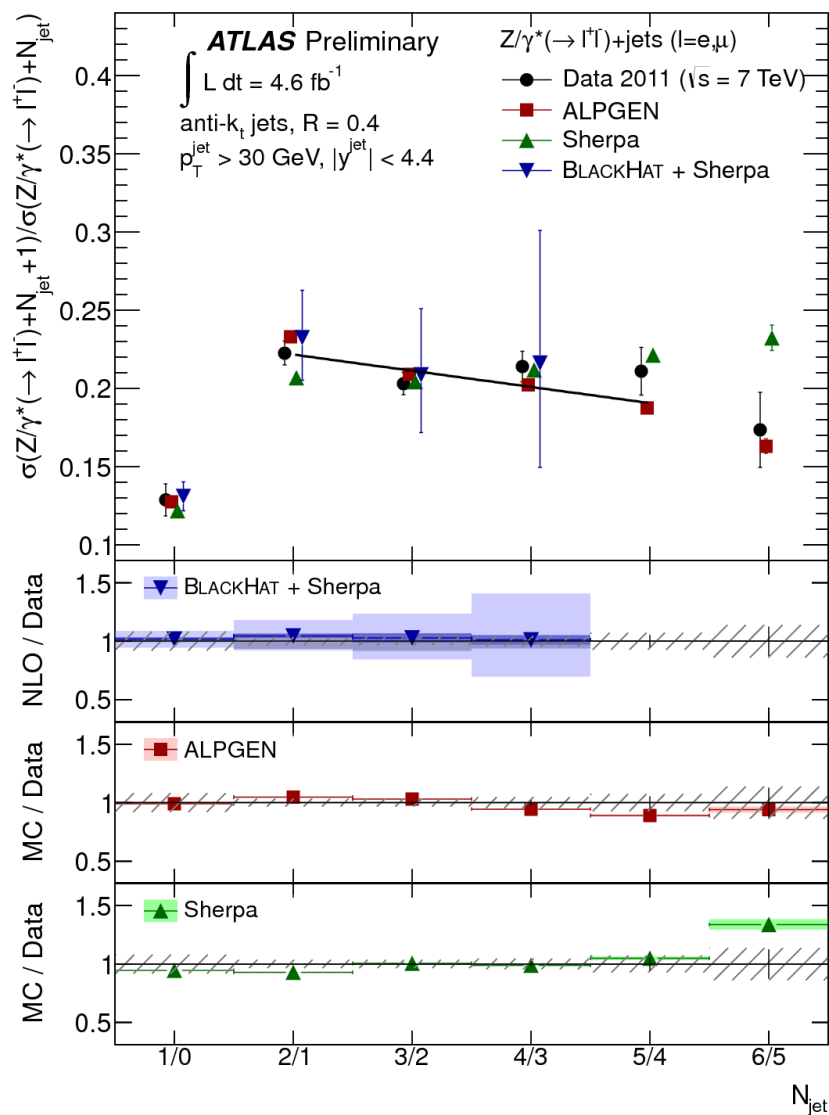
- Use ϕ_η^* defined purely by track directions instead of $p_T(\ell\ell)$ to reduce systematics

Experimental precision now one order of magnitude better than theoretical uncertainties



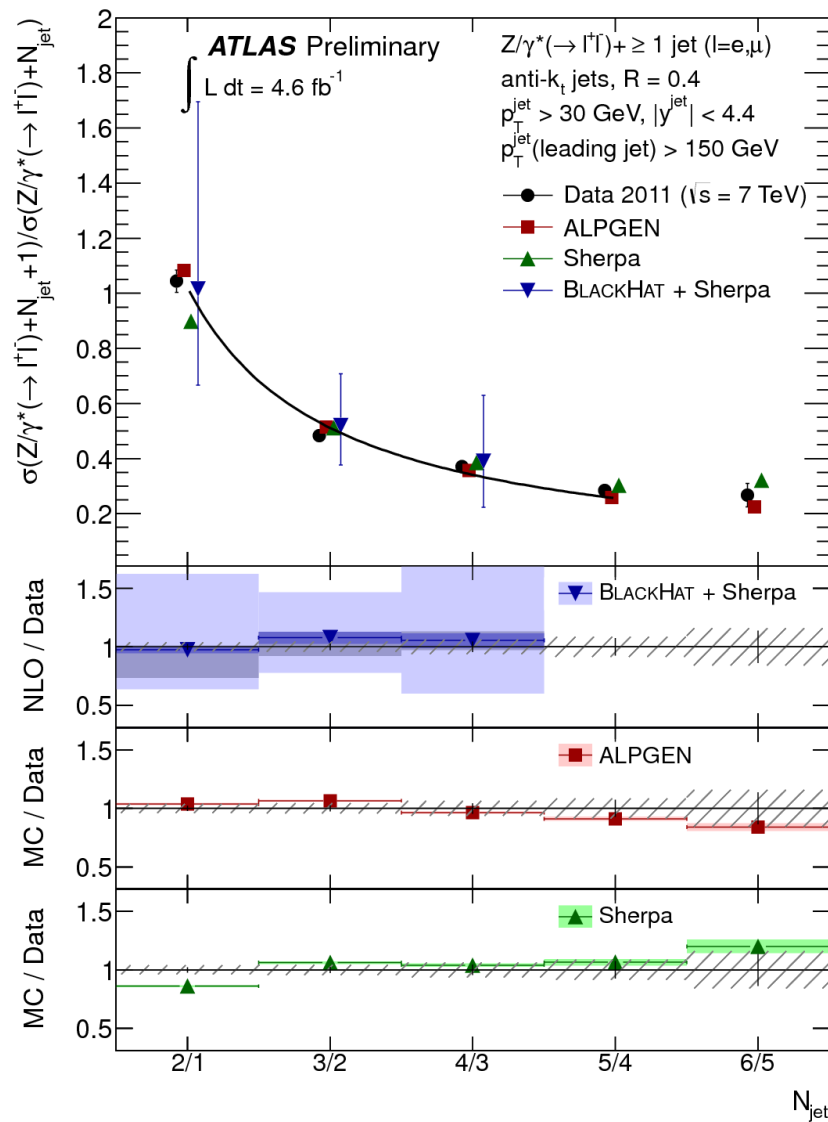
Z+Jets Exclusive Jet Multiplicities

Symmetric jet p_T selection



“Staircase” scaling

Hard leading jet selection

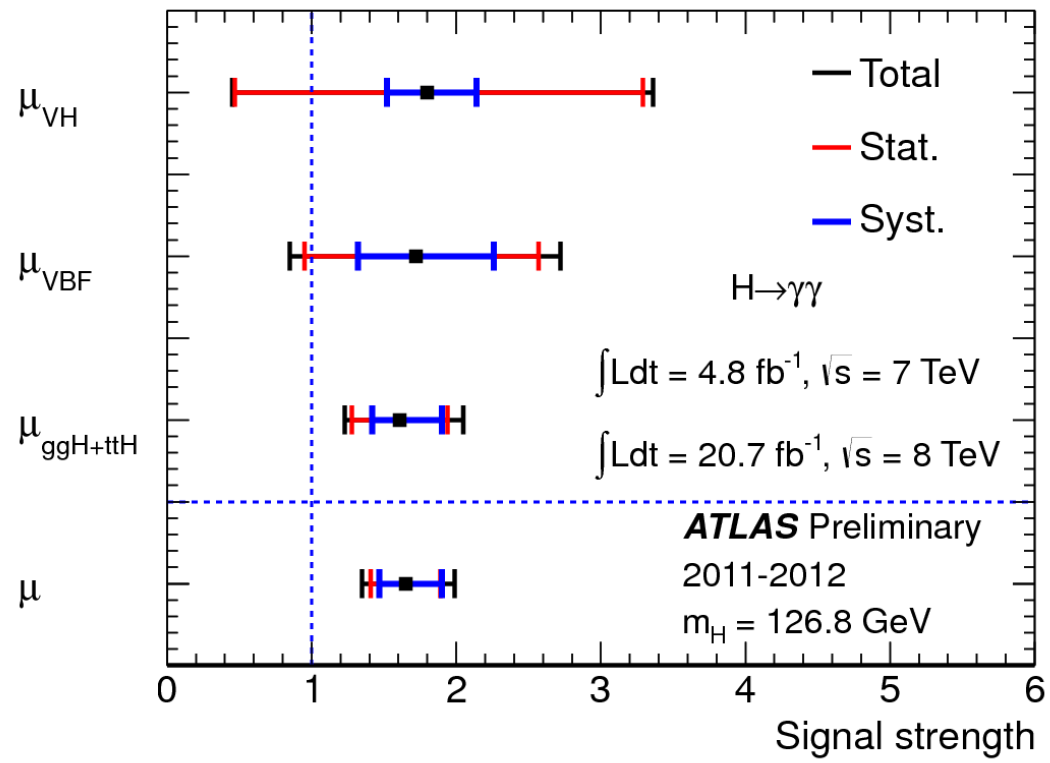
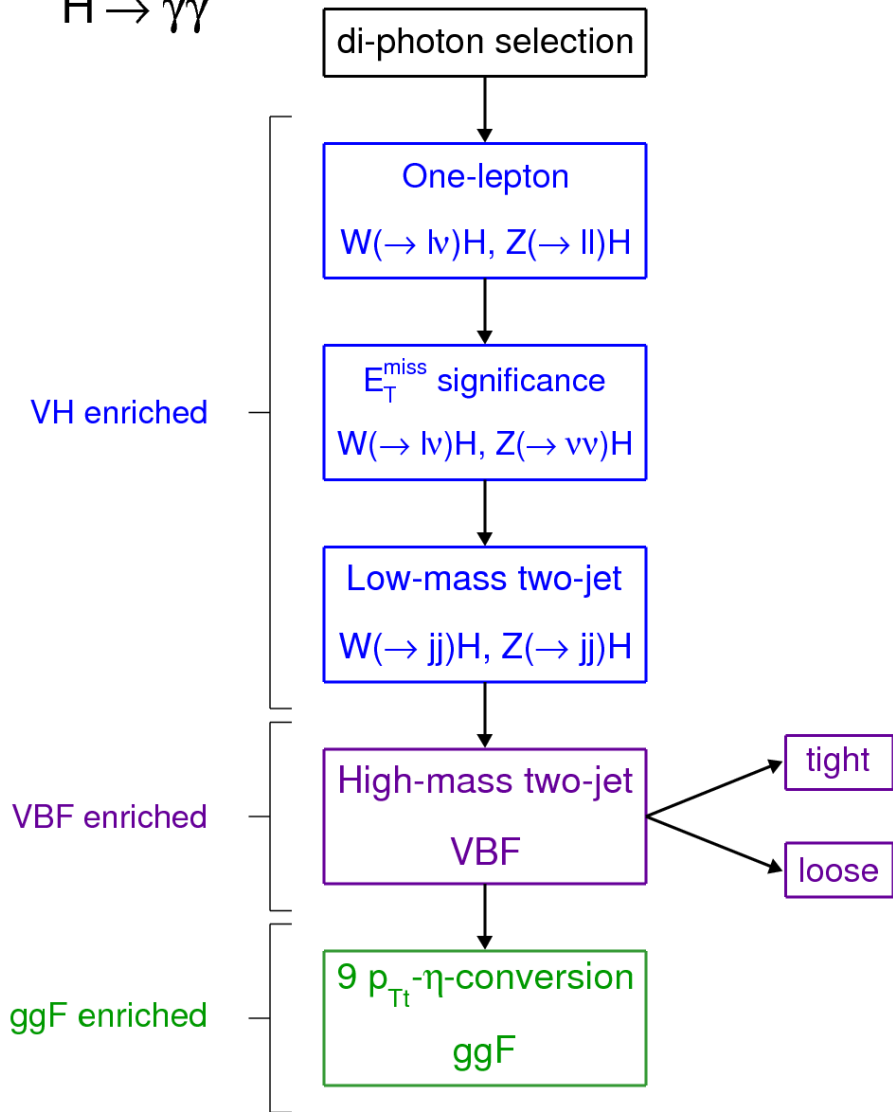


“Poisson” scaling

H → γγ Categorization

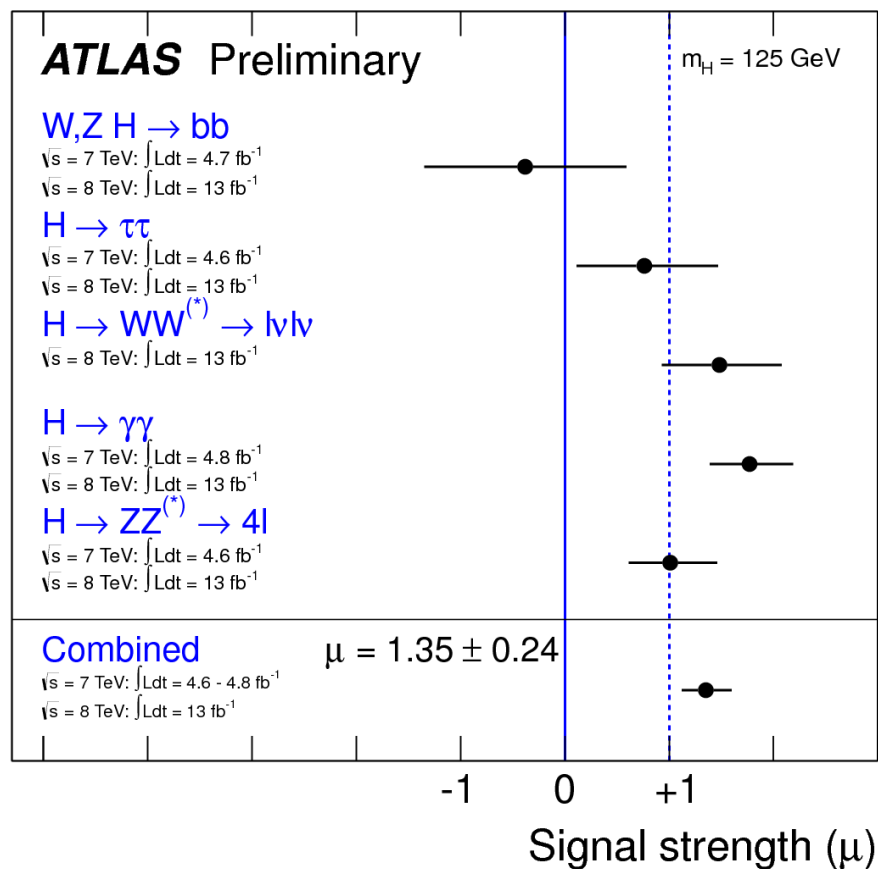
ATLAS Preliminary

H → γγ

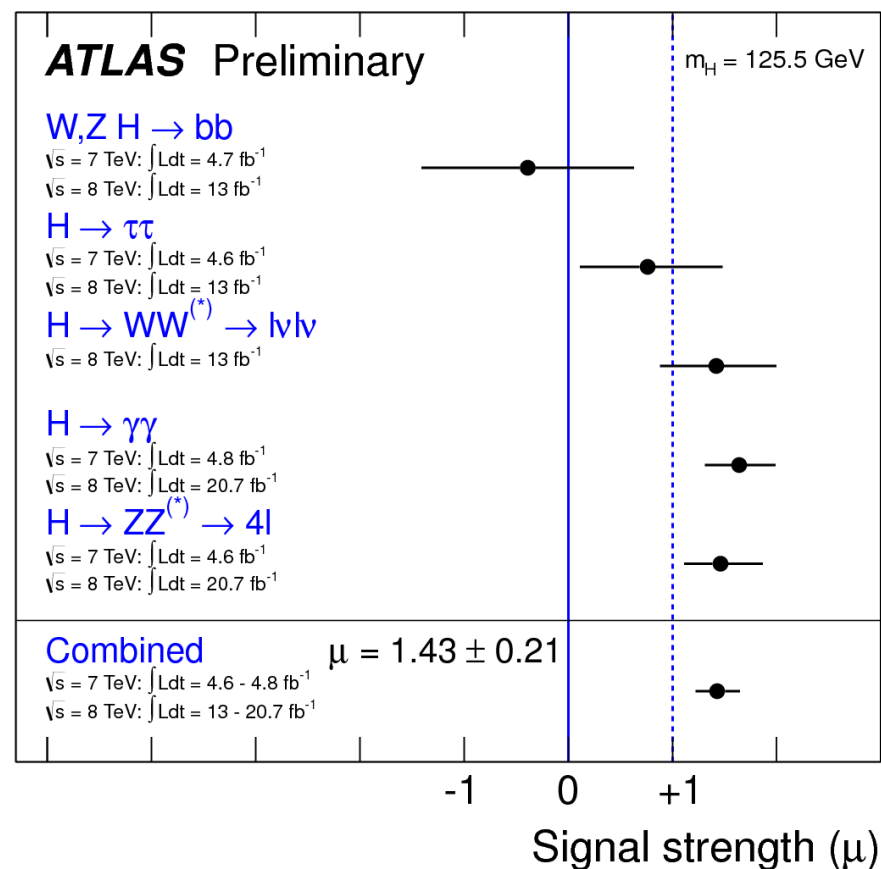


Signal Strength Comparison

December 2012



March 2013



Boson Mass Systematics

$H \rightarrow \gamma\gamma$ mass systematic uncertainties

Absolute energy scale from $Z \rightarrow ee$	0.3%
Uncertainties on upstream material simulation	0.3%
Pre-sampler energy scale	0.1%
Non-linearity of EM calo electronics	0.15%
Conversion fraction	0.1%
Relative calibration of first and second sampling	0.2%
Lateral leakage corrections	0.1%

+other smaller effects

Total systematic error is 0.55% (0.7 GeV)

4l mass measurement
dominated by the 4μ channel

Muon momentum scale	0.2%
Electron energy scale ($4e$)	0.4%
Low E_T electrons	0.1%

Possible local detector biases checked
event by event

ID and MS measurements also checked
separately

Spin-2 Model

General amplitude for spin-2 $H \rightarrow VV$

$$\begin{aligned}
 A(X \rightarrow VV) = \Lambda^{-1} & \left[2g_1^{(2)} t_{\mu\nu} f^{*1,\mu\alpha} f^{*2,\nu\alpha} + 2g_2^{(2)} t_{\mu\nu} \frac{q_\alpha q_\beta}{\Lambda^2} f^{*1,\mu\alpha} f^{*2,\nu,\beta} \right. \\
 & + g_3^{(2)} \frac{\tilde{q}^\beta \tilde{q}^\alpha}{\Lambda^2} t_{\beta\nu} (f^{*1,\mu\nu} f_{\mu\alpha}^{*2} + f^{*2,\mu\nu} f_{\mu\alpha}^{*1}) + g_4^{(2)} \frac{\tilde{q}^\nu \tilde{q}^\mu}{\Lambda^2} t_{\mu\nu} f^{*1,\alpha\beta} f_{\alpha\beta}^{*(2)} \\
 & + m_V^2 \left(2g_5^{(2)} t_{\mu\nu} \epsilon_1^{*\mu} \epsilon_2^{*\nu} + 2g_6^{(2)} \frac{\tilde{q}^\mu q_\alpha}{\Lambda^2} t_{\mu\nu} (\epsilon_1^{*\nu} \epsilon_2^{*\alpha} - \epsilon_1^{*\alpha} \epsilon_2^{*\nu}) + g_7^{(2)} \frac{\tilde{q}^\mu \tilde{q}^\nu}{\Lambda^2} t_{\mu\nu} \epsilon_1^* \epsilon_2^* \right) \\
 & \left. + g_8^{(2)} \frac{\tilde{q}_\mu \tilde{q}_\nu}{\Lambda^2} t_{\mu\nu} f^{*1,\alpha\beta} \tilde{f}_{\alpha\beta}^{*(2)} + g_9^{(2)} t_{\mu\alpha} \tilde{q}^\alpha \epsilon_{\mu\nu\rho\sigma} \epsilon_1^{*\nu} \epsilon_2^{*\rho} q^\sigma + \frac{g_{10}^{(2)} t_{\mu\alpha} \tilde{q}^\alpha}{\Lambda^2} \epsilon_{\mu\nu\rho\sigma} q^\rho \tilde{q}^\sigma (\epsilon_1^{*\nu} (q\epsilon_2^*) + \epsilon_2^{*\nu} (q\epsilon_1^*)) \right]
 \end{aligned}$$

Cannot exclude generic spin-2 with current data set

- Consider only minimal $g_1=g_5=1$ model for now

Spin-parity in $H \rightarrow 4\ell$

Table 9: For an assumed 0^+ hypothesis H_0 , the values for the expected and observed p_0 -values of the different tested spin and parity hypotheses H_1 for the BDT and J^P -MELA analyses. The results are given combining the $\sqrt{s} = 8$ TeV and $\sqrt{s} = 7$ TeV data sets. Also given is the observed p_0 -value where 0^+ is the test hypothesis and the other spins states are the assumed hypothesis (observed*). These two observed p_0 -values are combined to provide the CL_S confidence level for each test hypothesis. The production mode is assumed to be 100% ggF.

		BDT analysis				J^P -MELA analysis			
		tested J^P for an assumed 0^+		tested 0^+ for an assumed J^P	CL_S	tested J^P for an assumed 0^+		tested 0^+ for an assumed J^P	CL_S
		expected	observed	observed*		expected	observed	observed*	
0^-	p_0	0.0037	0.015	0.31	0.022	0.0011	0.0022	0.40	0.004
1^+	p_0	0.0016	0.001	0.55	0.002	0.0031	0.0028	0.51	0.006
1^-	p_0	0.0038	0.051	0.15	0.060	0.0010	0.027	0.11	0.031
2_m^+	p_0	0.092	0.079	0.53	0.168	0.064	0.11	0.38	0.182
2^-	p_0	0.0053	0.25	0.034	0.258	0.0032	0.11	0.08	0.116

Limits on Vector-like t' vs BR's

